

JANUARY 2024

FUGITIVE AND UNBURNED METHANE EMISSIONS FROM SHIPS (FUMES)

Characterizing methane emissions from LNG-fueled ships using drones, helicopters, and onboard measurements

Bryan Comer,¹ Jörg Beecken,² Robin Vermeulen,³ Elise Sturup,¹
Pierre Paschinger,³ Liudmila Osipova,¹ Ketan Gore,¹ Ann Delahaye,³
Vincent Verhagen,³ Bettina Knudsen,² Jon Knudsen,² and Ruud Verbeek³



¹International Council on Clean Transportation (ICCT); ²Explicit ApS; ³Netherlands Organization for Applied Scientific Research (TNO)

ACKNOWLEDGMENTS

The authors thank the owners and crew of the Aurora Botnia for granting access to their vessel for the onboard campaign and being responsive to their requests, and the LNG terminal operators who allowed the authors to fly within the terminal boundaries for the fugitive campaign. The authors also thank their colleagues at the ICCT, Explicit ApS, and TNO who reviewed earlier drafts of this report, in addition to experts representing engine manufacturers, shipowners, regulators, academics, advocates, and researchers who reviewed earlier versions of the plume results and this report. Finally, the authors thank Oceankind for funding this research.

International Council on Clean Transportation
1500 K Street NW, Suite 650
Washington, DC 20005

communications@theicct.org | www.theicct.org | [@TheICCT](https://twitter.com/TheICCT)

© 2024 International Council on Clean Transportation

SUMMARY

The use of liquefied natural gas (LNG) as a marine fuel is rapidly growing, doubling from 2.2 million tonnes (Mt) in 2018 to 4.4 Mt in 2022 for ships reporting to the European Union Monitoring Reporting and Verification system. Prior to this, the Fourth International Maritime Organization (IMO) Greenhouse Gas Study estimated that global LNG marine fuel consumption grew 30% between 2012 and 2018, resulting in an estimated 150% increase in methane (CH₄)¹ emissions. However, these estimates are uncertain because they rely on emission factors developed from only a few studies that used a mix of laboratory measurements of marine engines, including those provided by the engine manufacturers themselves, and onboard measurements of a few ships. More data are needed to understand the actual methane emissions from LNG-fueled ships under real-world conditions.

The Fugitive and Unburned Methane Emissions from Ships (FUMES) project collected the most comprehensive dataset of real-world methane emissions from LNG-fueled ships to date. Before the FUMES project, real-world measurements of methane slip were scarce, and the magnitude of ship-level methane emissions were largely unknown. FUMES is a collaboration between the International Council on Clean Transportation (ICCT), the measurement data service provider Explicit ApS, and the Netherlands Organization for Applied Scientific Research (TNO). Together, we conducted three measurement campaigns: plume, onboard, and fugitive. During the plume campaign, we measured methane in 45 plumes from 34 unique LNG-fueled ships. We used drones and helicopters to sample CH₄ in exhaust plumes for ships sailing near the coasts of the Netherlands, Denmark, Belgium, and Australia over the course of 2022. In our onboard campaign, we went on an LNG-fueled ferry that sails between Finland and Sweden, where we measured methane directly in the exhaust stack, as well as in the plume, in Spring 2023. During our fugitive campaign, we used a novel approach to quantify the rate of methane emissions from LNG cargo unloading operations of three LNG tankers at a European LNG terminal in September 2022.

Overall, we conclude that the use of LNG-fueled ships results in releases of methane to the atmosphere in the form of methane slip from their engines,² as well as fugitive methane emissions when LNG cargoes are unloaded from LNG tanker vessels. The specific conclusions from each campaign and the measurement approach used are provided below. We also offer policy recommendations to European Union (EU) and IMO policymakers based on the results of the study.

PLUME CAMPAIGN CONCLUSIONS

From the plume campaign, we conclude that low-pressure, dual-fuel, four-stroke (LPDF 4-stroke) engines, on average, emit more than twice as much methane slip than assumed by the EU and over 80% more than assumed by the IMO. Methane slip calculated from 22 measurements of 18 unique ships that exclusively used LPDF 4-stroke engines (L4 ships) averaged 6.42% with a median of 6.05%, as shown in Figure ES1. For six measurements at or above 50% combined engine load, the average was 6.07% and the median was 6.59%. Methane slip was greater than the EU assumption of 3.1% in 77% of the measurements. These same 77% of measurements were also greater than the IMO assumption of 3.5% methane slip.

Ships with LPDF 2-stroke main engines and LPDF 4-stroke auxiliary engines (L2L4) emitted the lowest ship-level methane slip. L2L4 ships emitted an average of 2.50% methane slip across all engine loads and 1.58% when operating above 10% main engine

¹ Throughout the study, we sometimes use the word methane and other times use CH₄. We use one or the other depending on context, with the goal of improving clarity and readability.

² Methane slip is the percentage of methane in fuel that is emitted unburned from an engine.

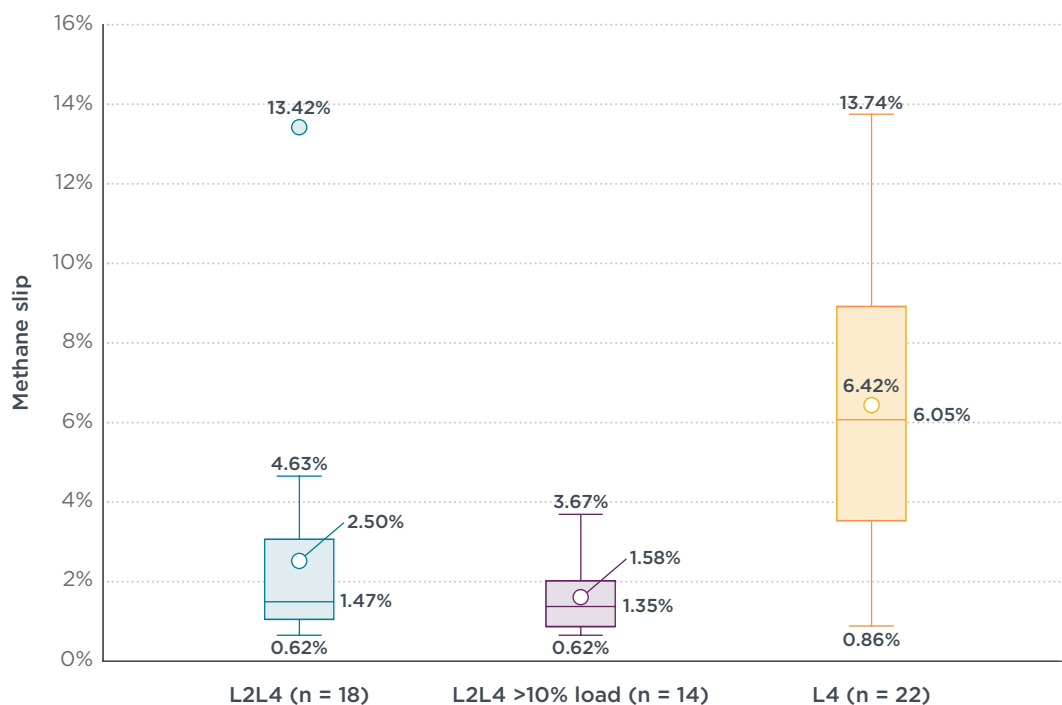
load. Median values were 1.47% and 1.35%, respectively. We found that LPDF 4-stroke auxiliary engine LNG consumption was significantly correlated with methane slip ($p = 0.017$); for every 10 percentage-point increase in LPDF 4-stroke auxiliary engine consumption, ship-level methane slip increased by 0.5 percentage points.

For ships with HPDF 2-stroke main engines and LPDF 4-stroke auxiliary engines (H2L4), we only obtained three measurements from two unique ships. Two measurements were performed when the ship was operating at below 10% main engine load, when we assume that only the LPDF 4-stroke auxiliary engines were operating on LNG, resulting in 3.47% and 6.12% methane slip. The other measurement was performed at 36% main engine load, when both the HPDF main engine and LPDF 4-stroke auxiliary engines were expected to be operating on LNG, resulting in 2.69% methane slip.

We cannot say whether the methane slip default values for HPDF 2-stroke or LPDF 2-stroke engines are reasonable, because we were not able to isolate methane slip emissions from these engines without interference from LPDF 4-stroke engines.

For ships with lean-burn spark-ignited (LBSI) engines, which do not have LNG-fueled auxiliary engines, we obtained two measurements from two unique ships and calculated a methane slip of 2.41% and 1.85% at 36% and 55% main engine load, respectively. This is lower than the EU and IMO assumption of 2.6% methane slip, but we do not have enough data to determine whether the default factor for LBSI engines is reasonable.

While our study is focused primarily on methane emissions, we find that most of the ships measured in the plume campaign could achieve nitrogen oxide (NO_x) emissions below weighted Tier III limits without the use of exhaust aftertreatment technologies.



Note: Dot shows outliers; whiskers show minimum and maximum (excluding outliers); circle inside box is the average; horizontal line is the median; box is the interquartile range.

Figure ES1. Boxplot of ship-level methane slip for ships with LPDF 2-stroke main engines and LPDF 4-stroke auxiliary engines (L2L4), and ships with only LPDF 4-stroke engines (L4).

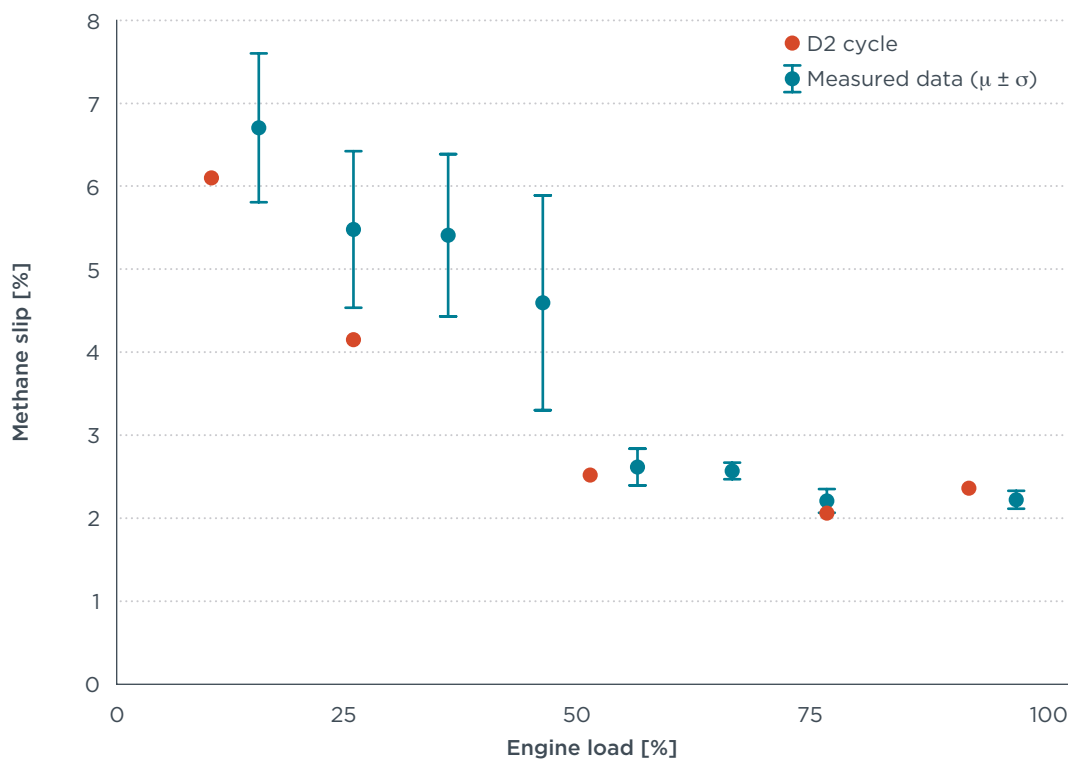
ONBOARD CAMPAIGN CONCLUSIONS

From the onboard campaign, we conclude that a modern LPDF 4-stroke engine can emit lower methane slip than assumed by the EU (3.1%) and the IMO (3.5%), but

methane slip can still be substantial, especially at low engine loads. Figure ES2 shows methane slip results in two ways: the orange circle shows the D2 cycle results, which were measured under constant engine load conditions when the engine was operated at approximately 10%, 25%, 50%, 75%, and 92% load (a proxy for the 100% engine load test point for the D2 cycle). The vertical bars show the average methane slip (dot) and standard deviation (whiskers) for all real-sailing measurements, binned by their nearest engine load at intervals of 15%, 25%, 35%, etc. We find that methane slip is highest at low engine loads, ranging from approximately 4%–7% at 25% engine load and below. Methane slip is also more variable below 50% engine load than above. Average real-sailing methane slip ranged from a minimum of approximately 2% for measurements near and above 75% load to a maximum of 6.7% for measurements near 15% load. Methane slip was about 2.5% at approximately 50% engine load. This is lower than the EU assumption of 3.1% at 50% load, and toward the lower end of the literature.

IMO’s assumption of 3.5% methane slip is meant to estimate emissions on the E2/E3 test cycle. Figure ES2 presents the results for the D2 cycle, which includes measurements at 10% load; the E2/E3 cycle omits the 10% load measurement and applies different weighting factors than the D2 cycle when calculating a weighted emission factor. The E2 test cycle is relevant for this engine and the measurements yielded a weighted methane slip of 2.0%, lower than IMO’s assumption of 3.5%. Note that although ships typically operate at lower loads than implied by the E2/E3 weighting factors, in this case, the ship tended to operate at higher engine loads.

We find that the engine can achieve weighted NO_x emissions that could comply with Tier III standards under the E2 test cycle, even though the engine is only required to be certified to less-stringent Tier II standards. However, we find that NO_x emissions (g/kWh) at around 10% engine load, which is not used in the E2 cycle, were 10-times greater than NO_x emissions near 75% engine load.



Note: Results shown when measured on the D2 cycle, which were measured at constant load, and results of all measured data binned by engine load (e.g., the first bar is centered at 15% engine load, the second at 25% engine load, etc.).

Figure ES2. Methane slip measured onboard a roll-on/roll-off passenger ferry with LPDF 4-stroke engines.

FUGITIVE CAMPAIGN CONCLUSIONS

From the fugitive campaign, we conclude that LNG cargo unloading operations can release 11–21 kilograms of methane per hour (kg/h) for a small, 10,000 cubic meter (m³) capacity LNG tanker that uses conventional diesel engines (i.e., does not use LNG as a fuel). The unloading operations of large 162,000–174,000 m³ capacity LNG tankers that use LPDF 4-stroke engines can result in fugitive methane emissions between 24 and 40 kg/h, including approximately 8 kg/h of methane slip from the engines. Figure ES3 shows an example; the hotspot on the left was determined to most likely be methane slip from the ship's LPDF 4-stroke engines, whereas the other areas show methane leaks associated with LNG cargo unloading operations. While the amount of methane released as a percentage of cargo unloaded is small, the methane emissions rates (kg/h) from unloading operations are estimated to be greater than the emission rates from the LPDF 4-stroke engines used by the large LNG tankers.

Map visualization

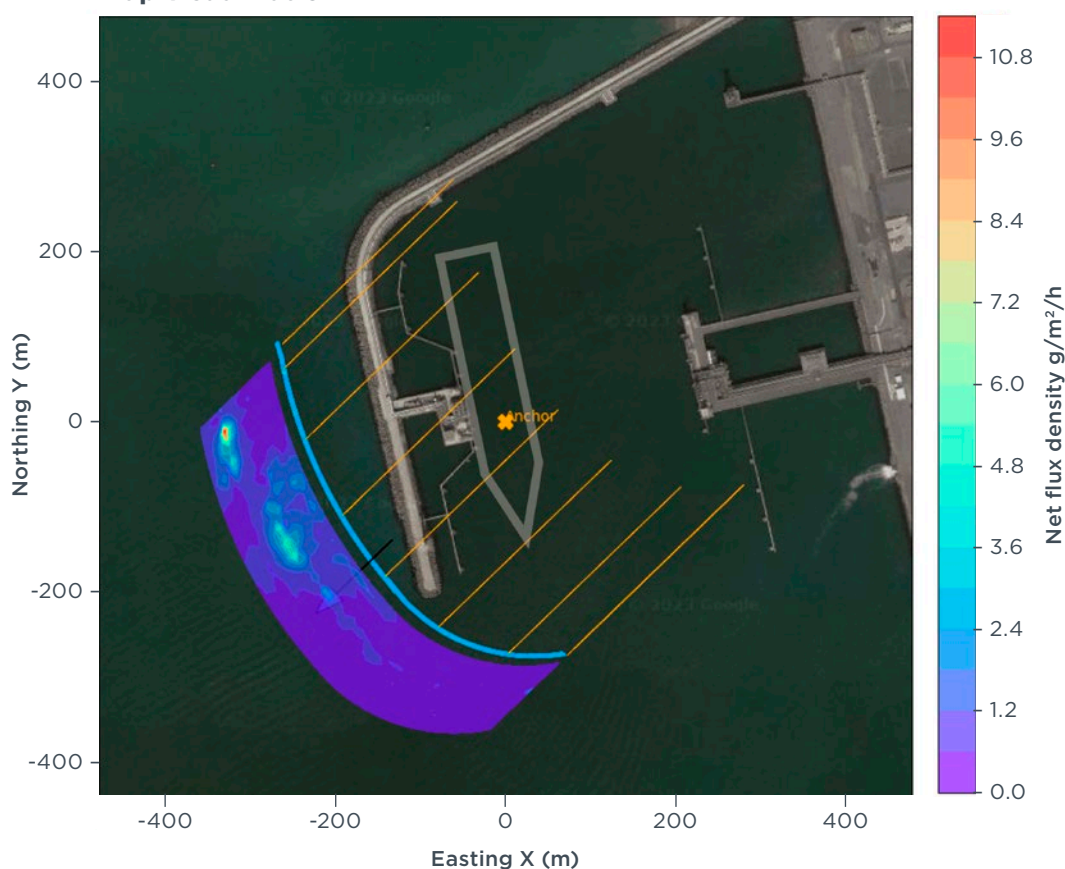


Figure ES3. Example of measured fugitive methane emissions from LNG cargo unloading operations that were visualized on a satellite map to identify the sources of methane (Maps data: Google, ©2023 CNES / Airbus, Maxar Technologies).

MEASUREMENT APPROACH CONCLUSIONS

We find that mounting sensors to drones and helicopters is useful for estimating ship-level methane slip from LNG-fueled ships and for estimating fugitive methane emissions from LNG cargo unloading operations. While measuring in the plume introduces more uncertainty compared with in-stack sensors, we nevertheless found good agreement in measured methane concentrations between the two approaches. Using drones and helicopters allows for the sampling of more ships at a lower cost than in-stack measurements. Moreover, there are fewer barriers to performing measurements: shipowner permission is not required; arranging schedules for boarding

and disembarking is not necessary; and equipment does not need to be loaded and unloaded from the ship. In-stack measurements are useful for accurately measuring methane emissions from individual engines onboard the ship, which is not possible when measuring in the plume unless only one engine is in operation. When measuring onboard, the emissions from the stack can be determined over the range of real sailing engine loads. When onboard, other methane sources can also be monitored, including any crankcase emissions or venting from the LNG fuel and cargo systems.

POLICY RECOMMENDATIONS

Regulators should consider the following policy actions which flow from the results of this study:³

EU and IMO policymakers should consider increasing the default methane slip value for LPDF 4-stroke engines from 3.1% (EU) or 3.5% (IMO) to at least 6%. This is based on our finding that the average and median methane slip for these engines was greater than 6%, even for measurements at higher engine loads. Shipowners that do not wish to take the default values could certify that the engines used on their ships emit less than the default methane slip values. We found in the onboard campaign that using a modern LPDF 4-stroke engine can result in lower-than-default emission values. However, any certification procedure should accurately reflect how the engine is operated in the real-world and account for methane slip variation by engine load.

EU policymakers should consider requiring LNG-fueled ships to plug into shore power or otherwise eliminate their at-berth emissions. Doing so would eliminate the use of LPDF 4-stroke auxiliary engines, the engine technology we found to have the highest methane slip.

EU policymakers should consider requiring monitoring, reporting, and verification of methane emissions at LNG storage and refueling points. We found that LNG cargo unloading operations can emit higher rates of methane emissions than LPDF 4-stroke engines. Current policies, such as the Alternative Fuels Infrastructure Regulation (AFIR), which requires investments in LNG infrastructure at major ports, may, therefore, be counterproductive to achieving EU climate goals. If data collected confirms that there are substantial methane emissions from LNG storage and refueling points, policymakers should consider regulations to address them.

IMO policymakers should consider adding a low-load test point to all engine emission certification test cycles. In the onboard measurements, we found that methane slip and work-specific NO_x emissions were highest at the lowest engine loads. To address this, IMO policymakers should consider adding a 10% engine load test point to all engine certification test cycles. They should also consider adjusting how emissions at each engine load test point are weighted to more accurately reflect real-world operations.

³ See the Policy Recommendations section of the report for specific ideas on when and how these recommendations could be implemented.

TABLE OF CONTENTS

Summary	i
Plume campaign conclusions.....	i
Onboard campaign conclusions.....	ii
Fugitive campaign conclusions.....	iv
Measurement approach conclusions.....	iv
Policy recommendations	v
Introduction	1
Background	2
LNG engine technologies	2
LNG engine installation and fuel consumption trends.....	3
Policy.....	6
Literature review	8
Laboratory, onboard, and review studies of methane emissions from ships	8
Remote-sensing measurement of methane.....	10
Strategies to reduce methane emissions.....	10
Air pollution impacts of using LNG as a marine fuel.....	13
Methods	14
Measuring methane and NO _x emissions in plumes.....	14
Measuring CH ₄ and NO _x in exhaust stacks (onboard).....	16
Cross-instrument comparison (on-land).....	20
Estimating methane slip in plumes.....	22
Estimating NO _x emission factors.....	26
Estimating fugitive methane emissions from stationary ships	28
Results and discussion	30
Plume campaign results	30
Onboard Campaign Results	45
Cross-instrument comparison (on-land) results.....	57
Fugitive Campaign Results	61
Limitations and future work	65
Policy recommendations	67
Conclusions	69
References	71
Appendixes	74
Appendix A: Auxiliary engine demand assumptions.....	74
Appendix B: Plume results figures in grams of methane per kilowatt hour (g CH ₄ /kWh)	75
Appendix C: Annual combined main engine load distributions for ships measured in the plume campaign	79
Appendix D: Supplemental material for plume and fugitive measurements.....	80

LIST OF FIGURES

Figure ES1. Boxplot of ship-level methane slip for ships with LPDF 2-stroke main engines and LPDF 4-stroke auxiliary engines (L2L4), and ships with only LPDF 4-stroke engines (L4).	ii
Figure ES2. Methane slip measured onboard a roll-on/roll-off passenger ferry with LPDF 4-stroke engines.	iii
Figure ES3. Example of measured fugitive methane emissions from LNG cargo unloading operations that were visualized on a satellite map to identify the sources of methane (Maps data: Google, ©2022 CNES / Airbus, Maxar Technologies)	iv
Figure 1. LNG-fueled fleet by number of ships, gross tonnage, and installed engine power, by ship type, for 2012–2022. Source: IHS Markit data as of July 2023.	4
Figure 2. Global LNG fuel consumption by main engine types, 2012–2017	4
Figure 3. Proportion of LNG fuel consumption by ships reporting to the EU Monitoring Reporting and Verification program, by engine type, 2018–2022. Source: Fuel consumption data from the EU Monitoring Reporting and Verification system paired with engine information from the ICCT’s SAVE model (Olmer et al., 2017).	5
Figure 4. Total LNG fuel consumption by ships reporting to the EU Monitoring, Reporting, and Verification program, by engine type, 2018–2022. Source: EU MRV fuel consumption data paired with engine information from the ICCT’s SAVE model (Olmer et al., 2017).....	6
Figure 5. The photograph shows a drone equipped with a Mini-Sniffer payload for sampling volume mixing ratios of CH ₄ and CO ₂ . The elongated nozzle at the front of the drone is the inlet nozzle for air samples. The sketch below illustrates the flight path of the aircraft for plume sampling. The “sweet spot” is a location within the plume where favorable concentration conditions are met. In the case of the applied Mini-Sniffers this is when the CO ₂ concentration within the plume is about 200 ppm above the background concentration.	15
Figure 6. Aurora Botnia roll-on/roll-off passenger ferry that was measured during the onboard campaign.....	16
Figure 7. Left: heated probe sampling hot gas from the exhaust after the turbine of main engine 4. Right: the FTIR instrument used to measure the concentrations of CO ₂ , CH ₄ , and NO _x (NO+NO ₂).....	18
Figure 8. Left: screen of main engine 4 power output over a selected time frame. Right: screen mode showing engine parameters.	19
Figure 9. Drone flight measuring CH ₄ , NO _x and CO ₂ concentrations in the exhaust plume of the Aurora Botnia when only main engine 4 was running. Fuel-fired boilers are switched off. The stacks are the stacks of the four main engines and two fuel-fired boilers. The high funnel in front contains the boil-off and crankcase gas venting pipes.	19
Figure 10. Schematic showing the land-based test set-up.....	21
Figure 11. The land-based test with a diesel genset with methane dosage in the exhaust and the drone mounted on a crane.	21
Figure 12. The photograph shows a drone equipped with a Mini-Sniffer. For the DFM method, the drone is additionally equipped with two wind sensors at extended beams to each side of the drone. The visualization below shows the evaluated, spatially resolved net flux densities superimposed to a map (Maps data: Google, ©2022 CNES / Airbus, Maxar Technologies). In combination with the wind information, individual sources can be identified and individually quantified.	28
Figure 13. Plume measurement locations and number of measurements in Europe and Australia, 2022.	30
Figure 14. Measurements by engine type.....	31
Figure 15. Measurements by ship type.	31
Figure 16. Measurements by combinations of ship types and engine types.	32

Figure 17. Unique ships measured by engine type.	32
Figure 18. Unique ships measured by ship type.	33
Figure 19. Unique ships by combinations of ship types and engine types.	33
Figure 20. Ship-level methane slip from all engine sources measured.	34
Figure 21. Boxplot of ship-level methane slip for ships with LPDF 2-stroke main engines and LPDF 4-stroke auxiliary engines (L2L4) and ships with only LPDF 4-stroke engines (L4).	35
Figure 22. Methane slip versus combined main engine load.	36
Figure 23. Methane slip by engine load for L4 ships that have only one LPDF 4-stroke main engine, with build year of the ship indicated.	38
Figure 24. Methane slip versus NO _x	39
Figure 25. Results of uncertainty calculation for plume measurements; the dashed yellow line represents a relative uncertainty of 15% of the methane slip.	41
Figure 26. Sensitivity analysis: Methane slip estimates with and without adjusting for CO ₂ from fuel oil consumption from pilot fuel or for two-stroke dual-fuel engines in diesel mode.	42
Figure 27. Sensitivity analysis: Methane slip results for L2L4 and L4 ships with and without adjusting for CO ₂ from fuel oil consumption from pilot fuel or for two-stroke dual-fuel engines operating in diesel mode.	43
Figure 28. Plot of the linear regression of the measurement of the ratio of CH ₄ to CO ₂ [mol/mol] with the in-stack measurement (FTIR) as explanatory variable (x-axis) and the drone measurement in the plume as the dependent variable (y-axis).	46
Figure 29. Plot of the linear regression of the measurement of the ratio of NO _x /CO ₂ [mol/mol] with the in-stack measurement (FTIR) as explanatory variable and the drone as the dependent variable.	47
Figure 30. Work-specific CO ₂ measured from the stack under constant engine loads for the D2 cycle and binned by engine load for all the measured data, which also contains data from transient operations near that load. Results are compared to a different campaign conducted on the same ship and engine (Lehtoranta et al., 2023). The result is calculated from the broadcasted fuel flow, an estimate of the pilot fuel rate, the fuels' carbon content, and broadcasted engine power.	48
Figure 31. Work-specific CH ₄ emissions measured in the stack under constant engine loads for the D2 cycle and binned by engine load for the measured data, which also contains data from transient operations near that load. Results are compared to a different campaign conducted on the same ship and engine (Lehtoranta et al., 2023).	49
Figure 32. Work-specific NO _x emissions measured in the stack under constant engine loads for the D2 cycle and binned by engine load for the measured data, which also contains data from transient operations near that load. Results are compared to those of a different campaign conducted on the same ship and engine (Lehtoranta et al. 2023).	50
Figure 33. Work-specific CO emissions as measured from the stack over various constant engine loads and off all measured data binned, which also contains data from transients. Engine load points are shown of the D2 test cycle, as binned data from all measurement data as tested during the campaign and of a different campaign conducted on the same ship and engine (Lehtoranta et al. 2023).	50
Figure 34. Methane slip measured on the D2 cycle and all measured data binned by engine load (e.g., the first bar is centered at 15% engine load, the second at 25% engine load, etc.)	51
Figure 35. CO ₂ -equivalent emissions based on the GWP of CO ₂ and CH ₄ emissions per engine load bin using all measured emissions data.	53
Figure 36. CO ₂ -equivalent emissions in kg/h based on the GWP of CO ₂ and CH ₄ per load bin using all measured emissions data.	54
Figure 37. Concentration of exhaust components during a trip from Umeå to Vaasa.	55

Figure 38. Screen of the engine load and fuel consumption of Main Engine 4 during a trip from Umeå to Vaasa. Orange line represents engine load in % of ME4. The pink line represents the fuel consumption of ME4 in kg/h.....	55
Figure 39. Screen of the engine load and fuel consumption of ME2 and 4 during a trip from Umeå to Vaasa. Blue line (ME4) and green line (ME2) represent load in %. Pink (ME4) and red (ME2) represent gas consumption in kg/h.....	56
Figure 40. Methane emissions expressed per unit of CO ₂ in g/kg and mol/mol as adjusted and measured by the mass flow controllers (CH ₄ setpoint), as measured by PEMS and as measured by the drone for the various methane slip levels selected in the program.	58
Figure 41. Methane emissions expressed per unit of CO ₂ in mol/mol as adjusted and measured by the mass flow controllers (CH ₄ setpoint), compared to PEMS and drone (Explicit) measurements during the on-land cross-instrument comparison.	59
Figure 42. Comparison of methane-to-CO ₂ concentrations (mol/mol) measured in-stack by the PEMS and in the plume by the drone (Explicit) for the various methane slip levels selected in the on-land cross-instrument comparison.	59
Figure 43. NO _x emissions expressed per unit of CO ₂ in mol/mol measured by the drone during the on-land cross-instrument comparison, compared to NO _x emissions measured by PEMS in the stack.	60
Figure 44. Map of the LNG Terminal with the marked locations of Jetty 1 where Case A was measured and Jetty 2 where Cases B and C were measured (Maps data: Google, ©2022, 2023 CNES / Airbus, Maxar Technologies).	61
Figure 45. Visualization of measured fugitive methane emissions while three different vessels were present for bunkering operations at two jetties of the LNG terminal. The visualized emission rates are combined emissions from the measurement scene.....	62
Figure B1. Ship-level methane slip from all engine sources (g/kWh).	75
Figure B2. Boxplot of ship-level methane slip for ships with LPDF 2-stroke main engines and LPDF 4-stroke auxiliary engines (L2L4) and ships with only LPDF 4-stroke engines (L4) in g/kWh.....	76
Figure B3. Methane slip (g/kWh) versus combine main engine load.	76
Figure B4. Methane slip (g/kWh) by engine load for ships that have only one LPDF 4-stroke main engine, with build year of the ship indicated.	77
Figure B5. Methane slip (g/kWh) versus NO _x	77
Figure B6. Sensitivity analysis: Methane slip estimates (g/kWh) with and without adjusting for CO ₂ from fuel oil consumption from pilot fuel or for two-stroke dual-fuel engines in diesel mode.	78
Figure B7. Sensitivity analysis: Methane slip results (g/kWh) for L2L4 and L4 ships with and without adjusting for CO ₂ from fuel oil consumption from pilot fuel or for two-stroke dual-fuel engines operating in diesel mode.	78

LIST OF TABLES

Table 1. Marine gas engine designs.	2
Table 2. Default methane slip emission factors used in IMO and EU policymaking.	7
Table 3. Main specifications of the ship.	16
Table 4. Overview of specifications of the ship's propulsion and power system.	17
Table 5. Overview of specifications of the fuels as delivered to the ship and as copied from the bunker delivery notes.	17
Table 6. Schedule of the onboard test campaign.	20
Table 7. Pilot fuel consumption equation parameters.	24
Table 8. Specific LNG fuel consumption assumptions.	24
Table 9. Input parameters for calculating uncertainty of estimated methane slip.	26
Table 10. Tests to compare the drone measurements and in-stack measurements of methane emissions from one LPDF 4-stroke main engine. The other main engines and boilers were shut down during these tests.	45
Table 11. Results over the D2 cycle modes and the weighted result of NO _x and CH ₄ emissions and methane slip for the D2 and E2 cycle.	53
Table 12. Summary of the measured emission rates from bunkering operations.	63
Table 13. Estimated fraction of the LNG cargo lost as fugitive methane emissions during unloading operations.	64
Table A1. Energy demand assumptions for auxiliary engines.	74

INTRODUCTION

The Fugitive and Unburned Methane Emissions from Ships (FUMES) project is a collaboration between the International Council on Clean Transportation (ICCT), the measurement data service provider Explicit ApS, and the Netherlands Organization for Applied Scientific Research (TNO). Together, we conducted emission measurement campaigns using three different approaches: plume, onboard, and fugitive. During the plume campaign, we measured methane in 45 plumes from 34 ships fueled with liquefied natural gas (LNG) that were operating under real-world conditions. We used drones and helicopters to sample methane (CH_4) in exhaust plumes for ships sailing near the coasts of the Netherlands, Denmark, Belgium, and Australia over the course of 2022. In our onboard campaign, we measured methane directly in the exhaust stack, as well as in the plume, from an LNG-fueled ferry sailing between Finland and Sweden in Spring 2023. During our fugitive campaign, we used a novel approach to quantify the rate of methane emissions from three LNG tankers while they were unloading cargo at a European LNG terminal in September 2022. For the plume and onboard campaigns, we also measured emissions of nitrogen oxides (NO_x). Our goal is to add to the body of literature on methane slip (unburned methane in ship exhaust) and fugitive methane emissions (methane leaks from LNG infrastructure), and to inform ongoing policy deliberations at the International Maritime Organization (IMO) and in the European Union on how to develop and enforce regulations that reduce methane and NO_x emissions.

This report is organized as follows: We begin with background information on the use of LNG as a marine fuel and how it has developed over the last decade. We then review the literature on measuring emissions from LNG-fueled engines. The methods section describes the methods and instrumentation used to measure and estimate methane and NO_x emissions from the plume, onboard, and fugitive campaigns. A cross-instrument comparison of the drone and in-stack methods was conducted, and the test setup for this comparison is described in the methods. The methods section also explains how we translated methane and NO_x concentrations in the samples into methane slip and NO_x emissions rates. A results and discussion section follows, which is divided into four parts. The first part covers the plume campaign, where we measured methane and NO_x using drones and helicopters. The second covers the onboard campaign, where we measured the same LNG-fueled ferry using both a drone and in-stack sensors. The third covers the on-land cross-instrument comparison between in-stack measurements and drone measurements. The fourth covers the fugitive campaign, where we used drone measurements to estimate methane emissions rates when LNG carriers were unloading LNG cargo. We then describe the limitations of our study and what it means for future work. Policy recommendations that flow from the results of this study are then presented. Lastly, we draw conclusions based on the FUMES project results.

BACKGROUND

Methane contributes to climate change, and its global warming potential is especially strong in the first decades after it is emitted. Methane's 100-year global warming potential is nearly 30 times stronger than the same amount of carbon dioxide (CO₂), and the 20-year global warming potential is even stronger at 82.5 (Intergovernmental Panel on Climate Change, 2021). As of August 2023, there are approximately 960 ships that can operate on LNG with nearly 900 additional LNG-capable ships on order.⁴ This is up from approximately 350 ships in 2012 (Pavlenko et al., 2020). As of August 2023, by capacity (gross tonnage, GT), 5% of the entire existing shipping fleet and 38% of ships on order are LNG-capable; of these, 100% of LNG carriers, 46% of cruise ships, 37% of oil tankers, and 29% of container ships are LNG-capable.⁵

The use of LNG as a marine fuel is growing because it makes it easier to comply with existing international environmental regulations that limit the CO₂ intensity of new and existing ships, the sulfur content of marine fuels, and nitrogen oxide (NO_x) emissions. Using LNG emits approximately 25% less direct (tank-to-wake) CO₂ than conventional marine fuels; plus, LNG contains virtually no sulfur, and using it in low-pressure, dual fuel engines results in low NO_x emissions without the use of expensive exhaust gas aftertreatment technologies (Pavlenko et al., 2020). While LNG represented only about 3% of marine fuel use in 2018, the use of LNG marine fuel grew nearly 30% between 2012 and 2018, leading to an estimated 150% increase in methane emissions from international shipping over that period (Faber et al., 2020). Looking ahead, Comer et al. (2022) estimate global demand for LNG marine fuels will triple between 2019 and 2030.

The amount of methane emitted by LNG-fueled ships is a function of engine type, engine load, and fugitive emissions from fuel tanks and cargo tanks. Estimates of total methane emissions are uncertain because they rely on emission factors developed from the existing literature, which is comprised of a few studies focused on limited onboard or laboratory measurements of individual engines. Also, improvements in engine design over recent years may not be fully captured in the earlier studies. More data are needed to understand the actual methane emissions from LNG-fueled ships under real-world conditions. Furthermore, because LNG-fueled ships are capable of using both fossil and renewable fuels, understanding the conditions under which methane emissions are high or low becomes a key component in identifying a net-zero greenhouse (GHG) gas pathway for shipping (Comer et al., 2022).

LNG ENGINE TECHNOLOGIES

Stenersen and Thonstad (2017) and Ushakov et al. (2019) identify five different gas engine design concepts, which are summarized in Table 1.

Table 1. Marine gas engine designs.

Concept	Cycle	Abbreviation in this study	Speed range	Power range
Lean-burn spark ignition	2/4-stroke	LBSI	medium-high	0.5–8.0 MW
Low-pressure dual-fuel	4-stroke	LPDF 4-stroke	medium	1.0–18.0 MW
Low-pressure dual-fuel	2-stroke	LPDF 2-stroke	low	5.0–63.0 MW
High-pressure dual-fuel	4-stroke	N/A	medium	2.0–18.0 MW
High-pressure dual-fuel	2-stroke	HPDF 2-stroke	low	>2.5 MW

Note: High-pressure, dual fuel, 4-stroke engines are not commercially available.

⁴ Clarksons World Fleet Register, accessed August 29, 2023.

⁵ Clarksons Green Technology Uptake statistics, accessed August 29, 2023.

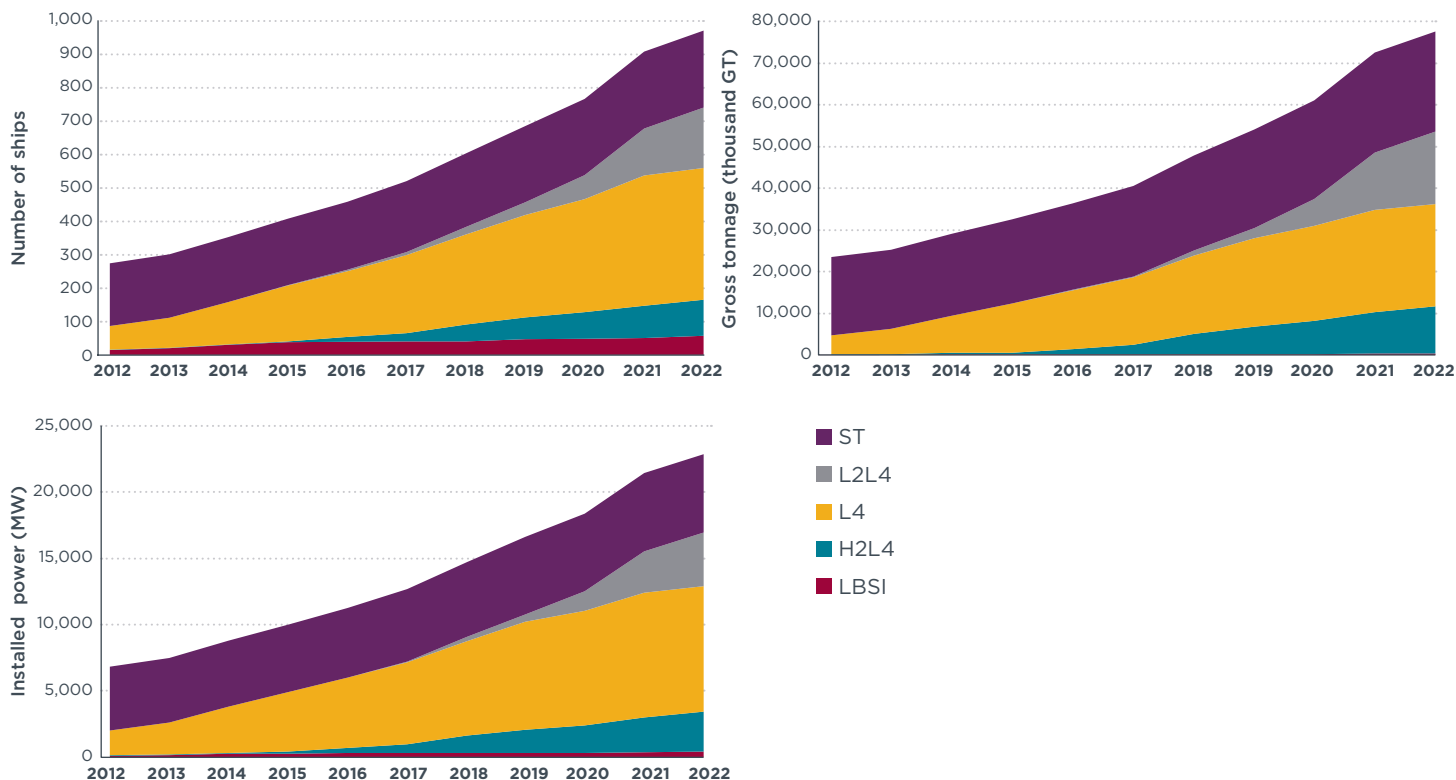
Natural gas has a low cetane number, meaning it has longer ignition delay than other fuels. Therefore, to combust the air-gas mixture in the cylinder, spark ignition, used in lean-burn spark ignition (LBSI) engines, or compression ignition with injection of a pilot fuel, used in low-pressure dual fuel (LPDF) and high-pressure dual fuel (HPDF) engines, is needed. Depending on the type of engine and the operating condition, the pilot fuel contributes between 1%–30% to the total heating value of the fuel in the cylinder. Newer engine models usually use lower amounts of pilot fuel than older engines. (cf. Corbin et al., 2020; Korakianitis et al., 2011; Stenersen & Thonstad, 2017).

These engine designs use the Otto cycle, mixing air and gas prior to the compression stroke, with the exception of the HPDF engines, where gas is injected via jets at the end of the compression stroke. There are two main reasons for methane slip in engines according to Stenersen and Thonstad (2017): dead volume in the combustion chamber and quenching at cold parts of the cylinder. In both cases, the local fuel-air mixture is not combusted completely due to an unfavorable composition of the charge or too low temperatures. Furthermore, a blow-through of methane might occur if the valve overlap time is too long (Stenersen & Thonstad, 2017). According to Stenersen and Thonstad (2017), ranking of the four designs from highest to lowest methane slip would be: LPDF 4-stroke, LBSI, LPDF 2-stroke, and HPDF.

LNG ENGINE INSTALLATION AND FUEL CONSUMPTION TRENDS

Between 2012 and 2018, methane emissions from ships grew 150% compared to a 10% increase in CO₂ emissions over the same period (Faber et al., 2020). Much of the increase in methane emissions is because ships use engines that emit unburned methane to the atmosphere. Figure 1 shows trends in LNG engine installations over time, based on IHS Markit data.⁶ Ships can have a combination of different LNG engine types onboard. In the figure and throughout the report, LBSI refers to ships with lean-burn spark ignition engines; H2L4 refers to ships with HPDF 2-stroke main engines with LPDF 4-stroke auxiliary engines; L4 refers to ships with LPDF 4-stroke for all engines; L2L4 refers to ships with LPDF 2-stroke main engines with LPDF 4-stroke auxiliary engines; and ST refers to ships with steam turbines. As shown in Figure 1, the number, gross tonnage, and installed engine power for STs has remained relatively stable over the last 10 years, whereas L4 ships have steadily grown, and H2L4 and L2L4 ships have increased rapidly. The number of LBSI ships account for a small share of the total. There is a transition away from STs, despite their negligible methane slip, because they are much less efficient than internal combustion engines (Pavlenko et al., 2020).

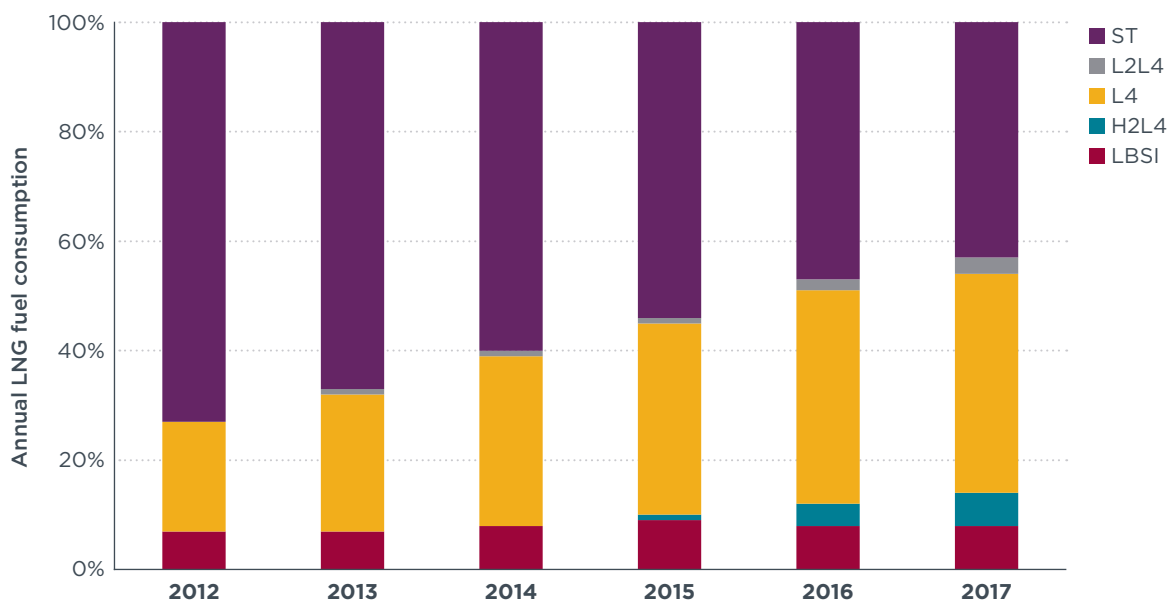
⁶ The ICCT has a bespoke ship characteristics database purchased from IHS Markit. More information on the IHS Markit data is available at <https://cdn.ihsmarkit.com/www/pdf/0920/Bespoke-Data-Solutions.pdf>.



LBSI is lean-burn spark ignition; H2L4 is high-pressure, dual-fuel, 2-stroke (HPDF 2-stroke) main engines with low-pressure, dual-fuel, 4-stroke (LPDF 4-stroke) auxiliary engines; L4 is LPDF 4-stroke for all engines; L2L4 is low-pressure, dual-fuel 2-stroke (LPDF 2-stroke) main engines with LPDF 4-stroke auxiliary engines; ST is steam turbine.

Figure 1. LNG-fueled fleet by number of ships, gross tonnage, and installed engine power, by ship type, for 2012–2022. Source: IHS Markit data as of July 2023.

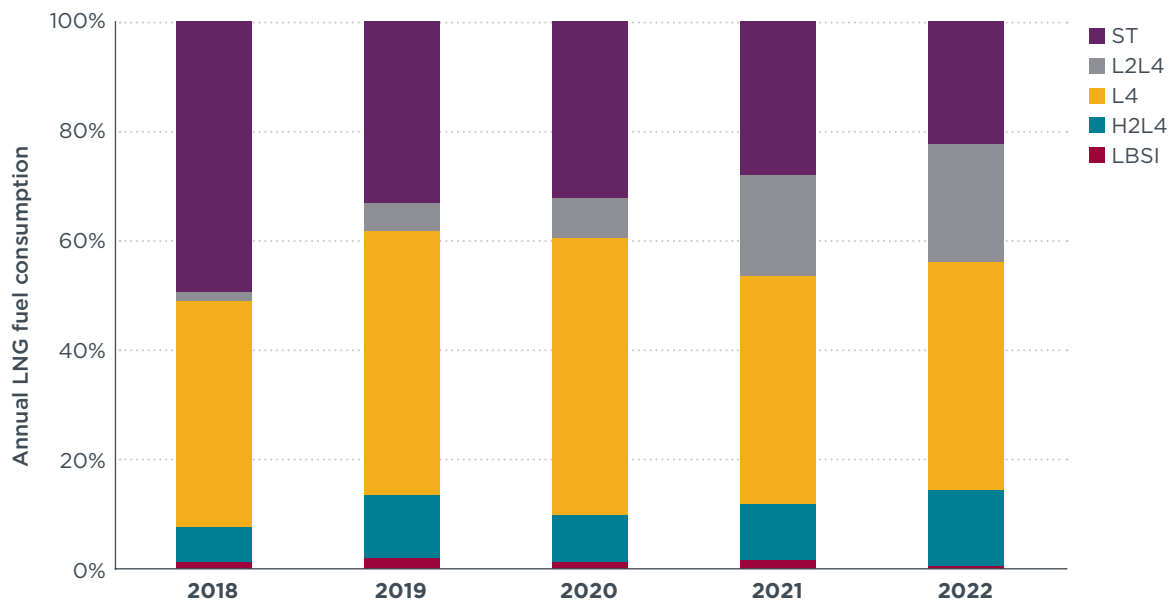
Figure 2 shows the proportion of LNG consumption by engine type, based on data from Faber et al. (2020). The share of fuel consumption by ST ships has decreased over time, in favor of dual-fuel internal combustion engines that are more efficient. There is a particularly pronounced growth in the use of LNG in L4 ships, doubling from 20% of fuel consumption in 2012 to 40% in 2017.



LBSI is lean-burn spark ignition; H2L4 is high-pressure, dual-fuel, 2-stroke (HPDF 2-stroke) main engines with low-pressure, dual-fuel, 4-stroke (LPDF 4-stroke) auxiliary engines; L4 is LPDF 4-stroke for all engines; L2L4 is low-pressure, dual-fuel 2-stroke (LPDF 2-stroke) main engines with LPDF 4-stroke auxiliary engines; ST is steam turbine.

Figure 2. Global LNG fuel consumption by main engine types, 2012–2017. Source: Faber et al. (2020).

This global trend is also reflected in the EU Monitoring Reporting and Verification dataset, which reports fuel consumption by ships on voyages to, from, or between EU ports (Figure 3).⁷ In 2018, ST ships comprised half of LNG fuel consumption and L4 ships represented more than 40%. By 2022, L4 ships were still responsible for around 40% of the total but ST ships only accounted for 22%, as other engine types, like H2L4 and especially L2L4, were responsible for an increasingly large share of fuel consumption. The share of LNG fuel consumption by H2L4 ships grew from 6% in 2018 to 14% in 2022. Meanwhile, L2L4 ships grew tenfold between 2018 and 2022, increasing from just 2% of LNG fuel consumption in 2018 to 21% in 2022.

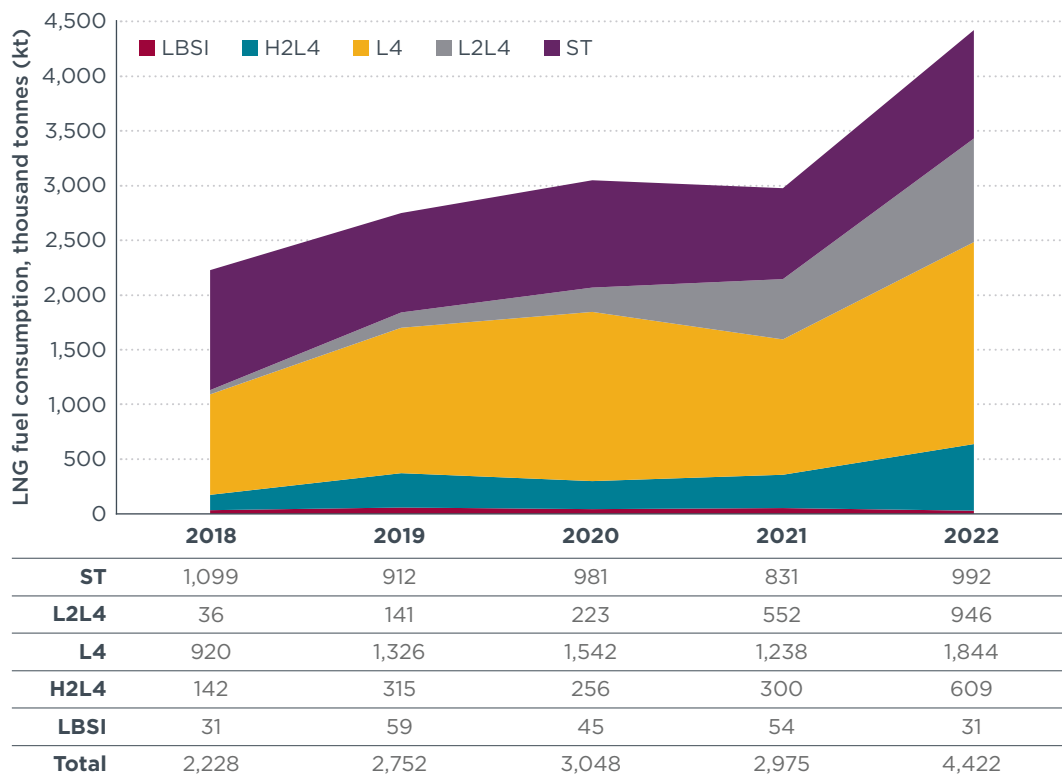


LBSI is lean-burn spark ignition; H2L4 is high-pressure, dual-fuel, 2-stroke (HPDF 2-stroke) main engines with low-pressure, dual-fuel, 4-stroke (LPDF 4-stroke) auxiliary engines; L4 is LPDF 4-stroke for all engines; L2L4 is low-pressure, dual-fuel 2-stroke (LPDF 2-stroke) main engines with LPDF 4-stroke auxiliary engines; ST is steam turbine.

Figure 3. Proportion of LNG fuel consumption by ships reporting to the EU Monitoring Reporting and Verification program, by engine type, 2018–2022. Source: Fuel consumption data from the EU Monitoring Reporting and Verification system paired with engine information from the ICCT’s SAVE model (Olmer et al., 2017).

Total LNG fuel consumption has doubled from 2.2 million tonnes in 2018 to 4.4 million tonnes in 2022, as shown in Figure 4. The total amount of LNG consumed in ST engines is stable over time, at about 1 million tonnes per year, and the use of LNG in LBSI engines is insignificant. Therefore, the growth in the use of LNG as a marine fuel has been driven by new ships with dual-fuel engines. The use of LNG in L4 ships doubled from 920 thousand tonnes (kt) in 2018 to 1,844 kt in 2022. Meanwhile, there was a fourfold increase in LNG use by H2L4 ships, from 142 kt in 2018 to 609 kt in 2022, and a twenty-six-fold increase for L2L4 ships, from 36 kt in 2018 to nearly 1 million tonnes in 2022. Overall, engines with low-pressure LNG injection are dominant over engines with high-pressure injection.

⁷ Available for download at <https://mrv.emsa.europa.eu/#public/emission-report>. Versions used to produce the figure are as follows: 2018 v269; 2019 v215; 2020 v191; 2021 v170; 2022 v51.



LBSI is lean-burn spark ignition; H2L4 is high-pressure, dual-fuel, 2-stroke (HPDF 2-stroke) main engines with low-pressure, dual-fuel, 4-stroke (LPDF 4-stroke) auxiliary engines; L4 is LPDF 4-stroke for all engines; L2L4 is low-pressure, dual-fuel 2-stroke (LPDF 2-stroke) main engines with LPDF 4-stroke auxiliary engines; ST is steam turbine.

Figure 4. Total LNG fuel consumption by ships reporting to the EU Monitoring, Reporting, and Verification program, by engine type, 2018–2022. Source: EU MRV fuel consumption data paired with engine information from the ICCT’s SAVE model (Olmer et al., 2017).

POLICY

The IMO has implemented several regulations in recent years to control shipping emissions and their subsequent negative impacts on the environment. For example, to regulate sulfur oxide (SO_x) emissions, the IMO has approved several Emission Control Areas (ECAs) with a fuel sulfur cap of 0.1% and imposed a global fuel sulfur cap of 0.5% that came into effect in 2020. Additionally, tiered NO_x emission limits have been imposed by the IMO, ranging from 2.0–3.4 g/kWh within ECAs to 7.7–14.4 g/kWh for ships operating outside of such zones (Zhao et al., 2021; IMO, 2019).

The IMO does not currently regulate methane. However, researchers and advocates have proposed several ways to include CH₄ in regulations (Laskar & Giang, 2023; Maersk Mc-Kinney Møller Center for Zero Carbon Shipping, 2022; Republic of Korea, 2022; Stamatis, 2021):

- » Including methane slip in IMO’s guidelines on life cycle GHG intensity of marine fuels (LCA guidelines), which are currently being developed;
- » Including methane in future phases of Energy Efficiency Design Index (EEDI) (ISWG-GHG 7/3 and MEPC 75/7/10); and
- » Measuring methane slip during parent engine certification.

The EU’s “Fit-for-55” package aims to reduce the region’s economy-wide net GHG emissions by 55% by 2030 compared to 1990 levels. Methane emissions from ships have been incorporated into these targets through various measures (Bernard, 2023; DNV, 2023; European Parliament and the Council of the European Union, 2023;

Gozillon, 2022; Maersk Mc-Kinney Møller Center for Zero Carbon Shipping, 2022; Olczak et al., 2022):

- » By December 31, 2024, the EU Commission will assess the impact on the global climate of GHGs other than CO₂, including CH₄, N₂O, and particles with a global warming potential, from ships arriving at or departing from EU ports.
- » By December 31, 2025, the EU Commission is required to set a binding 2030 methane emissions reduction target covering all relevant sectors, including maritime.
- » Methane slip has been included in the FuelEU Maritime regulation. This regulation will limit well-to-wake CO₂e emissions from ships starting from 2025.
- » Starting in 2024, CH₄ and N₂O emissions from ships are included in the EU Monitoring, Reporting, and Verification regulation, which applies to ships above 5,000 gross tonnage (GT) on voyages to, from, or between EU ports.
- » The shipping sector is covered under the EU Emission Trading System (ETS) starting in 2024. While initially it will only cover CO₂ emissions, starting in 2026, CH₄ and N₂O emissions will also be included within the EU ETS.
- » By January 1, 2025, EU Member States are required to make an “appropriate number” of LNG refueling points available in major EU ports under the Alternative Fuels Infrastructure Regulation (AFIR). In this case, the regulation may increase fugitive methane emissions.

Table 2 summarizes the default methane slip emission factors used in IMO and EU policymaking. The IMO values are derived from Faber et al. (2020) and have been included in the IMO’s LCA Guidelines that were adopted in July 2023 (International Maritime Organization, 2023). These guidelines contain initial emission factors for various fuel and engine combinations, including methane slip from LNG-fueled marine engines. These factors are being refined by an IMO Correspondence Group. Ultimately, the IMO will amend the LCA Guidelines to include default (rather than initial) emission factors. Potential default emission factors will first be considered at IMO’s 81st Marine Environment Protection Committee meeting in 2024. The EU values are contained in Annex II of Regulation (EU) 2023/1805 of the European Parliament and of the Council of 13 September 2023 on the use of renewable and low-carbon fuels in maritime transport, and amending Directive 2009/16/EC, i.e., the FuelEU Maritime regulation (European Parliament and the Council of the European Union, 2023).

Table 2. Default methane slip emission factors used in IMO and EU policymaking.

Engine	IMO	EU
LPDF 4-stroke	3.5%	3.1%
LPDF 2-stroke	1.7%	1.7%
HPDF 2-stroke	0.15%	0.2%
LBSI	2.6%	2.6%

To comply with these regulations, fossil LNG may be gradually replaced by renewable liquefied methane. Comer et al. (2022) showed that unless methane slip from marine engines is reduced, even using renewable LNG can result in growing methane emissions from ships over time as demand for LNG increases. Methane slip will make it more difficult for LNG-fueled ships to comply with regulations that limit the GHG intensity of marine fuels, and it will make it more expensive to comply with economic measures that put a price on GHG emissions, such as the EU ETS and any economic element included in the IMO’s mid-term GHG measures that could enter into force as early as 2027.

LITERATURE REVIEW

This section reviews the literature related to emissions from LNG-fueled engines. We begin with studies conducted in the laboratory or onboard that measured methane emissions from ships; we also include studies that review those measurements. We then summarize studies that measured methane from ships using remote sensing technology. Next, we discuss the literature which provides ways to reduce methane emissions from LNG-fueled ships. Lastly, we provide an overview of the literature on the air pollution impacts of using LNG as a marine fuel, with a focus on NO_x.

LABORATORY, ONBOARD, AND REVIEW STUDIES OF METHANE EMISSIONS FROM SHIPS

Several studies have measured methane slip from LNG-fueled marine engines (Anderson, Salo, & Fridell, 2015; Grönholm et al., 2021; Peng et al., 2020; Rochussen et al., 2023; Sommer et al., 2019; Stenersen & Thonstad, 2017). Others have investigated fugitive emissions from leaks and venting onboard (Balcombe et al., 2022). The effects on methane slip from new engine combustion concepts has also been studied (Lehtoranta et al., 2023). Broadly, the studies found that LPDF 4-stroke engines emit the greatest amount of methane slip, followed by LBSI and LPDF 2-stroke engines, according to independent testing and engine manufacturer data. In addition, HPDF 2-stroke engines emit very low amounts of methane slip, according to engine manufacturer data. The works also determined that methane slip increases as engine load decreases; this trend is especially pronounced for LPDF 4-stroke engines.

Stenersen and Thonstad (2017) from SINTEF published a report on methane slip from (at the time) state-of-the-art of marine gas engine technology, which was also summarized by Ushakov et al. (2019). The authors conducted a measurement campaign on six ships and one testbed engine. In addition, recent data of two more ships was included in the analysis. Nine measurements of LBSI engines and seven measurements of LPDF 4-stroke engines (two by SINTEF; five by the engine manufacturer) were included in the study. The authors found a considerable reduction in the emissions of NO_x and CO₂ compared to diesel engines, but LNG-fueled engines had higher total hydrocarbons and CH₄ emissions. Based on the results, new methane slip factors of 2.32% for LBSI engines and 4.01% for LPDF 4-stroke engines were proposed (Stenersen & Thonstad, 2017, p. 6). These were significantly lower compared to previous results in Nielsen and Stenersen (2010). NO_x emission factors were suggested as 0.9 g/kWh for LBSI and 1.9 g/kWh for LPDF 4-stroke.

Pavlenko et al. (2020) estimated methane slip emission factors for marine engines over the E2/E3 test cycle based on the work of Stenersen and Thonstad (2017), Ushakov et al. (2019), Sommer et al. (2019), Thinkstep (2019), and several additional researchers.⁸ They estimated the following methane slip for each engine technology: 5.5 g/kWh for LPDF 4-stroke, equivalent to 3.5% methane slip; 4.1 g/kWh (2.6%) for LBSI; 2.5 g/kWh (1.7%) for LPDF 2-stroke; and 0.20 g/kWh (0.15%) for HPDF 2-stroke. These emission factors were subsequently used by Faber et al. (2020) and are currently being used as the initial factors in IMO's LCA Guidelines adopted at MEPC 80 in July 2023.

Peng et al. (2020) measured a roll-on/roll-off ferry in North America in 2019 with LPDF 4-stroke engines. They measured an average methane slip of 11.5 g/kWh based on the engine's actual operational load profile, compared to 6.6 g/kWh using the weighting factors from the E2 test cycle. The same ship was measured again by Rochussen et al. (2023) after the shipowners had implemented GHG reduction measures, which included deactivating one or more cylinders depending on load, employing closed loop

⁸ See Appendix B of Pavlenko et al. (2020) for a detailed explanation of the sources used to develop each emission factor.

combustion phasing control, revising charge air pressure mapping, and implementing a lower air-fuel ratio. Rochussen et al. (2023) estimated the engine can achieve methane slip of 3.9 g/kWh based on the engine's actual operational load profile or 4.2 g/kWh on the E2 test cycle. This demonstrated that actions can be taken to modify existing, in-use engines to reduce methane slip.

Schuller et al. (2021) from the research group Sphera (formerly Thinkstep) estimated methane slip on the E2/E3 test cycle for marine engine technologies based on recent engine manufacturer data. They arrived at the following methane slip values: 3.98 (2.6%) for LPDF 4-stroke; 2.14 (1.5%) for LPDF 2-stroke; 2.00 (1.3%) for LBSI; and 0.23 (0.17%) for HPDF 2-stroke. The LPDF 4-stroke and LBSI emission factors are toward the lower end of those found in the literature.

The Maersk Mc-Kinney Møller Center for Zero Carbon Shipping (2022) defined representative methane slip for new dual-fuel engines based on engine manufacturer data. LPDF 4-stroke engines had the highest CH₄ slip, varying between 1.5% and 3.3% for engine loads above 50%. LPDF 2-stroke engines without exhaust gas recirculation (EGR) ranged from 1.1% to 1.4% methane slip at engine loads between 85% and 25%. LPDF 2-stroke engines with EGR ranged from 0.8% to 1.0% methane slip for the same engine load ranges. HPDF 2-stroke engines showed very low methane slip of approximately 0.19%. These results are based upon testbed data for engines operated under controlled and stable conditions. The conditions under vessel operations are more dynamic and variable, which can result in higher CH₄ emissions compared to testbed measurements.

Balcombe et al. (2022) studied methane slip onboard an LNG carrier on a month-long, round-trip voyage between the United States and Belgium. The researchers measured methane slip from the engines, as well as fugitive and venting emissions. The ship used two LPDF 2-stroke main engines and four LPDF 4-stroke auxiliary engines. Each main engine had a power output of 11,530 kW. Two auxiliary engines (G1 and G4) had a power output of 3,840 kW and the other two (G2 and G3) had a power output of 2,880 kW. During the voyage, 68 tons of CH₄ and 4,600 tons of CO₂ were emitted. The LPDF 4-stroke auxiliary engines produced nearly 60% of total CH₄ emissions, and the main engines contributed 39%. Methane emissions from venting and fugitive emissions contributed only a small proportion of total emissions, at about 0.23%. The two main engines showed average slip rates of 2.3% and 1.9%. Higher methane slip was observed from the LPDF 4-stroke auxiliary engines. Engines G1 and G3, which operated 96% and 97% of the time, respectively, averaged 7.9% and 8.5% methane slip. Engines G2 and G4, which operated 14% and 5% of the time, respectively, had average methane slip rates of 12% and 16%. Engine G4, which had 16% methane slip, had about twice as much methane slip as G1 (7.9%), despite being the same engine model and power rating. The relationship between methane slip and engine load (higher slip at lower loads) was more pronounced for the LPDF 4-stroke auxiliary engines compared with the LPDF 2-stroke main engines. Across all main and auxiliary engines, the average ship-level methane slip was 3.8%, which equaled 0.1% of the delivered LNG.

Kuittinen et al. (2023) provided a review of the published literature on methane slip by engine type and engine load, complemented by the latest ship owner data covering measurements for LBSI, LPDF 2-stroke, LPDF 4-stroke, and HPDF engines. For HPDF engines, the methane slip emission factor was reported to be low, ranging from 0.2–0.3 g/kWh, while LBSI engines manufactured between 2010 and 2015 showed methane slip ranging from 2.1–25.5 g/kWh at engine loads between 100%–25%. For the newest LPDF 4-stroke engines manufactured between 2020–2022, methane slip measured on the testbed was found to vary between 2.6–4.1 g/kWh at 100%–75% load and 6.6–13.05 g/kWh at 25% load. Methane slip had greater variation and higher maximum when measured onboard, at 1.9–6.4 g/kWh for 100%–75% load and 70 g/kWh with 25% load.

LPDF 2-stroke engines manufactured between 2019 and 2022 had methane slip ranging from 1.9–7.2 g/kWh between 100%–25% load. Onboard and testbed measurements of LPDF 2-stroke engines showed similar results.

The work of Lehtoranta et al. (2023) is of particular interest for this study because the measurements were carried out on the same ship as our onboard campaign, and the results are compared in the onboard campaign section of this report. In Lehtoranta et al. (2023), emissions of CH₄, CO₂, CO, NO_x, formaldehyde (HCHO), and particle number (PN) of two 4-stroke LPDF engines were measured. One of the engines was fitted with a new combustion concept intended to reduce the methane slip (ME3), while the other engine was in the standard configuration (ME4). The researchers showed a clear trend of lower methane slip at higher engine loads for both engines. For ME4, methane slip ranged from around 3 g/kWh at high loads (≥75%) to more than 12 g/kWh at 10% load. For the ME3 engine, methane slip ranged from below 2 g/kWh at loads less than 75% to below 4 g/kWh at 10% load. Overall, the new combustion concept engine emitted 50%–65% lower methane slip than the standard engine setup for engine loads between 50%–90%. Both engines measured had lower CH₄ emissions compared to previous onboard measurement studies (Anderson et al., 2015; Balcombe et al., 2022; Corbin et al., 2020; Peng et al., 2020; Sommer et al., 2019; Ushakov et al., 2019). This came at the cost of elevated PN emissions.

REMOTE-SENSING MEASUREMENT OF METHANE

Remote measurement and monitoring techniques have been developed to research emissions from ships to assess compliance with regulations. There are two main approaches: measuring the emissions of passing ships with land-based equipment and the use of drones and aircraft. Beecken et al. (2019) reviewed the state of the art of remote measuring systems, the analysis of collected data, and the reporting of the results. Few studies have used remote sensing to measure methane emissions, and this report aims to add to the literature.

Grönholm et al. (2021) carried out research on the possibilities of ground-based measurements of maritime CH₄ emissions. Between 2015–2021 the $\Delta\text{CH}_4/\Delta\text{CO}_2$ ratio in parts per million (ppm) was measured by a remote measuring station located in the Baltic Sea. The peak values of $\Delta\text{CH}_4/\Delta\text{CO}_2$ ranged from 1%–9%, with a median of 3% for LPDF 4-stroke engines. For HPDF 2-stroke engines, $\Delta\text{CH}_4/\Delta\text{CO}_2$ ranged from 0.1%–0.5%. $\Delta\text{NO}_x/\Delta\text{CO}_2$ and varied between 0.5 parts per thousand and 8.7 parts per thousand, with an average of 4 parts per thousand; there was no significant difference between engine types. Based on the results, the authors proposed a not-to-exceed value of 1.4% for mass-based (not ppm) $\Delta\text{CH}_4/\Delta\text{CO}_2$ so that the 100-year climate forcing impacts of using LNG would not exceed that of using diesel engines.

The Danish company Explicit developed a method and a drone setup for measuring the emissions of ships by sampling their exhaust plumes (Patent No. EP3100022, US10416672, CN106170685, 2016). This method has been applied since 2016 in national and international monitoring programs (Explicit ApS, 2018; Knudsen et al., 2022). In this project, it is used to measure the CH₄-to-CO₂ ratios in the plumes of individual vessels to calculate methane slip. Another approach, the Drone Flux Measurement (DFM) method to quantify fugitive emissions, has successfully been used in several projects at various on- and offshore sources (De Rossi, 2021; De Rossi & Knudsen, 2022; Knudsen & De Rossi, 2022). The DFM method is used in this study to determine fugitive methane emissions during unloading operations of LNG tankers at an LNG terminal.

STRATEGIES TO REDUCE METHANE EMISSIONS

Strategies to reduce methane slip from marine engines fall into three categories: operational changes, engine modifications, and exhaust aftertreatment technologies.

Operational changes include efforts to run engines at higher engine loads, where methane slip is lower. This can include switching off engines so that the remaining engines operate at higher loads and plugging into shore power to eliminate at-berth methane emissions. Engine modifications include reducing crevices and pockets where gas can be trapped and not combusted, as well as reducing the size of the area between the piston head and the cylinder heads. One can also adjust the valve timing and when the fuel is injected, in addition to deactivating cylinders to maintain a higher effective engine load. Aftertreatment technologies include EGR, methane oxidation catalysts (MOCs), and plasma reduction systems (PRSs).

Overall, the literature suggests that operational changes are the easiest way to reduce methane slip, and they can be quite effective. There is a wide baseline range to consider, but researchers report that a 50% reduction in methane slip is possible using operational strategies to reduce low-load operations. Engine modifications have also helped to reduce methane slip but they tend to occur as new engines are put on the market, although retrofits are possible. The use of aftertreatment technologies to control methane is rare and EGR, which is mainly used to reduce NO_x emissions, is the only technology that can be readily used today. EGR increases fuel consumption and increases engine wear but can reduce methane slip by 20%-50% according to the literature cited in this section. MOCs can be highly effective at reducing methane emissions (70%+ according to the literature cited in this section), but performance degrades over time and they face practical challenges, including sulfur contamination from pilot fuels and lubrication oils. Moreover, MOCs perform best at high exhaust temperatures that usually are not achieved by LPDF engines, which are the technology that has the greatest need for reducing methane slip. PRSs are not yet commercially available and their overall impacts on fuel consumption and total GHG emissions is not known.

Sommer et al. (2019) studied strategies to reduce methane slip from 4-stroke LPDF engines. During the project, a portable CH₄ sensor using wavelength modulation spectroscopy was developed and placed onboard to take in-stack measurements of CH₄ concentrations. They found that deactivating cylinders when the engine was operating at low-load conditions below 15% can substantially reduce methane slip. In addition, changing how the ship was operated to minimize low-load operations—including using only one engine more frequently and plugging into shore power—reduced methane slip even further. Using a combination of cylinder deactivation and operational changes, total methane emissions were reduced by 23%-33%. Based on these results, Sommer et al. (2019) modeled an ideal scenario that could result in up to a 60% reduction in total methane emissions.

A report issued by the Mærsk Mc-Kinney Møller Center for Zero Carbon Shipping (2022) summarized sources of methane emissions from vessels and technologies to reduce them. For HPDF 2-stroke engines, which already have low methane slip, any aftertreatment technology to further reduce methane slip would actually increase total GHG emissions. For LPDF 2-stroke engines, a combination of EGR and PRS can reduce methane slip but can also lead to an overall increase in GHG emissions. A new LPDF 2-stroke engine with EGR (and without PRS) is expected to emit about half as much methane slip as a first-generation LPDF 2-stroke engine with EGR. Laboratory tests yielded a 78% conversion rate of methane to CO and H₂O using PRS, and higher exhaust gas temperatures of about 150°C-400°C can further improve performance. However, using the PRS increases fuel consumption, which increases CO₂ emissions, in addition to the CO₂ generated by converting methane slip to CO₂. The effect on total GHG emissions is still unknown as the PRS technology is still under development and onboard validation is pending. For LPDF 4-stroke engines, MOC could reduce methane slip 70%-99%. However, MOCs require high exhaust gas temperatures of above 390°C. Since such high temperatures are usually not reached by 4-stroke engines downstream

of the turbocharger, further study of the technical feasibility of integrating the MOC upstream of the turbocharger is necessary. An additional barrier to using MOCs is sulfur contamination: low-sulfur pilot fuel and lubrication oil are required and sulfur traps could offer additional protection.

The performance of MOCs has also been studied by Lehtoranta et al. (2021), using an MOC in experiments in lean-burn conditions of LNG engines. Because even low concentrations of sulfur in the exhaust significantly reduces the efficiency of the catalyst, a regeneration cycle at stoichiometric conditions and a sulfur trap were part of the study. The authors concluded that MOC technology can reduce the methane slip by up to 70%–80%. This efficiency, however, decreases over time.

Carr et al. (2023) provided an overview of technological choices and operational measures for mitigating methane slip. Their study found in terms of operational measures, increasing engine loads can reduce methane slip by 50%, while also offering better fuel efficiency. This strategy works best for LPDF 4-stroke engines because larger 2-stroke engines show less variability in methane slip with engine load. Ships can also switch to diesel fuel when operating at lower engine loads; however, this increases air pollutant emissions, including NO_x , compared to LNG. With regards to engine-level modifications, minimizing empty combustion chamber volume in combination with early pilot fuel injection can lead to reduction in CH_4 slip by nearly 50%, but this would require retrofitting the engine. Another engine-level strategy referred to as skip-firing, or cylinder deactivation at low loads, can reduce methane slip by nearly 55%. Regarding the use of exhaust aftertreatment technologies, it was recognized that MOCs could reduce methane slip, especially at higher exhaust temperatures, but their use will require possible installation of sulfur traps. While technologies such as EGR could also reduce methane slip by up to 20% alongside NO_x emissions, their use leads to possible increase in carbon monoxide and black carbon emissions, while also increasing engine wear.

Rochussen et al. (2023) characterized tank-to-wake GHG (CH_4 and CO_2) emissions for two roll-on/roll-off cargo ferries operating LPDF 4-stroke engines. The first ship, built in 2016, can run on LNG or diesel fuel using Wärtsilä LPDF 4-stroke engines. The second ship, built in 2021, can run on LNG or diesel using MAN LPDF 4-stroke engines. Rochussen et al. (2023) estimated the GHG benefits of a new calibration strategy for the 2016 vessel, which included deactivating one more cylinders depending on load, closed loop combustion phasing control, revised mapping of charge air pressure, and a lower air-fuel ratio. This calibration strategy reduced methane slip by 24% for a one-way trip. Lesser methane slip reductions were achieved at very low loads of less than 20% due to higher air-fuel ratio; reducing the air-fuel ratio at low loads would likely necessitate further modifications in engine hardware. Combining the new engine calibration with better operating strategies such as single engine operation and shore power was found to reduce GHG emissions by 57% relative to stock LPDF calibration, with most of this reduction due to a decrease in unburned CH_4 emissions of 82%, while a GHG reduction of 24% was observed for this combination against diesel operation. Despite being 5 years newer, the CH_4 slip from the 2021 ferry was found to be similar to (and slightly higher than) that of the stock LPDF calibration of the 2016 ferry. The authors hypothesize that the 2021 ship could benefit from applying a similar reduction strategy as the 2016 ship. Finally, the authors emphasized the importance of developing emission inventories based on measured emission factors from typical vessel operations, as the E2 test-cycle would have underestimated methane slip from the 2016 ship by 74% based on Peng et al. (2020), whereas it would have overestimated methane slip by 8%–30% when the ship was implementing its new GHG reduction strategies.

AIR POLLUTION IMPACTS OF USING LNG AS A MARINE FUEL

Due to growing concerns surrounding the environmental impacts of pollutants like NO_x and particulate matter (PM), several studies have estimated the air pollution impacts of using LNG compared to conventional marine fuels. The research shows that using LNG results in lower NO_x and PM emissions compared with conventional fuels, but higher methane and CO, as well as more HCHO.

Anderson et al. (2015) measured emissions onboard a ferry in 2013 using LPDF 4-stroke engines. They found that NO_x, CO₂, and particle emissions were significantly lower when the ship was running on LNG compared to marine gas oil (MGO). Methane emissions were higher when running LNG due to a 7% methane slip, and CO emissions were also higher. Consequently, the authors identified measuring methane slip from dual-fuel engines as worthy of further investigation. Other studies also found that particle emissions are lower using gas instead of MGO. For example, Lehtoranta et al. (2019) showed that using compressed natural gas in a dual fuel engine can reduce PM levels by 63%–69% compared with MGO. Trivanovic et al. (2019) also discussed that while PM emissions from the use of LNG in dual-fuel engine system are low, they are not negligible and are most likely caused by the pilot fuel.

Peng et al. (2020) performed onboard measurements on a roll-on/roll-off ferry that used LPDF 4-stroke engines. They found lower emissions of PM, black carbon, NO_x, and CO₂ when the engine ran on LNG instead of diesel. As expected, emissions of CH₄ were much higher (11.5 g/kWh on average), and there were also higher levels of HCHO and CO. Corbin et al. (2020) measured PM onboard a ship using LPDF 4-stroke engines, with a particular focus on black carbon. They found that PM emissions were similar when the engine was idling on either LNG or diesel; they suggest that idling at low loads be avoided for this reason. However, PM emissions, including black carbon, were lower when operating LNG.

METHODS

This section describes the methods used for measuring methane and NO_x in the plume and in the stack; conducting an on-land cross-instrument comparison; estimating methane slip and NO_x emissions rates for the plume measurements; and estimating fugitive methane emissions for LNG cargo bunkering operations.

MEASURING METHANE AND NO_x EMISSIONS IN PLUMES

This section describes the methods used to remotely assess, via drones and helicopters, the ratios of CH₄ or NO_x to CO₂ for methane slip or NO_x emission calculations from ships.

Instrumentation

Measurements were conducted using Explicit's Mini-Sniffer systems, which contain sensor assemblies to extract air samples for analysis of the abundant mixing ratios of targeted species. Their compact dimensions and light weight allow for the use as payload on commercial drones (Beecken et al., 2019).

The applied Mini-Sniffer Units used in the FUMES project are in-house developments which are quality controlled by FORCE Technology, the Danish government reference laboratory for air emissions. Mini-Sniffers are equipped with sensors for the quantification of CO₂, SO₂, NO, and NO₂. The concentration of CO₂ is quantified based on non-dispersive infrared spectroscopy, while SO₂, NO, and NO₂ are measured using electrochemical cells. The Mini-Sniffer, as well as Explicit's patented method to measure emissions in ship plumes, is described in a report prepared for the Danish Environmental Protection Agency (Explicit ApS, 2018).

For the measurement of CH₄, the units were additionally equipped with a separate methane sensor using tunable diode laser spectrometry. The two primary measured species in the FUMES deployments are CH₄ and CO₂.

The overall response time is dominated by the CO₂ sensor, which showed the slowest response time with T₉₀ of about 20 s while the response time of the fastest sensor, the CH₄ sensor, is about 1.8 s. The sampling frequency of the overall system is 2 Hz. For evaluating methane slip, the respective concentrations are integrated over time for the duration of the plume sampling before the CH₄-to-CO₂ ratio is taken. This also compensates for the differences in the response times and yields an average ratio for the time of sampling.

For quality assurance, the Mini-Sniffer with the methane sensor was performance tested for linearity, cross-sensitivity, and other dependencies such as temperature, relative humidity, and drift over time by reference laboratories. FORCE Technology tested the mini-sniffers and conducted calibrations of new sensors before they were deployed. As the electrochemical sensors deteriorate non-linearly over time, they are regularly replaced. The performance tests showed that the lifetime of a sensor is at least 100 hours of operation. The CH₄ sensors were initially tested by FORCE Technology before deployment. A follow-up test of CH₄ sensors at the Swedish reference laboratory RI.SE confirmed the values from FORCE Technology after being deployed in the field.

The uncertainties of the provided CH₄ to CO₂ ratios were found to be around 15.1% based on the sensor characterization. In the case of the NO_x to CO₂ ratios, the uncertainty is around 18.7% using this method.

Principle of operation

Methane slip is calculated based on the CH₄ to CO₂ ratio measured in the exhaust plume of the ship. The applied principle is a patented method for the aerial monitoring

of sulfur emissions and other pollutants in IMO-designated ECAs (Patent No. EP3100022, US10416672, CN106170685, 2016).

The CH₄ to CO₂ ratio is assessed by individual simultaneous measurements of each of the two species within 25 to 100 meters of the stack using aerial Mini-Sniffer sensors onboard drones or helicopters.

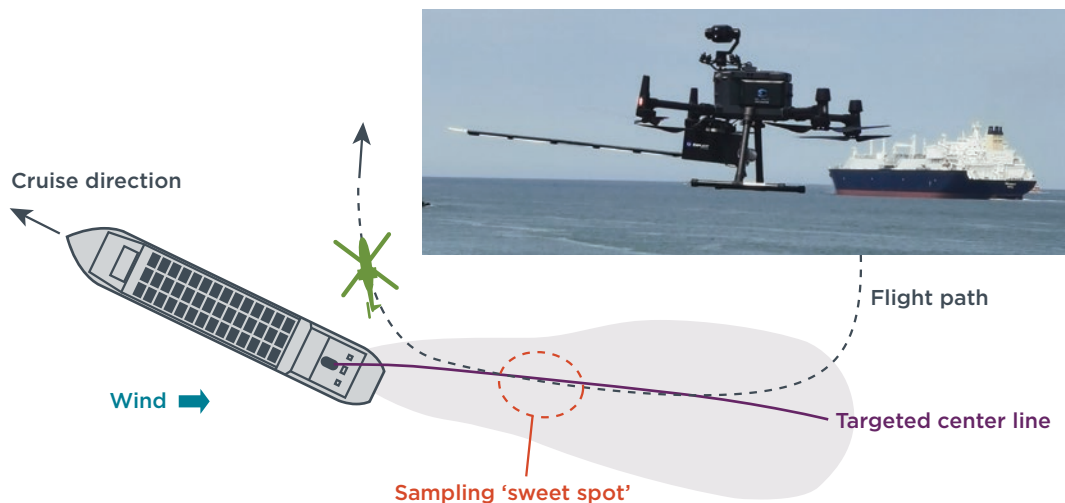


Figure 5. The photograph shows a drone equipped with a Mini-Sniffer payload for sampling volume mixing ratios of CH₄ and CO₂. The elongated nozzle at the front of the drone is the inlet nozzle for air samples. The sketch below illustrates the flight path of the aircraft for plume sampling. The “sweet spot” is a location within the plume where favorable concentration conditions are met. In the case of the applied Mini-Sniffers this is when the CO₂ concentration within the plume is about 200 ppm above the background concentration.

The sampling procedure for drones and crewed aircraft is illustrated in Figure 5. To obtain a sample, the aircraft approaches the target from downwind direction. During a measurement, a CO₂ concentration at about 200 ppm above background is targeted, which corresponds to a total concentration of around 600 ppm. Carbon dioxide is used as a guiding signal to indicate a favorable position within the plume for obtaining measurements. The other concentrations are measured at their then present abundancies. At the favorable position, the measured concentrations are typically at the required levels to reliably quantify them with respect to the sensors' measurement ranges and precisions. The aircraft remains in this spot for about 20–30 seconds to enhance the measurement quality before it leaves the plume to sample ambient air again. The sample inlet is positioned in such a way that it is not affected by the aircraft itself. The emission contribution from the ship is the difference between the concentrations of CH₄ and CO₂ within the plume and within the ambient air. Though the absolute concentrations of the targeted species reduce with increasing distance from the stack due to dilution of the exhaust plume, the ratio of these two gases remains stable in the mixed, turbulent plume that is emitted from stack. Two to three replications of each sample were attempted, but this was not feasible in all cases, particularly when operating the drone from shore due to requirements like the need for a line of sight.

The time stamped measurements from the gas sensors, the simultaneously recorded Global Navigational Satellite Systems (GNSS) data from the drone, and the received Automatic Identification Signals (AIS) data received from the ships in the vicinity were transmitted to a central cloud system which combines the data to determine the individual CH₄ to CO₂ ratios of the measured exhaust plumes. Emissions of NO and NO₂ are measured simultaneously and processed in a similar way. The total NO_x emission is calculated as the sum of these two nitrogen oxide species.

MEASURING CH₄ AND NO_x IN EXHAUST STACKS (ONBOARD)

To obtain real world emissions data from a ship running on LNG as its primary fuel, and to compare the methane slip emissions levels determined by drone measurements with an accurate reference, measurements of emissions levels were obtained onboard from the exhaust stack.

Ship and usage

The ship selected for the campaign was the Aurora Botnia, a modern roll-on/roll-off passenger ferry from Wasaline (Figure 6). The ship's specifications are included in Table 3. The Aurora Botnia transports passengers, cars, and lorries between Umeå, Sweden, and Vaasa, Finland, in a weekly fixed schedule with two to four return trips a day.



Figure 6. Aurora Botnia roll-on/roll-off passenger ferry that was measured during the onboard campaign.

Table 3. Main specifications of the ship.

Ship name, flag, owner	Aurora Botnia, Finland, Wasaline
IMO number	9878319
Keel laid	February 2020
Into service	August 2021
Type of ship	Ropax (Roll-on, roll-off passenger ferry)
Capacity (# passengers, lane length [m])	935, 1500
Dimensions [m] Length overall, beam, design draught	150, 26, 6.1
Maximum speed [knots] / [km/h]	20 / 37
Tonnage, gross / net / deadweight	24,036 / 7,264 / 3,500

Propulsion and engines

An overview of the ship's propulsion and power systems is provided in Table 4. The ship has a serial hybrid powertrain with two ABB electrical pulling thruster Azipods, a 2 megawatt-hour (MWh) battery stack, and four LPDF 4-stroke engines, each driving a generator. Battery power is used for port entry and departure, hotel load, and boost power. Batteries act as an accumulator between the provided generator power and power demand, which includes auxiliary power demand.

All four engines (ME1-4) are 8V31DF engines manufactured by Wärtsilä. ME3 is a development engine for Wärtsilä and has a technology package aimed primarily at reducing methane emissions. ME2 and ME3 have an SCR system, which are used when the engines are running on fuel oil.

LNG is stored under low pressure in two tanks, and the gas is heated and evaporated before being fed to the engines. An integrated gas valve unit controls the gas feed pressure according to engine load, ensures safe maintenance on the engine, and performs a leak test of the automatic shut of valves before operating on gas. The unit can be fed with inert nitrogen in case of hazard. Gas is transferred to the engine in a double-walled pipe. The space between the two pipes is ventilated, and leakage of the inner pipe can be detected in the ventilation flow of the outer pipe before the extraction fan. Crankcase gases are vented in the open air via a separate funnel where there are also pipes to release boil-off gas.

Table 4. Overview of specifications of the ship's propulsion and power system.

Configuration	Diesel-electric (Serial hybrid electrical with LPDF 4-stroke engines)
Engines	4x Wärtsilä 8v31DF V8 engines (LPDF 4-stroke) 4800kW rated power @ 750 rpm
Propulsion	2x ABB Azipod Pulling thrusters, 5.8 MW each 2x Wärtsilä transverse (bow) thrusters WE TECH Hybrid system
Battery	2 MWh
Generator	WEG
Fuel system	Dual fuel oil/gas with integrated gas valve unit. 2x Wärtsilä LNGPacs with IMO Type C LNG fuel tanks
Emissions control	Engines are IMO Tier II certified in liquid fuel mode and Tier III certified in gas fuel mode. The two main engines with SCR are certified to Tier III in gas and liquid modes.

Fuel

The ship has four main engines that can run in single fuel mode using fuel oil or in dual fuel mode using LNG plus marine diesel oil (MDO) as pilot fuel. Table 5 gives an overview of the fuel specifications.

Table 5. Overview of specifications of the fuels as delivered to the ship and as copied from the bunker delivery notes.

	MDO	LNG 26 May 2023	LNG 31 May Truck 1	LNG 31 May Truck 2
Density (kg/m³)		441	443	445
Density (kg/m³) at 15 °C	872			
Delivery (kg)	39,108	21,680	21,580	21,740
LHV (MWh)		299	295	297
LHV (MJ/kg)	42.58	49.62	49.19	49.16
Methane (mol-%)		96	94	94
Ethane (mol-%)		4	5	4.93
Propane (mol-%)		0.434	0.706	0.679
Remainder (mol-%)		<0.1	<0.1	<0.1
Sulfur (wt-%)	0.02			
Carbon (wt-%)	86.5			
Fuel carbon dioxide intensity (g CO₂/g fuel) calculated using above alkane mol-%.		2.76	2.77	2.77

Measurements

The main goal of the tests was to determine the methane slip levels of the LPDF 4-stroke engines in the stack and in the plume and to compare the results. The program consisted of three steps:

1. Commissioning: In addition to setup and checking the equipment, we confirmed the availability of data from the ship.
2. Drone comparison: We performed several tests with fixed engine loads done simultaneously, measuring exhaust gas concentrations in the stack and in the plume with the drone.
3. Engine real sailing conditions: Tests were performed with several load points and at different engine running conditions. The D2 test cycle was used for constant-speed measurements. In addition, emissions were sampled during a whole trip.

In-stack measurement

The testing setup is shown in Figure 7. A Gaset DX4000 FTIR (Fourier-transform infrared spectroscopy) and Horiba PEMS (Portable Emissions Measurement System) OBS-One GS were selected to measure the concentrations of gases in the exhaust in the stack of two of the four main engines. The FTIR was adjusted to measure CH₄, CO₂, water (H₂O), CO, ethane (C₂H₆), propane (C₃H₈), and HCHO. Oxygen (O₂) was measured with a separate zirconia-based sensor in the pump unit. The Horiba OBS-One PEMS uses different measurement techniques: Flame Ionization Detection to measure total hydrocarbons (THC); Non-Dispersive Infrared to measure CO and CO₂; and heated chemiluminescence detector (CLD) to measure NO and NO₂. Each engine has a socket located after the turbine in the exhaust pipe which can be used to sample exhaust gas. For the FTIR a PSP4000 probe (180°C) and a heated sample line were used. The FTIR was checked prior to the program in the lab with a mixture of calibration gases with known concentrations (N₂, O₂, water vapor, CH₄, and CO₂). The mixing was done using mass flow controllers in a lab set-up. At-site on the ship, nitrogen was used for zeroing and class 4.0 (99.99%) CO₂ was used for the leak checks.



Figure 7. Left: heated probe sampling hot gas from the exhaust after the turbine of main engine 4. Right: the FTIR instrument used to measure the concentrations of CO₂, CH₄, and NO_x (NO+NO₂).

During the installation of the instruments, the control module of the PEMS did not start and, with internal checks, no cause could be found at site. This rendered the instrument useless for the duration of the measuring period. The FTIR was used stand-alone to measure the concentrations of CH₄, C₂H₆, C₃H₈, CO, CO₂, O₂, NO, NO₂, and HCHO. A Testo 350 was used in series, connected to the exhaust of the FTIR, to check the measured CO₂ and NO_x concentrations of the FTIR in the stack.

Engine and ship data

To calculate mass emissions and work-specific emissions from measured concentrations using the carbon balance method, data broadcasted by the engine control unit was used. Screens in the ship control room (Figure 8) show the actual engine speed, power, main fuel consumption, pilot fuel consumption, intake pressures and temperatures, as well as ship speed, draught, wind direction, and current. Trends of engine parameters over time can be visualized and signals can be averaged over selected periods. The trends could be printed but not extracted as data-files.

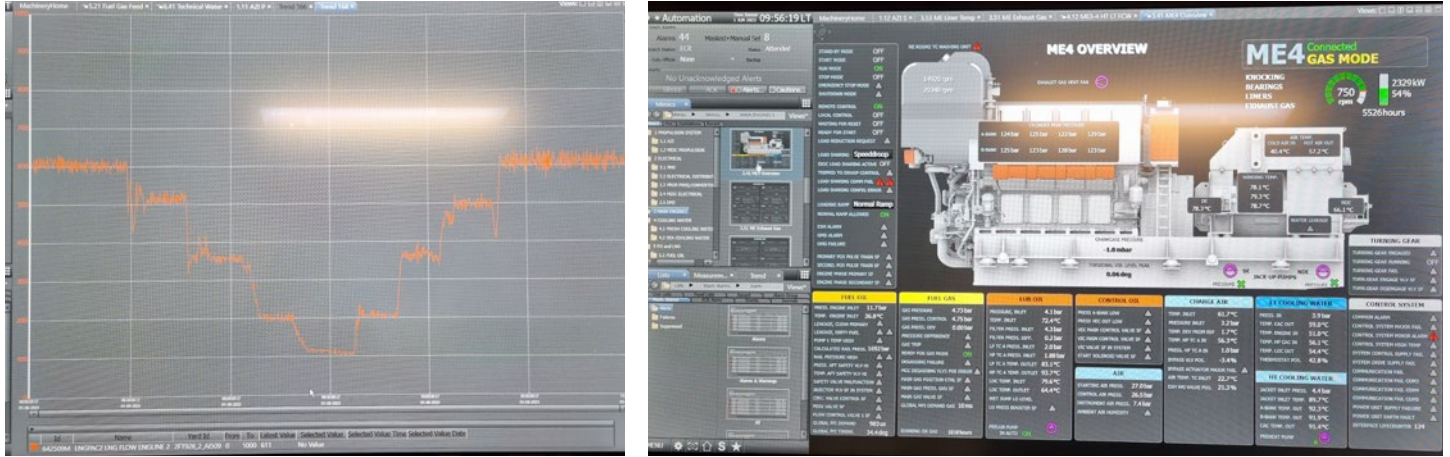


Figure 8. Left: screen of main engine 4 power output over a selected time frame. Right: screen mode showing engine parameters.

Drone measurement

Figure 9 shows the stack arrangement at the Aurora Botnia: one for each of the four main engines and two for the fuel-fired boilers (not well visible in this picture). The high funnel in front contains the boil-off and crankcase gas venting pipes. During measurement, the drone flies downwind in the exhaust plume to sample diluted gas. The plume is located by observing a display on the drone's control device which shows the actual CO_2 , NO_x , and CH_4 concentrations. As part of the sampling procedure, the measurements before and after sampling the plume were conducted in ambient air to define the respective background concentrations.



Figure 9. Drone flight measuring CH_4 , NO_x and CO_2 concentrations in the exhaust plume of the Aurora Botnia when only main engine 4 was running. Fuel-fired boilers are switched off. The stacks are the stacks of the four main engines and two fuel-fired boilers. The high funnel in front contains the boil-off and crankcase gas venting pipes.

Test schedule

Table 6 shows the schedule of the program as executed on the Aurora Botnia.

Table 6. Schedule of the onboard test campaign.

Date [dd.mm.yyyy]	Part of test program	Weather conditions (wind speed [km/h] and direction, ambient pressure [mbar], temperature [°C], RH [%])
30.05.2023	Boarding, installation equipment	
31.05.2023	Commissioning equipment	
31.05.2023	Switching to LNG (low tank level and pressure)	
31.05.2023	Drone, in-stack load points	16, WNW, 1009, 10, 50
31.05.2023	Bunkering LNG (truck 1 and 2)	
01.06.2023	D2 load points	24, NNW, 1010, 7, 52
01.06.2023	Drone, in-stack load points	21, NNW, 1010, 7, 48
01.06.2023	Whole trip Umeå-Vaasa	21, NNW, 1010, 7, 48
01.06.2023	Drone, in-stack load points	22, NW, 1012, 6, 88%
02.06.2023	De-installation equipment, disembarking	

CROSS-INSTRUMENT COMPARISON (ON-LAND)

A land-based cross-instrument comparison was carried out to compare the CH₄ to CO₂ concentration ratios measured by the drone in the exhaust gas plume to an accurate reference measurement of the concentrations in the stack. This set-up ensures that the comparison can be made across the whole range of CH₄ to CO₂ ratios which can be measured in the plumes. The comparison was conducted prior to the onboard campaign.

The test setup is depicted in Figure 10 and Figure 11. It consisted of a diesel-fueled generating set which served as the source of exhaust gas emitted to the air and mass flow controllers which controlled different known quantities of methane into the exhaust gas in the stack of the generator set to represent various levels of methane slip. To vary the load and the exhaust mass flow of the diesel engine, a load bank was used. The concentrations of CH₄ and CO₂, as well as of other exhaust components such as NO_x, were measured in the stack of the genset with PEMS, which uses an FID to measure the total hydrocarbon emissions and remotely by means of sensors installed on a drone operated by Explicit. Additionally, a portable gas analyzer for in-stack emissions measurement manufactured by ABB was used to assess its feasibility for the onboard measurements and compare its performance to PEMS.

The test setup consisted of:

- » A generator (John Deere, 100 kVA/80 kW, Stage IIIB diesel engine)
- » A loadbank (300 kW, a variable electric resistor to vary the power of the generator)
- » Three calibrated Bronkhorst mass flow-controllers (MFC)⁹ to inject CH₄ to the exhaust of the engine
- » A calibrated HORIBA OBS-ONE-GS12 PEMS
 - » with FID to measure total hydrocarbons
 - » a pitot tube to measure exhaust mass flow
- » An ABB LGR-ICOS™ GLA131 microportable GHG analyzer

⁹ TUI-numbers: 94017729, 33071026, 41124344; Accuracy: ±0.5% RD plus ±0.1% FS

» Explicit's sensors on a drone (mounted on a crane to place it at reasonable distance from the exhaust pipe)

The concentration of CH₄ in the exhaust of the diesel engine was controlled by injecting different known amounts of CH₄ to the exhaust to represent levels of methane slip between approximately 0.05% and 15.0% for molCH₄/molCO₂, which equals roughly 0.05% to 13% methane slip (CH₄ slip/CH₄ used), neglecting different properties of pilot fuel.

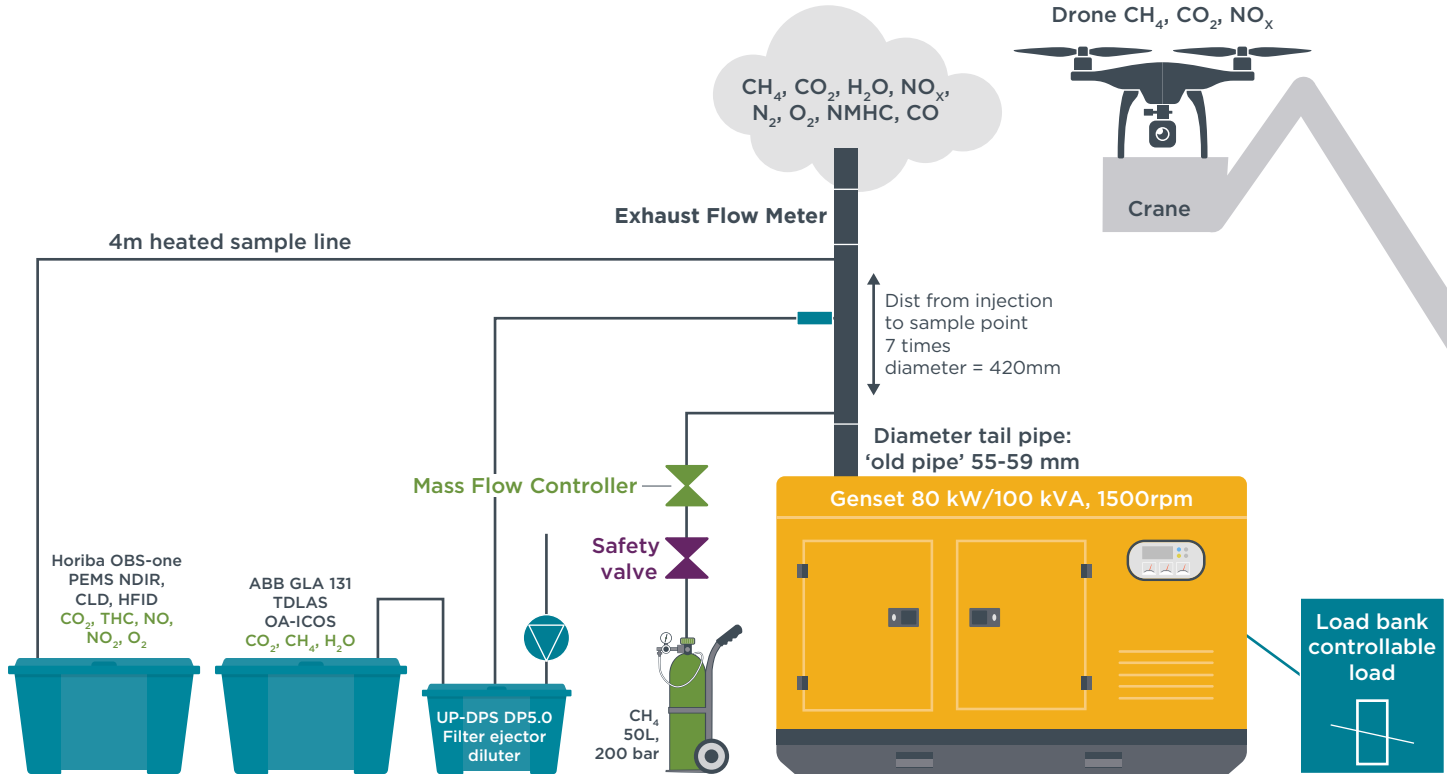


Figure 10. Schematic showing the land-based test set-up.



Figure 11. The land-based test with a diesel genset with methane dosage in the exhaust and the drone mounted on a crane.

ESTIMATING METHANE SLIP IN PLUMES

Plume measurements of CH₄ and CO₂ can be converted to a fuel methane factor using Equation 1. The numerator in the first element is the net methane concentration in parts per million, which subtracts the measured methane concentration in the plume from the background concentration. The denominator begins with the net CO₂ concentration measured in the plume.

The next part of the denominator is a value less than 1. Multiplying the net CO₂ concentration by this value adjusts the CO₂ concentration down by removing the CO₂ from the MGO pilot fuel so that only the CO₂ from LNG is used.¹⁰ This isolates LNG fuel consumption, which is important because essentially all methane measured in the plume will be from LNG, not pilot fuel. The contribution of CO₂ from the pilot fuel varies depending on engine load because the rate of pilot fuel injection is kept approximately constant across engine loads. Therefore, at lower loads, the pilot fuel contributes a larger proportion of CO₂ than at higher loads. We assume that below 10% main engine load, HPDF 2-stroke and LPDF 2-stroke engines switch to diesel mode; during this time, any methane slip is solely from LPDF 4-stroke auxiliary engines. Note that there may be other sources of CO₂ in the plume that we have not accounted for. These could include emissions from gas combustion units used by LNG carriers to burn excess boil-off gas to maintain safe cargo tank pressures. In instances such as these, the actual methane slip from the engines would be higher than we have estimated in this study.

The last two elements of the equation are used to convert from volume of CO₂ to grams of LNG. First, the ratio of molar mass of methane to carbon (16/12) is multiplied by the fuel carbon content by mass. The fuel carbon content (FCC) of LNG is assumed to be 0.75 g C/g LNG, so multiplying by 16/12 equals 1. Therefore, after the CO₂ from pilot fuel is subtracted, the resultant ratio of net CH₄ to net CO₂ equals the fuel methane factor (FMF). Importantly, the FMF results in units of g CH₄/g LNG combusted; this is not the same as methane slip. Using the FMF alone would overestimate methane slip because it does not add the uncombusted methane to the denominator. To calculate the methane slip, we use Equation 2.¹¹

Equation 1. Fuel methane factor (g CH₄/g LNG combusted)

$$FMF = \frac{CH_{4_{meas}} - CH_{4_{bg}}}{\left(CO_{2_{meas}} - CO_{2_{bg}} \right) \times \left(1 - \frac{CO_{2_{pilot}}}{CO_{2_{total}}} \right)} \times \frac{16 \text{ g } CH_4 \times \text{mol}^{-1}}{12 \text{ g } C \times \text{mol}^{-1}} \times FCC$$

Where:

FMF is the fuel methane factor, which is the mass of CH₄ emitted divided by the mass of LNG combusted.

CH_{4_{meas}} is the concentration of CH₄ in the plume in ppm.

CH_{4_{bg}} is the background concentration of CH₄ in ppm.

CO_{2_{meas}} is the concentration of CO₂ in the plume in ppm.

CO_{2_{bg}} is the background concentration of CO₂ in ppm.

CO_{2_{pilot}} is the CO₂ in the plume from MGO pilot fuel, which can be estimated as follows:

10 Some ships with LPDF 2-stroke main engines have both LPDF 4-stroke auxiliary engines and diesel auxiliary engines. In this case, our default assumption is that only the LPDF 4-stroke auxiliary engines are used because doing so makes it easier to comply with the ECA fuel sulfur limits.

11 Other carbon-containing pollutants, such as CO are not explicitly accounted for in the equation. However, based on emission factors from Faber et al. (2020) and measured CO values from the onboard campaign in this study, accounting for CO would reduce the estimates of methane slip by less than half a percent in most instances, and approximately 1% at engine loads 25% and below. As an example, if we estimated methane slip of 5.00% at 25% load, the actual methane slip could instead be 4.95%.

$$CO_{2\text{pilot}} = SFC_{ME\text{pilot}} \times Cf_{\text{pilot}} \times P_{ME\text{load}} + SFC_{AE\text{pilot}} \times Cf_{\text{pilot}} \times P_{AE\text{phase}}$$

$CO_{2\text{total}}$ is the total CO_2 in the plume, which represents the sum of CO_2 from LNG and CO_2 from MGO pilot fuel, as follows:

$$CO_{2\text{total}} = CO_{2\text{pilot}} + \left(SFC_{ME\text{load}} \times Cf_{LNG} \times P_{ME\text{load}} + SFC_{AE} \times Cf_{LNG} \times P_{AE\text{phase}} \right)$$

$SFC_{ME\text{pilot}}$ is the main engine pilot fuel consumption in g MGO/kWh, which varies by engine model and engine load based on the parameters reported in Table 7. For HPDF 2-stroke engines made by MAN ES operating at and above 10% main engine load, and for LPDF 4-stroke engines made by MAN operating at all main engine loads, we assume that $SFC_{ME\text{pilot}}$ at a given engine load equals the specific pilot fuel consumption at 100% ME load (a) divided by the engine load (l), per the following equation:

$$SFC_{ME\text{pilot_MAN}} = a/l$$

For LPDF 2-stroke engines made by WinGD operating at and above 10% main engine load, and for LPDF 4-stroke engines made by Wärtsilä and all other manufacturers operating at all main engine loads, we apply the following equation, where a and b are parameters (see Table 7) derived from a power regression of pilot fuel consumption values reported by engine manufacturers at various engine loads (l):

$$SFC_{ME\text{pilot_others}} = a \times l^{-b}$$

For HPDF 2-stroke and LPDF 2-stroke engines operating below 10% main engine load, we assume they switch from gas mode to diesel mode and that any methane slip is associated only with their LPDF 4-stroke engines. To model this, for 2-stroke main engine loads <10%, $SFC_{ME\text{pilot}}$ in the $CO_{2\text{pilot}}$ equation is replaced with $SFC_{ME\text{load}}$ (defined below) multiplied by (48/42.7) to convert LNG specific fuel consumption (SFC) to MGO SFC. The 48 value represents the IMO-defined lower heating value (LHV) of LNG of 48 MJ/kg and MGO of 42.7 MJ/kg. Further, the $SFC_{ME\text{load}}$ is set to zero in the $CO_{2\text{total}}$ equation. For the ships with LBSI main engines in our dataset, which have diesel auxiliary engines but no pilot fuel, we replace $CO_{2\text{pilot}}$ with SFC_{AE} at a value of 210 g/kWh based on relevant engine product guides to reflect fuel oil consumption, rather than LNG.

Cf_{pilot} is the carbon factor of the pilot fuel in g CO_2 /g fuel, which is assumed to be 3.206 for MGO pilot fuel, according to IMO guidelines and Faber et al. (2020).

$P_{ME\text{load}}$ is the main engine power at the main engine load, calculated as the vessel's speed through water divided by its maximum speed and then raised to the power of 3, according to the Propeller Law.

$SFC_{AE\text{pilot}}$ is the auxiliary engine specific pilot fuel consumption, which we assume is 1.47 g MGO/kWh, based on the equation for calculating $SFC_{ME\text{pilot}}$ for Wärtsilä LPDF 4-stroke engines operating at 75% load.

Cf_{LNG} is the carbon factor of LNG, which is assumed to be 2.750 g CO_2 /g fuel based on IMO guidelines and Faber et al. (2020).

$P_{AE\text{phase}}$ is the total auxiliary engine power demand, which is a function of ship type, size, and operating phase (cruising, maneuvering, at anchor, at berth), according to the methods of Faber et al. (2020), as presented in Appendix A.

SFC_{AE} is the auxiliary engine SFC, which we assume is 156 g LNG/kWh, aligned with the SFC of LPDF 4-stroke engines in Table 8.

$SFC_{ME\text{load}}$ is the main engine LNG SFC, which varies by engine type and engine load, per the following equation from Faber et al. (2020):

$$SFC_{ME\text{load}} = SFC_{\text{base}} \times \left(0.455 \times l^2 - 0.71 \times l + 1.28 \right)$$

Where:

SFC_{base} is the base SFC of the LNG engine, which varies by engine type (see Table 8); and

l is engine load, which is calculated as $\left(\frac{v}{v_{max}}\right)^3$, where v is the vessel's speed through water and v_{max} is the vessel's maximum speed; when $l < 0.05$, $l = 0.05$.

FCC is the fuel carbon content which we assume to be 0.75 g C/g LNG based on IMO guidelines and Faber et al. (2020).

Table 7. Pilot fuel consumption equation parameters.

Engine	Model	a	b	Reference
LPDF, 4-stroke	All MAN engines	3.7	N/A	Personal communication with MAN
	Wärtsilä and all others	1.0	1.237	Wärtsilä 50DF product guide
LPDF, 2-stroke	Flex50DF	1.5	0.664	Personal communication with WinGD
	X62DF	1.0	0.664	
	X72DF	1.0	0.664	
	X92DF	0.8	0.664	
HPDF, 2-stroke	All	4.8	N/A	Personal communication with MAN ES

Notes: "a" is equivalent to the pilot fuel consumption at 100% engine load in g MGO/kWh, and "b" defines the shape of the curve used to vary pilot fuel consumption with engine load. For MAN LPDF 4-stroke and HPDF 2-stroke engines, there is no "b" variable because the equation to estimate pilot fuel consumption is simply "a" divided by the engine load.

Table 8. Specific LNG fuel consumption assumptions.

Engine	Model	SFC _{base} for LNG (g/kWh)
LPDF, 4-stroke	All	156
LPDF, 2-stroke	Flex50DF	139
	X62DF	139
	X72DF	136
	X92DF	138
HPDF	All	135
LBSI	All	156

Notes: Data are based on relevant engine product guides and Faber et al. (2020). The SFC values are for LNG only and exclude pilot fuel consumption. Pilot fuel consumption is estimated separately; it varies by engine load depending on the parameters in Table 7, which feed into the equations outlined above to calculate specific pilot fuel consumption.

To calculate methane slip, Equation 2 accounts for the uncombusted methane in the denominator, resulting in a percent methane slip in terms of the mass of methane emitted from the engine divided by the mass of methane injected into the engine as fuel (i.e., the mass of LNG). Note that Equation 2 calculates the ship-wide methane slip from all LNG-fueled engines. We cannot use this method to estimate the methane slip from each engine independently.

Equation 2. Percent methane slip (g CH₄/g LNG)

$$\% CH_4 slip = \frac{FMF}{(1 + FMF)}$$

Where:

$\% CH_4 slip$ is the percent methane slip in g CH₄/g LNG.

FMF is the fuel methane factor, which is g CH₄/g LNG combusted, as calculated by Equation 1.

When multiple measurements were taken of the same ship during the same measurement session, we calculate and report the average methane slip value.

An energy-based emission factor (g/kWh) can be determined using Equation 3, which multiplies the percent methane slip from Equation 2 by the SFC of the main engine and auxiliary engines, weighted by the proportion of total energy output from the main and auxiliary engines. The result is an emission factor EF_{CH_4} in units of g CH_4 /kWh. Like Equation 2, this method produces a ship-wide emission factor and the emissions from each individual LNG-fueled engine cannot be estimated independently. However, when the main engine and auxiliary engines are the same type, e.g., for ships with diesel-electric propulsion that use LPDF 4-stroke engines, which includes many LNG carriers, ferries, and cruise ships, the emission factor represents the weighted emission factor for that engine type. This can be useful for generating an emission factor for LPDF 4-stroke engines. It is more difficult to estimate emission factors using this method when the main engines and auxiliary engines are different engine types.

Figures reporting plume results in units of g CH_4 /kWh are presented in Appendix B.

Equation 3. Methane slip emission factor (g CH_4 /kWh)

$$EF_{CH_4} = \%CH_4\ slip \times \left(SFC_{ME_{load}} \times \left(\frac{P_{ME_{load}}}{P_{ME_{load}} + P_{AE_{phase}}} \right) + SFC_{AE} \times \left(\frac{P_{AE_{phase}}}{P_{ME_{load}} + P_{AE_{phase}}} \right) \right)$$

Where:

- EF_{CH_4} is the methane emission factor in units of g CH_4 /kWh.
- $\%CH_4\ slip$ is the percent methane slip from Equation 2.
- $SFC_{ME_{load}}$ is the main engine specific LNG fuel consumption, which varies by engine type and engine load, as described below Equation 1.
- $P_{ME_{load}}$ is the main engine power at the main engine load.
- $P_{AE_{phase}}$ is the total auxiliary engine power demand.
- SFC_{AE} is the auxiliary engine SFC, which we assume is 156 g LNG/kWh based on LPDF 4-stroke SFCs from Table 8.

When multiple measurements were taken of the same ship during the same measurement session, we calculate and report the average methane slip value.

Estimating uncertainty in plume measurements of methane slip

The uncertainty of the methane slip calculated using Equation 2 was determined according to the Guide to the expression of Uncertainty in Measurement (GUM) 1995 (ISO/IEC GUIDE 98-3:2008(E), 2008). The combined variance $u_c^2(y)$ of the result is obtained from the variances $u^2(x_i)$ of the input parameters by applying Equation 4.

Equation 4. Combined variance according to GUM 1995 used to calculate uncertainty in the methane slip estimates

$$u_c^2(y) = \sum_{i=1}^N \left(\frac{\delta f}{\delta x_i} \right)^2 u^2(x_i)$$

Here, f denotes the function given by Equation 2, including the input of Equation 1, and x_i is the input parameters listed in Table 9. Note that the ratio of the above-ambient values of CH_4 and CO_2 is considered as one input parameter. Table 9 also contains the assumed standard deviations of the listed input parameters.

Table 9. Input parameters for calculating uncertainty of estimated methane slip.

Parameter	Unit	Engine type	Assumed standard deviation	Source
$\frac{CH_{4_{meas}} - CH_{4_{bg}}}{CO_{2_{meas}} - CO_{2_{bg}}}$	unitless	n/a	15%	Reference laboratory testing and confirmatory testing in FUMES on-land and onboard campaigns
SFC_{base}	g LNG/kWh	Main engine	5%	Typical tolerances from engine manufacturers
SFC_{AE}	g LNG/kWh	Auxiliary engine	5%	Typical tolerances from engine manufacturers
Engine load	%	Main engine	20%	Authors' expert opinion based on experience modeling power demand, ship design, and ship parameters. Also depends on accuracy of reported or estimated maximum speed.
Cf_{pilot}	g CO ₂ /g fuel	Main and auxiliary engines	3%	Authors' estimate based on the fact that carbon content can vary depending on the composition of MGO fuel.
Cf_{LNG}	g CO ₂ /g fuel	Main and auxiliary engines	2%	Authors' estimate based on the fact that carbon content can vary depending on the composition of LNG fuel.
a	-	Main engine	5%	Based on potential variability in pilot fuel consumption
b	-	Main engine	5%	Based on potential variability in pilot fuel consumption
$P_{AE_{phase}}$	kW	Auxiliary engine	20%	Authors' expert opinion based on experience modeling power demand, ship design, and ship parameters, as well as onboard variability
Engine load	%	Auxiliary engine	20%	Authors' expert opinion based on experience modeling power demand, ship design, and ship parameters, as well as onboard variability.
a	-	Auxiliary engine	5%	Based on potential variability in pilot fuel consumption
b	-	Auxiliary engine	5%	Based on potential variability in pilot fuel consumption

ESTIMATING NO_x EMISSION FACTORS

Based on the sampled concentrations of NO_x and CO₂ in each ship plume, an individual emission factor per ship was calculated using Equation 5.¹² The first two elements result in grams of NO_x per gram of carbon. The rest of the equation in the large parentheses and before the final element results in grams of carbon per kWh. It is weighted by the various fuel carbon contents and SFCs of LNG and MGO pilot fuel for main and auxiliary engines. Multiplying all three elements together results in g NO_x/kWh. The final element accounts for methane slip. The SFCs in the equation reflect both combusted and uncombusted methane. Using the ratio of NO_x to CO₂ only measures CO₂ from the LNG that was combusted, so the SFCs are adjusted down to reflect only the grams of LNG fuel combusted. The last element (1 - %CH₄slip) accomplishes this.

12 Other carbon-containing pollutants, such as CO are not explicitly accounted for in the equation. However, based on emission factors from the Fourth IMO GHG Study (Faber et al. 2020) and measured CO values from the onboard campaign in this study, accounting for CO would reduce the estimates of NO_x by less than half a percent in most instances, and approximately 1% at engine loads 25% and below.

Equation 5. NO_x emission factor (g NO_x/kWh)

$$EF_{NO_x} = \frac{NO_{x_{meas}} - NO_{x_{bg}}}{CO_{2_{meas}} - CO_{2_{bg}}} \times \frac{46 \text{ g } NO_x \text{ mol}^{-1}}{12 \text{ g C mol}^{-1}}$$

$$\times \left(\left(\left(FCC_{LNG} \times SFC_{ME_{load}} + FCC_{pilot} \times SFC_{ME_{pilot}} \right) \times \left(\frac{P_{ME_{load}}}{P_{ME_{load}} + P_{AE_{phase}}} \right) \right) \right.$$

$$\left. + \left(\left(FCC_{LNG} \times SFC_{AE} + FCC_{pilot} \times SFC_{AE_{pilot}} \right) \times \left(\frac{P_{AE_{phase}}}{P_{ME_{load}} + P_{AE_{phase}}} \right) \right) \right) \times (1 - \%CH_4 \text{ slip})$$

Where:

- EF_{NO_x} is the NO_x emission factor in units of g NO_x/kWh.
- $NO_{x_{meas}}$ is the concentration of NO_x in the plume, measured in ppm.
- $NO_{x_{bg}}$ is the background concentration of NO_x, measured in ppm.
- $CO_{2_{meas}}$ is the concentration of CO₂ in the plume, measured in ppm.
- $CO_{2_{bg}}$ is the background concentration of CO₂, measured in ppm.
- 46/12 is the ratio of molar mass of NO_x (based on NO₂) to carbon.
- FCC_{LNG} is the fuel carbon content of LNG, which is assumed to be 0.75.
- FCC_{pilot} is the fuel carbon content of MGO pilot fuel, which is assumed to be 0.87.
- $SFC_{ME_{load}}$ is the main engine specific LNG fuel consumption, which varies by engine type and engine load. The base SFC for each main engine is listed in Table 8, in g LNG/kWh.
- $SFC_{ME_{pilot}}$ is the main engine specific pilot fuel consumption, which varies by engine type and engine load, as explained below Equation 1, in g MGO/kWh.
- SFC_{AE} is the auxiliary engine SFC, which we assume is 156 g LNG/kWh.
- $SFC_{AE_{pilot}}$ is the auxiliary engine specific pilot fuel consumption, which we assume is 1.47 g MGO/kWh.
- $P_{ME_{load}}$ is the main engine power at the main engine load.
- $P_{AE_{phase}}$ is the total auxiliary engine power demand.
- $\%CH_4 \text{ slip}$ is the percent methane slip from Equation 2.

When multiple measurements were taken of the same ship during the same measurement session, we calculate and report the average NO_x value.

ESTIMATING FUGITIVE METHANE EMISSIONS FROM STATIONARY SHIPS

Fugitive emissions originating from cargo or fuel were measured from ships at berth using a drone-borne method. The methane emissions are quantified using the DFM method (De Rossi, 2021; Knudsen & De Rossi, 2022), depicted in Figure 12.

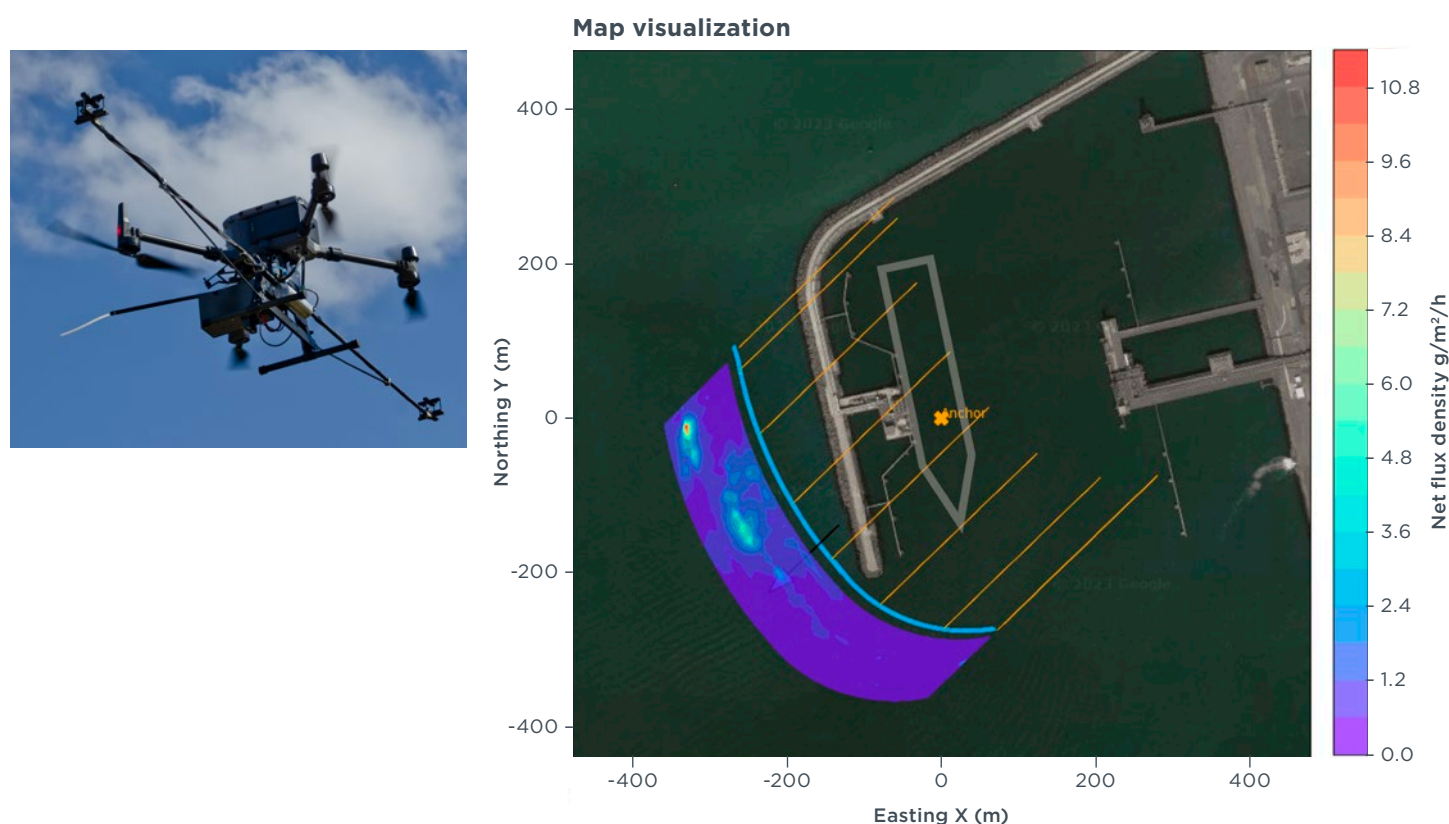


Figure 12. The photograph shows a drone equipped with a Mini-Sniffer. For the DFM method, the drone is additionally equipped with two wind sensors at extended beams to each side of the drone. The visualization below shows the evaluated, spatially resolved net flux densities superimposed to a map (Maps data: Google, ©2022 CNES / Airbus, Maxar Technologies). In combination with the wind information, individual sources can be identified and individually quantified.

The DFM method was developed by Explicit to monitor total net fugitive emission rates from facilities that emit methane. It is in accordance with the Oil and Gas Methane Partnership 2.0 requirements for site-level reporting (level 5), and the DFM method has subsequently been accredited according to ISO 17025 for the quantification of methane emissions. A drone follows a predefined pattern which is set up downwind of the facility. The pattern is described by waypoints defining horizontal transects and vertical altitude steps between each transect. During the measurement, the drone flies along the horizontal transect at a predefined speed. After each horizontal path is completed, the drone automatically rises to the next altitude before continuing with the next transect in the opposite direction. The result is a virtual vertical wall forming a cross-section through the fugitive emission plume(s).

Air samples are taken and analyzed continuously along the flight path. The concentration data, as well as the simultaneously measured wind and positional data, are collected and processed, and a background level of CH₄ is statistically evaluated for each transect and used as a correction as part of the evaluation.

The strength of this method is that the wind is measured at the same spot where the air is sampled. This makes it possible to accurately calculate spatially resolved

flux densities from emissions sources (see Figure 12) and to quantify total net fluxes. Using the superimposed visualization overlaid on a map, further information about the origin of the emissions is gained by backtracing the emissions using the wind information.

This method measures fluxes of CH₄ with a certainty of about ±20 % with 95% confidence at emission rates as low as 300 g/h with three repetitions. Accuracy can be improved by further repetitions (De Rossi & Knudsen, 2022).

RESULTS AND DISCUSSION

PLUME CAMPAIGN RESULTS

Overview

We obtained 45 measurements of 34 unique vessels over the course of 2022 using sensors mounted to drones and helicopters. The locations and number of measurements in each are shown in Figure 13.

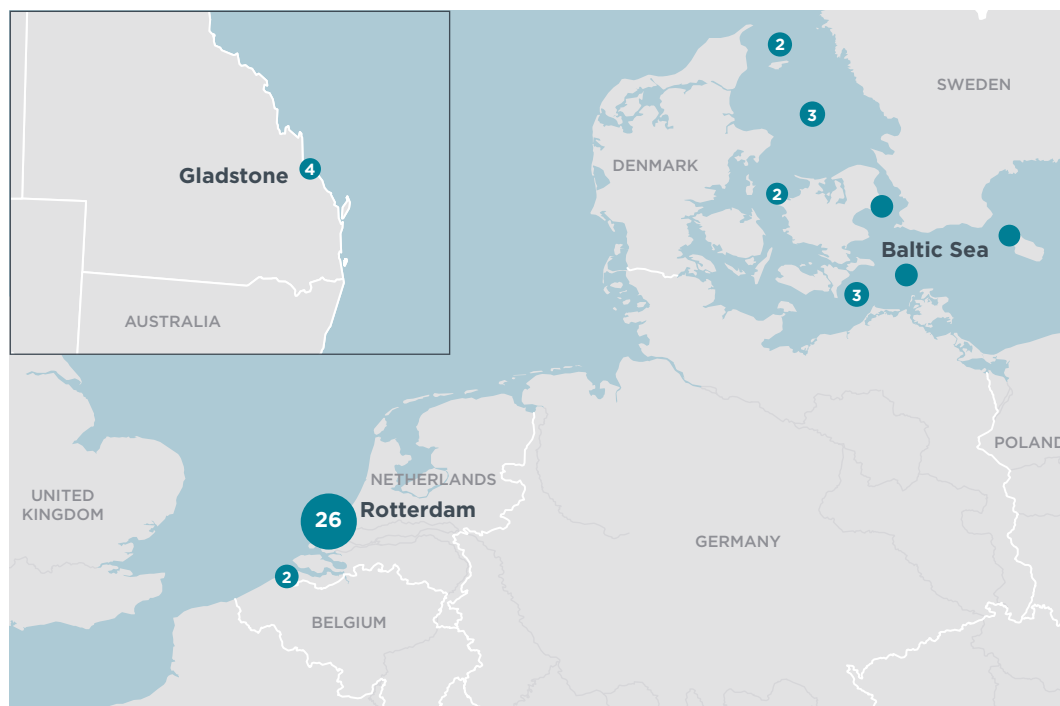
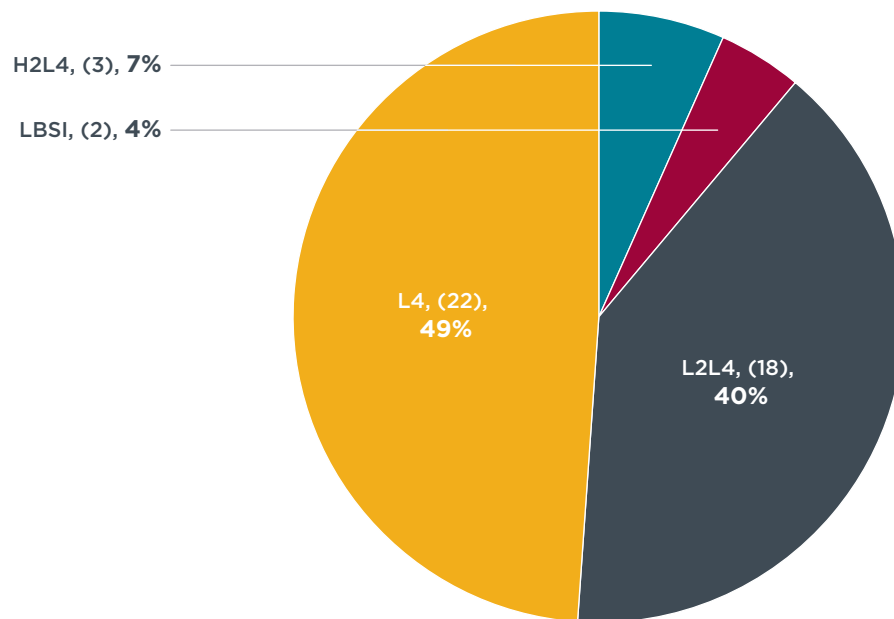


Figure 13. Plume measurement locations and number of measurements in Europe and Australia, 2022.

When measuring in the plume, the drone sampled the combined exhaust from all engines that were operating at the time. Ships with HPDF 2-stroke and LPDF 2-stroke main engines also had LPDF 4-stroke auxiliary engines onboard. We label these ships as H2L4 and L2L4, respectively. Some L2L4 ships also had diesel auxiliary engines in addition to LPDF 4-stroke auxiliary engines. Other ships used one or more LPDF 4-stroke engines for both propulsion and auxiliary power; we label these ships L4. Lastly some ships used LBSI engines along with diesel auxiliary engines, we leave these labeled as LBSI.

Of the 45 measurements, approximately half (49%) were from L4 ships and 40% were from L2L4 ships. Three measurements (7%) were obtained from H2L4 ships, and two measurements (4%) were from ships with LBSI engines (Figure 14).



Note: H2L4 are ships with HPDF 2-stroke main engines and LPDF 4-stroke auxiliary engines; LBSI ships are those with only LBSI LNG-fueled engines; L2L4 are ships with LPDF 2-stroke main engines and LPDF 4-stroke auxiliary engines; L4 are ships are those with only LPDF 4-stroke engines.

Figure 14. Measurements by engine type.

Of the 45 measurements, 44% were from LNG tankers and 29% were from container ships, with the rest being a mix of service vessels, roll-on/roll-off ferries, chemical tankers, one offshore vessel, and one cruise ship (Figure 15).

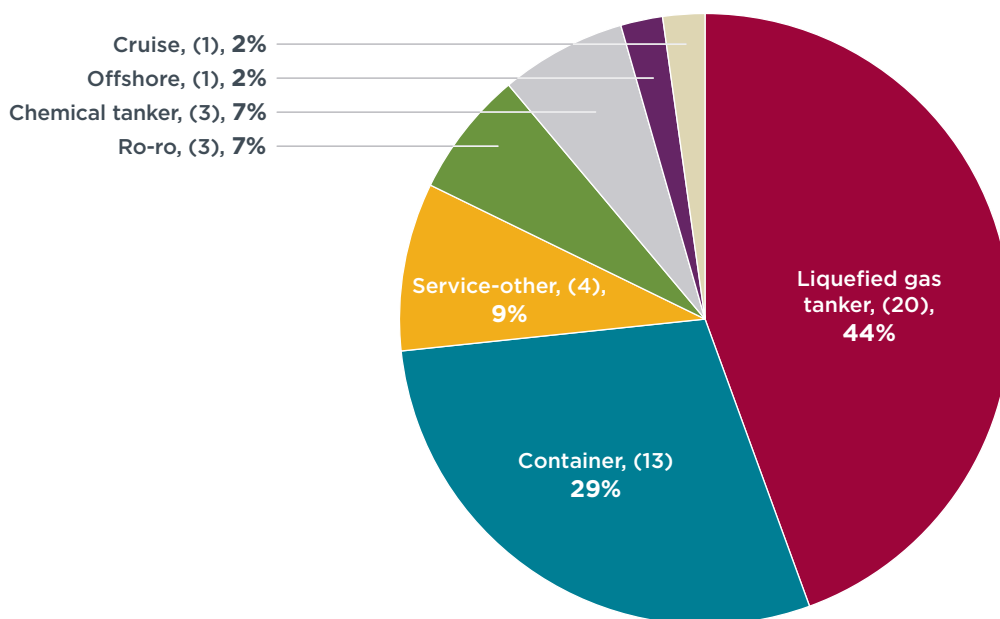
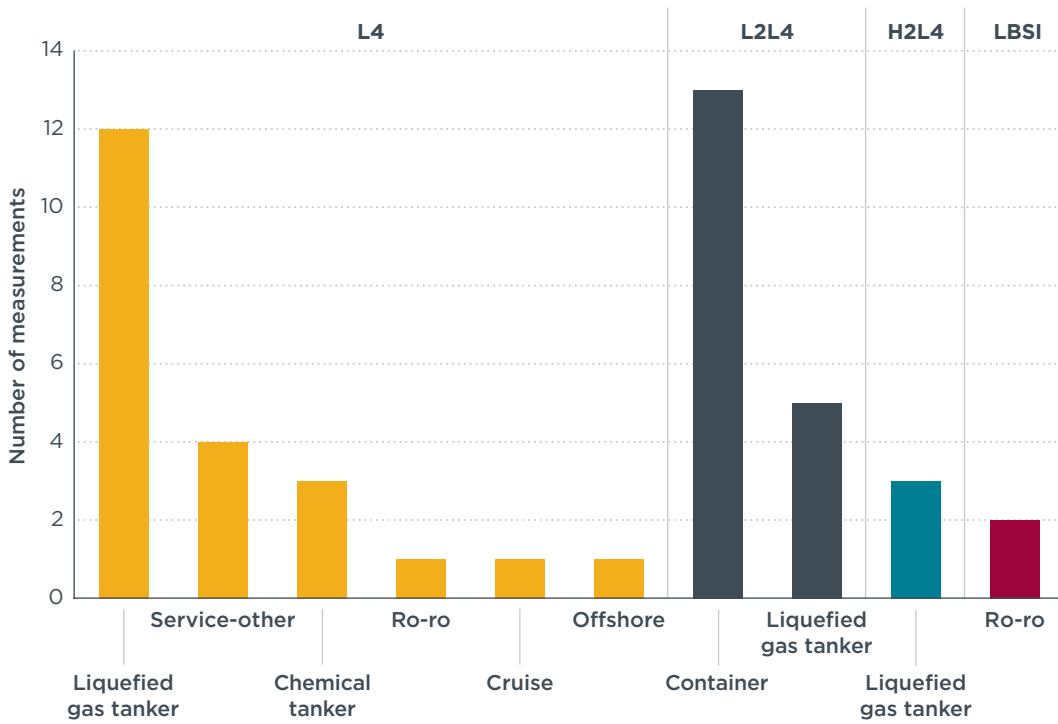


Figure 15. Measurements by ship type.

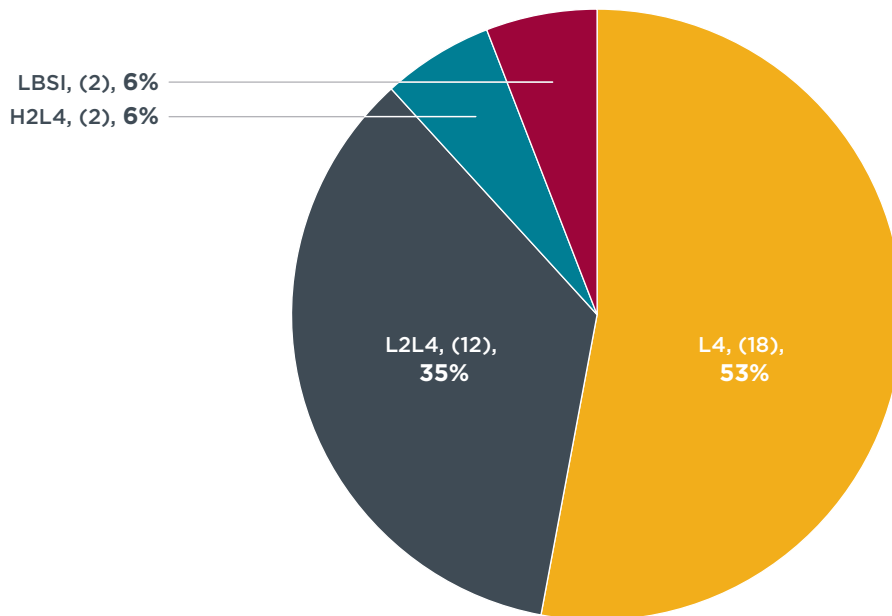
Of the 45 measurements, 13 (29%) were from L2L4 container ships, 12 (27%) were from L4 LNG tankers, 7 (11%) were from L2L4 LNG tankers, 4 (9%) were from L4 service vessels, and the remainder were from other combinations of ship types and engine types (Figure 16).



Note: H2L4 are ships with HPDF 2-stroke main engines and LPDF 4-stroke auxiliary engines; LBSI ships are those with only LBSI LNG-fueled engines; L2L4 are ships with LPDF 2-stroke main engines and LPDF 4-stroke auxiliary engines; L4 are ships are those with only LPDF 4-stroke engines.

Figure 16. Measurements by combinations of ship types and engine types.

Of the 34 unique vessels, 53% were from L4 ships, 35% were from L2L4 ships, 6% were from H2L4 ships, and 6% were from LBSI ships (Figure 17).



Note: H2L4 are ships with HPDF 2-stroke main engines and LPDF 4-stroke auxiliary engines; LBSI ships are those with only LBSI LNG-fueled engines; L2L4 are ships with LPDF 2-stroke main engines and LPDF 4-stroke auxiliary engines; L4 are ships are those with only LPDF 4-stroke engines.

Figure 17. Unique ships measured by engine type.

Of the 34 unique vessels, 19 ships (56%) were LNG tankers, 7 (20%) were container ships, 3 (9%) were roll-on/roll-off ferries, 2 (6%) were chemical tankers, 1 (3%) was an offshore supply vessel, and 1 (3%) was a cruise ship, as shown in Figure 18.

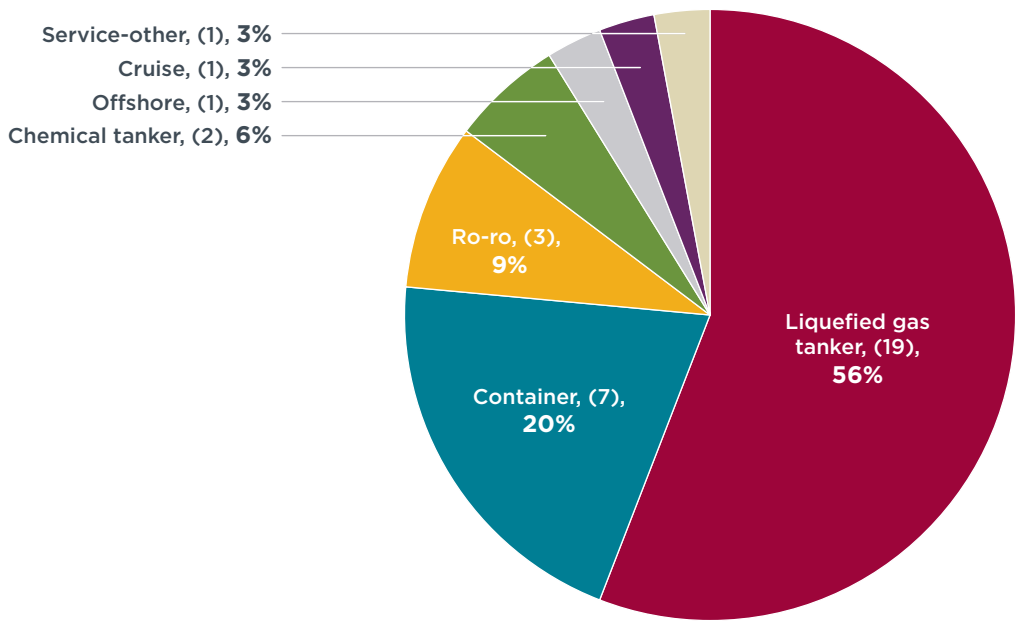
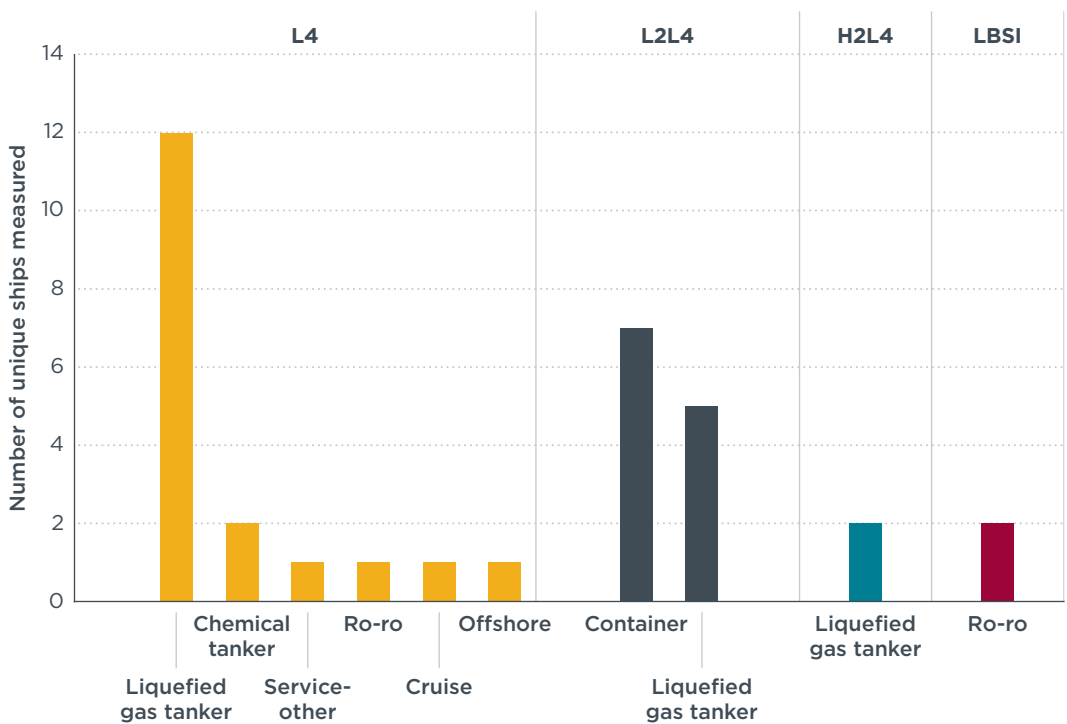


Figure 18. Unique ships measured by ship type.

As shown in Figure 19, of the 34 unique vessels, 12 (35%) were L4 LNG tankers, 7 (20%) were L2L4 container ships, 5 (15%) were L2L4 LNG tankers, and the remainder were a combination of engine types and ship types.



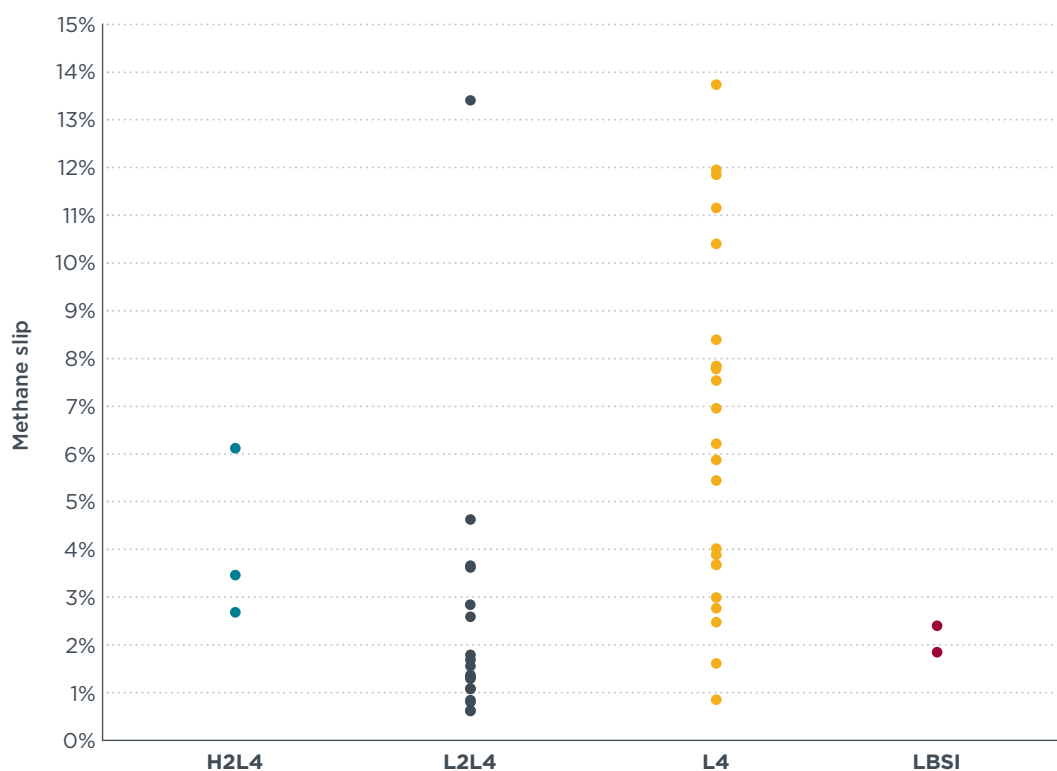
Note: H2L4 are ships with HPDF 2-stroke main engines and LPDF 4-stroke auxiliary engines; LBSI ships are those with only LBSI LNG-fueled engines; L2L4 are ships with LPDF 2-stroke main engines and LPDF 4-stroke auxiliary engines; L4 are ships are those with only LPDF 4-stroke engines.

Figure 19. Unique ships by combinations of ship types and engine types.

Ship-level methane slip

Figure 20 shows each measurement for ship-level methane slip for H2L4, L2L4, L4, and LBSI ships. (The relationship between these measurements and engine load is presented in Figure 22.) Three measurements were obtained from H2L4 ships and

two were taken from LBSI ships. We see the tightest measurement distribution for the L2L4 ships and the largest distribution for L4 ships. The measured methane emissions sources depend on which engines are operating while the ship is being measured. For H2L4 and L2L4 ships operating below 10% main engine load, the 2-stroke main engines are assumed to switch from gas mode to diesel mode, and only the LPDF 4-stroke auxiliary engines are operating on LNG. The two highest methane slip measurements for H2L4 ships are associated with <10% main engine load and reflect methane slip only from the LPDF 4-stroke auxiliary engines. Similarly, four measurements for L2L4, including the outlier that shows methane slip greater than 13%, are associated with low-load operations where only the LPDF 4-stroke auxiliary engines are assumed to be operating on LNG. For the L4 and LBSI ships, only one engine technology is responsible for methane slip; however, multiple engines may be operating at the same time and at different engine loads. The impact of engine load on methane slip is examined in more detail below.



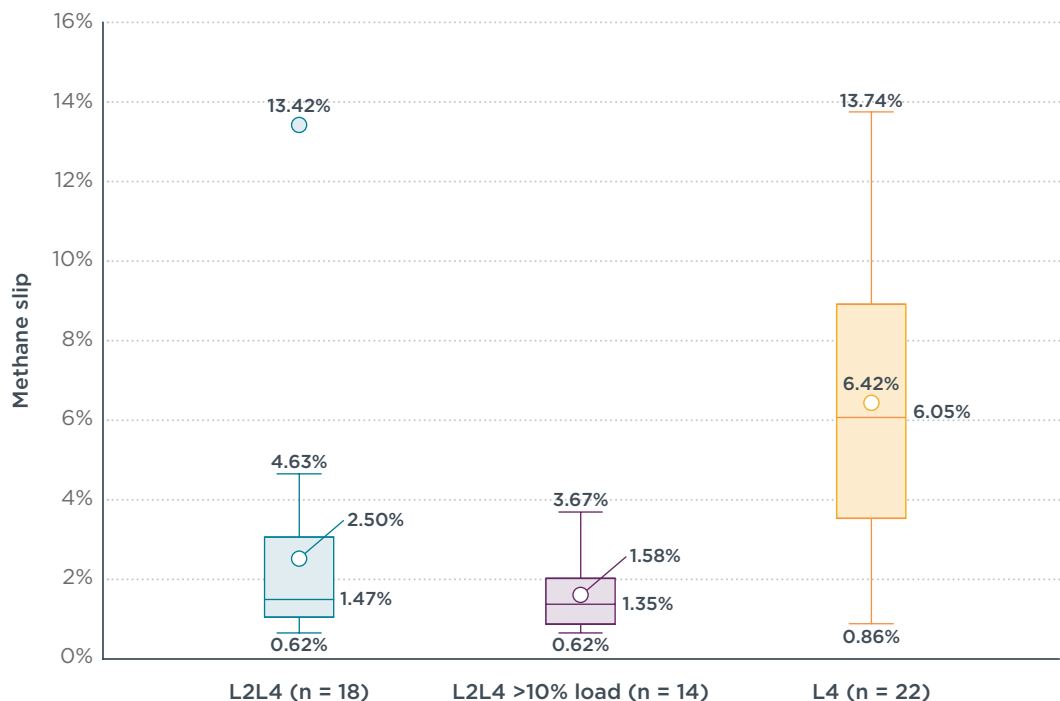
Note: H2L4 are ships with HPDF 2-stroke main engines and LPDF 4-stroke auxiliary engines; LBSI ships are those with only LBSI LNG-fueled engines; L2L4 are ships with LPDF 2-stroke main engines and LPDF 4-stroke auxiliary engines; L4 are ships are those with only LPDF 4-stroke engines.

Figure 20. Ship-level methane slip from all engine sources measured.

Methane emission statistics for L2L4 and L4 ships are presented in the boxplot in Figure 21. The mean and median ship-level methane slip is lower for L2L4 than for L4, and the interquartile ranges do not overlap. The maximum value for L2L4 (13.42%) was measured when the ship was operating at <10% main engine load, meaning that the LPDF 2-stroke main engine was assumed to have switched over to diesel mode and the methane slip was only from the LPDF 4-stroke auxiliary engines. The second-highest methane slip (4.63%) is also associated with <10% main engine load. If we exclude the four measurements taken at <10% main engine load for L2L4 ships, the maximum methane slip falls from 13.42% to 3.67%, the average decreases from 2.50% to 1.58%, and the median is reduced from 1.47% to 1.35%.

The maximum value for L4 ships was 13.74%, with a mean of 6.42% and a median of 6.05%. The minimum methane slip value for L4 ships of 0.86% was associated with

higher-than-expected sulfur emissions, suggesting that one or more of the LPDF 4-stroke engines on the ship was using petroleum fuel and not LNG. If so, this would artificially lower the estimated methane slip because the CH₄-to-CO₂ ratio is used to estimate methane slip and a portion of the CO₂ in the plume would be from the higher-sulfur petroleum fuel. We do not know how much high-sulfur, non-LNG fuel was consumed in this case; we leave this measurement in the dataset for completeness. The second-lowest methane slip value for L4 ships was 1.6%.

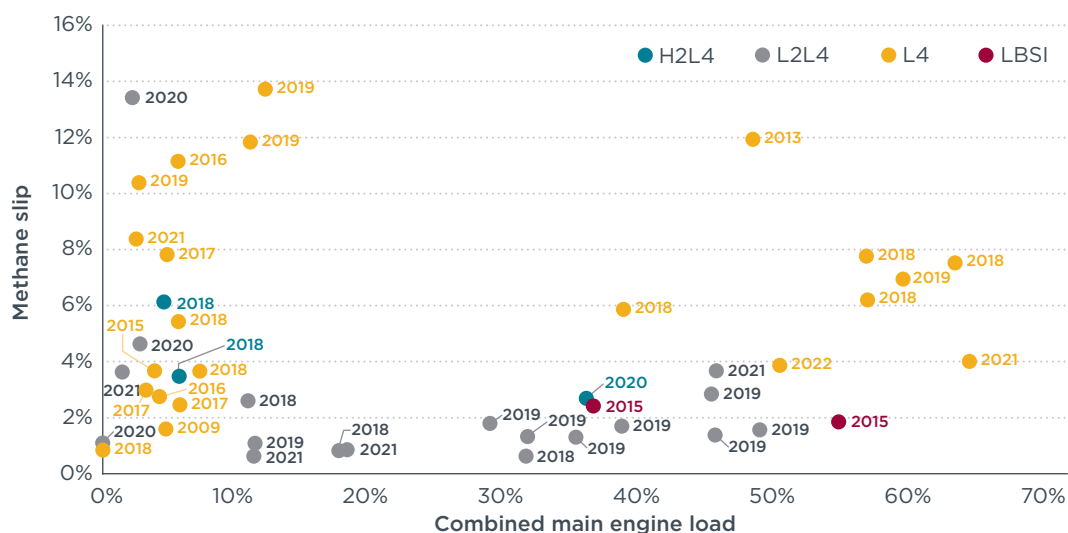


Note: Dot shows outlier; bars show minimum and maximum (excl. outliers); circle inside box is the average; horizontal line is the median; box is the interquartile range

Figure 21. Boxplot of ship-level methane slip for ships with LPDF 2-stroke main engines and LPDF 4-stroke auxiliary engines (L2L4) and ships with only LPDF 4-stroke engines (L4).

Methane slip, engine load, and engine age

Figure 22 shows ship-level methane slip emissions compared to the combined main engine load at the time the measurement was taken, with the build year of the ship indicated. The engine load is estimated based on the speed of the ship, reflecting the main engine propulsion power demanded at that time divided by the total installed main engine power.



reason, in Figure 22, there is no clear pattern between combined main engine load and methane slip for L2L4 ships.

For ships with LBSI engines, which do not have LNG-fueled auxiliary engines, we obtained two measurements from two unique ships, with methane slips of 2.41% and 1.85% at 36% and 55% main engine load, respectively. This is lower than the EU and IMO assumption of 2.6% methane slip, but we do not have enough data to determine whether the default factor for LBSI engines is reasonable.

With regard to engine age (using ship build year as a proxy), we ran a regression for all of the measured values from L2L4 ships with combined main engine loads above 10% and controlled for combined engine load. The regression model was not statistically significant (F statistic >0.05). Therefore, our dataset does not provide evidence that ship age affects methane slip for the L2L4 ships we measured. One explanation could be that the variability in methane slip due to the influence of the LPDF 4-stroke auxiliary engines, combined with only a 4-year spread of ship builds, prevents us from determining any significant relationship. Additionally, there may be only one or two engine generations reflected in the data.

For L2L4 ships, there are sufficient data points to run a regression on the influence of auxiliary engine LNG consumption on methane slip. Methane slip was used as the dependent variable and percent auxiliary engine LNG consumption was used as the independent variable. The p-value for percent of auxiliary engine LNG consumption was significant at the 95% confidence level ($p < 0.05$, at 0.017). The coefficient was 0.050, meaning that every 10 percentage-point increase in LPDF 4-stroke auxiliary engine LNG consumption increased ship-level methane slip by 0.5 percentage points. For example, if methane slip was 5% when LPDF 4-stroke auxiliary engines represented 40% of LNG fuel consumption, increasing auxiliary engine LNG consumption to 50% would be expected to result in 5.5% methane slip. The coefficient is sensitive to the 13.74% methane slip measurement at 100% auxiliary engine fuel consumption. To test if the relationship still held had we not measured this high methane slip value, we re-ran the regression without it. In this case, the p-value for percent of auxiliary engine LNG consumption was 0.08 (less significant) and the coefficient fell to 0.017, meaning that a 10 percentage-point increase in LPDF 4-stroke auxiliary engine LNG consumption would be expected to increase ship-level methane slip by 0.17 percentage points. The finding that LPDF 4-stroke auxiliary engines can increase ship-level methane slip for ships with LPDF 2-stroke main engines is consistent with Balcombe (2022).

Data for the L4 ships can be divided into two groups: one close to or below 10% combined engine load and one at or above approximately 40% combined engine load, with 6 of 22 measurements at or above 50% combined engine load. For the low-load group, the methane slip ranges from 0.86% to 13.74%. For the higher-load group, the methane slip ranges from 3.89% to 11.96%. For the six measurements at or above 50% engine load, methane slip ranges from 3.89% to 7.78%, with an average of 6.07% and a median of 6.59%; four of the six measurements fell between 6% and 8% methane slip. For comparison, the FuelEU Maritime regulation assumes that methane slip for LPDF 4-stroke engines is 3.1% at 50% engine load, with the implication that methane slip is higher than that below 50% engine load and lower than that above 50% engine load. The Fourth IMO GHG Study assumes LPDF 4-stroke engines emit approximately 3.5% on the E2/E3 test cycle (Faber et al., 2020). For the L4 ships, 17 of 22 measurements (77%) showed greater than 3.1% methane slip. The same number were greater than 3.5%. Recall that these measurements represent the ship-level methane slip and not the slip from each engine, except for the five L4 ships that have only one LPDF 4-stroke engine.

To investigate the relationship between methane slip and engine age for L4 ships, we first combined the full L4 dataset with all H2L4 and L2L4 measurements below

10% combined engine load, and assumed that only the LPDF 4-stroke engines were operating on LNG. This resulted in 28 measurements from LPDF 4-stroke engines. In this dataset, the minimum methane slip was 0.86%, the maximum was 13.74%, the mean was 6.20%, and the median was 5.67%. The ships included one built in 2009, one built in 2013, and the rest built between 2015 and 2022. From this dataset, we ran a regression and controlled for combined engine load. The model was not significant (F statistic $\gg 0.5$). Therefore, this dataset does not provide evidence that ship age affects methane slip for the LPDF 4-stroke engines that we measured. A similar finding was made by Rochussen et al. (2023). One explanation could be that the variability in methane slip due to the influence of multiple LPDF 4-stroke engines overcomes any relationship we might be able to see if we were to test individual engines at the same load points.

There are five measurements from ships that have only one LPDF 4-stroke engine (see Figure 23). There are two measurements with nearly 12% methane slip. The first is for a ship built in 2019 operating near 10% load. That same ship was later measured at 60% load, and its methane slip was 7%; this is lower but still more than twice as high as the FuelEU Maritime regulation’s assumption of 3.1% methane slip for this engine technology (when operating at 50% load). The other measurement near 12% methane slip was taken from a ship built in 2013 operating near 50% load. The two remaining measurements showed approximately 4% methane slip at 50% and 65% load from ships built in 2022 and 2021, respectively. The range of single-engine methane slip from this study (4%–12%) can be compared to those from Sommer et al. (2019), which measured 5%–8% methane slip for a single LPDF 4-stroke engine.

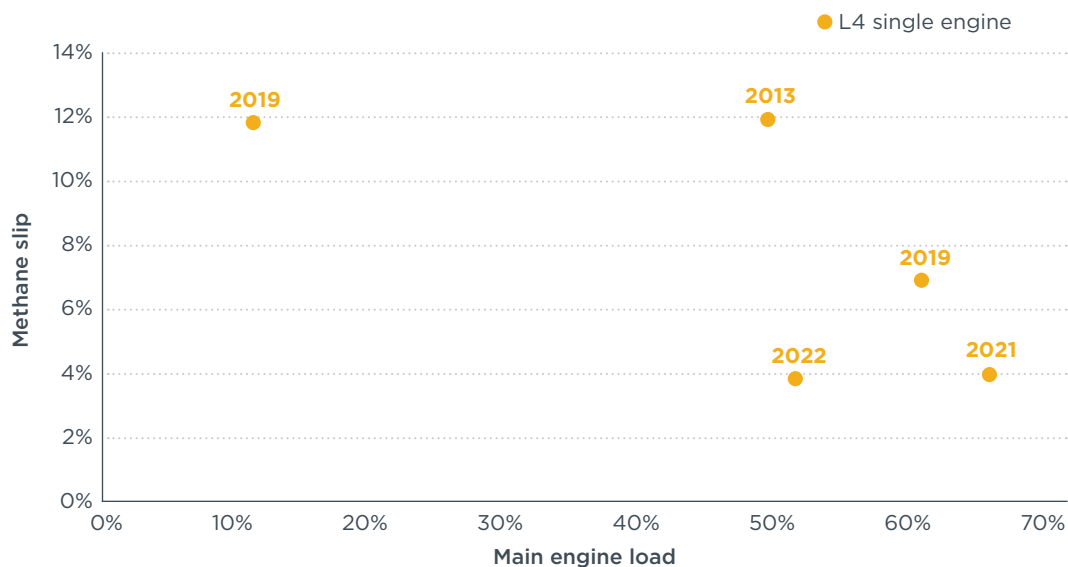
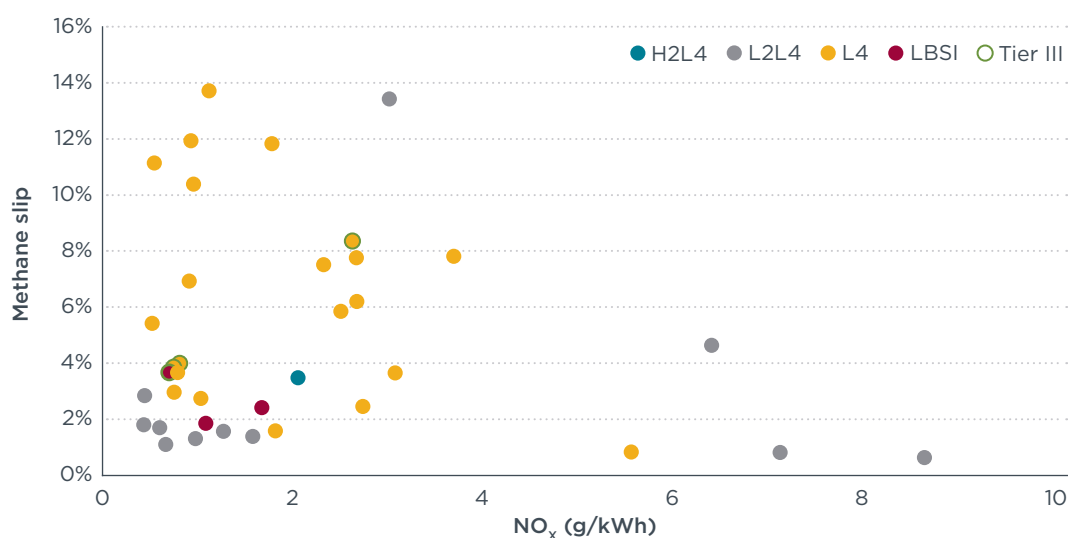


Figure 23. Methane slip by engine load for L4 ships that have only one LPDF 4-stroke main engine, with build year of the ship indicated.

Methane slip versus NO_x

We obtained 37 measurements representing 29 unique ships that contained data for both CH₄ and NO_x. The results are shown in Figure 24. All the ships were required to at least achieve Tier II NO_x limits, and four were required to achieve Tier III. All measured values are below the NO_x Tier II emissions limit, which ranges from 7.7 to 14.4 g/kWh

depending on engine rpm and applies to ships built from 2011 through 2020.¹³ Four of the 29 ships were built in 2021 or later, meaning that each engine onboard would be required to achieve Tier III when operating in the Baltic and North Sea ECAs. Tier III limits range from 2.0–3.4 g/kWh, depending on engine rpm. For all ships of all tiers, 32 (86%) of the measurements were below 3.4 g NO_x/kWh and 23 (62%) were below 2.0 g NO_x/kWh. For the four ships required to meet Tier III limits, two had SCR systems that would be used in diesel mode, but these two ships were likely operating in gas mode when they were measured because they were sailing at 46% and 64% combined main engine load, respectively. The measurements from three of the four ships were below 1 g/kWh and, therefore, fall below the weighted Tier III limit. The fourth was 2.59 g/kWh; the ship's LPDF 4-stroke engines have rpms of 514 and 720, which would require achieving less than 2.59 and 2.41 g/kWh on the NO_x test cycle. This fourth ship has LPDF 4-stroke engines and did not have SCR.



achieve Tier II limits, which would be 14.4 g/kWh for the main engine, which can likely be achieved without SCR, even in diesel mode. Therefore, the SCR system would not need to be activated in this case.

We observed four measurements with NO_x emissions above 5 g/kWh. The L4 ship NO_x value of 5.48 g/kWh was associated with 0.86% methane slip, a data point that has higher sulfur emissions than we would expect if all engines were running only on LNG. This helps explain the high NO_x value because running an LPDF 4-stroke engine in diesel mode would result in higher NO_x emissions than in gas mode. A value of 0.86% methane slip is also low relative to the median and mean methane slip for L4 ships, which also supports the hypothesis that one or more engines were running on fuel oil instead of LNG because the measured methane-to-CO₂ ratio in the plume would be smaller due to the extra CO₂ generated by burning the fuel oil. The other three outlier values were for L2L4 ships, two of which have both dual-fuel LNG auxiliary engines and diesel auxiliary engines. These two measurements were from the same ship at two different times, and both measurements had low methane slip estimates; this supports the idea that the diesel auxiliary engines were operating when the ship was measured. The measured sulfur emissions were not high for these measurements, but it could reflect running the auxiliary engines on low sulfur MGO instead of higher sulfur fuel oil, which is what we suspect was used for the 0.86% methane slip L4 measurement. The remaining higher NO_x L2L4 measurement of 6.32 g/kWh has relatively high methane slip (4.63%), and, unlike the other L2L4 ship with higher NO_x emissions, this ship does not have a diesel auxiliary engine. We cannot explain this higher NO_x value.

Uncertainty analysis

The results of the uncertainty analysis are depicted in Figure 25. On the x-axis, the values of the methane slip according to Equation 2 are plotted; on the y-axis, the standard deviation is shown, i.e., the square root of the calculated uncertainty. The absolute value of the uncertainty increases with the methane slip; the relative value of the standard deviation, however, is around 15% of the methane slip for lower values of methane slip (e.g., at 2.5% calculated methane slip, one standard deviation results in a range of 2.125%–2.875% methane slip; i.e., 2.5% ± 15%). This is due to the predominant influence of the relative standard deviation of the measured ratio of CH₄/CO₂ which was determined to be 15% (cf. Table 9), based on the results of sensor tests conducted at the two reference laboratories. (Note that the similarly obtained uncertainty for the NO_x to CO₂ ratio by FORCE Technology is 18.7%.) At higher methane slip, other factors become more important and the uncertainty relative to the methane slip decreases.

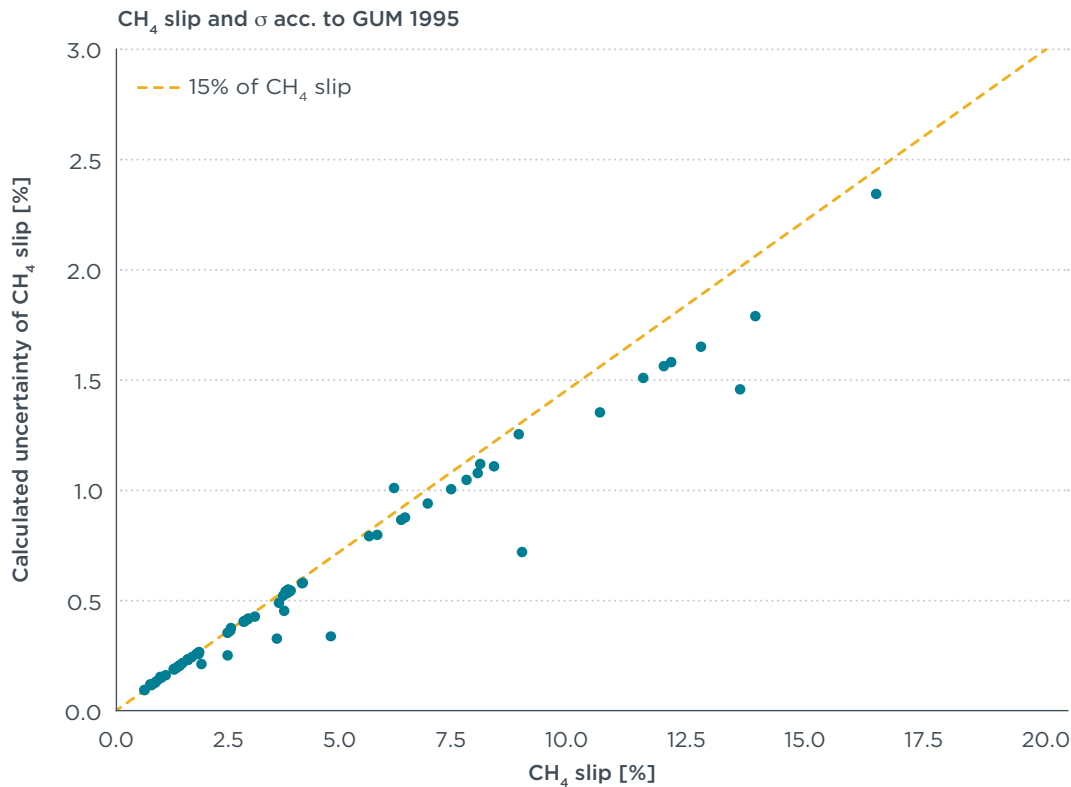


Figure 25. Results of uncertainty calculation for plume measurements; the dashed yellow line represents a relative uncertainty of 15% of the methane slip.

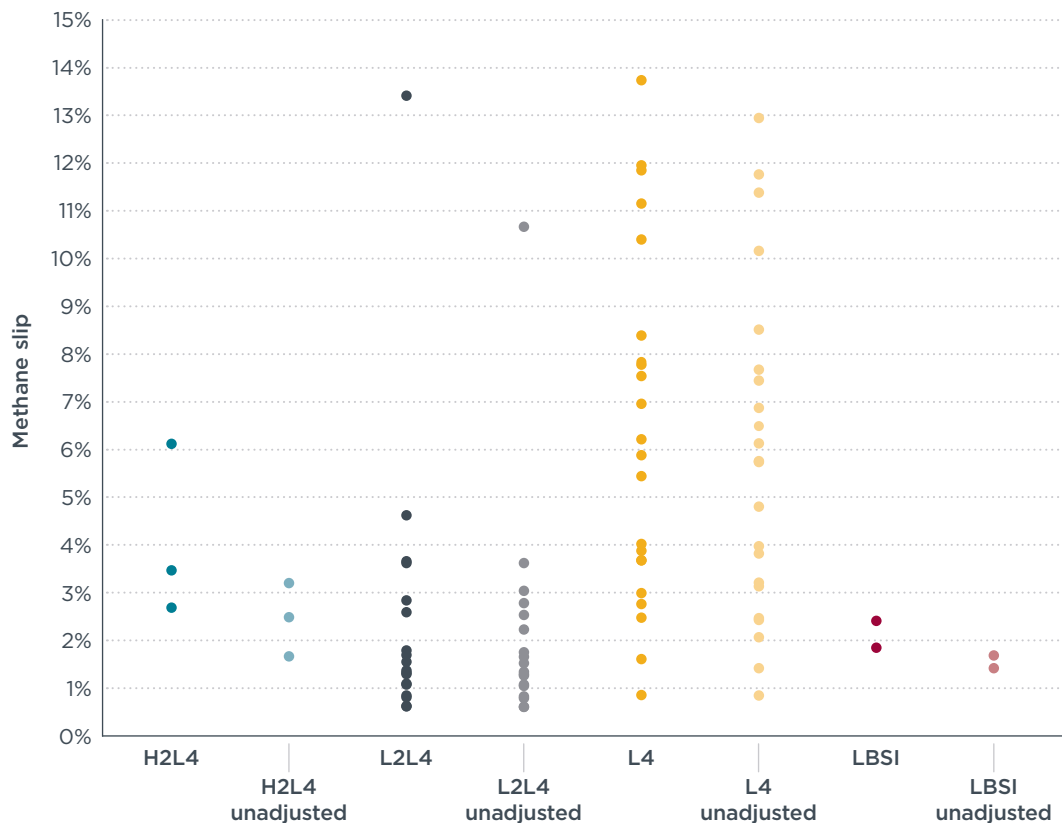
Sensitivity analysis

The methane slip results are sensitive to assumptions about how much CO₂ measured in the plume originates from consuming fuels other than LNG, including pilot fuel for dual fuel engines, fuel oil consumption for 2-stroke engines operating below 10% load, and fuel oil consumption from diesel auxiliary engines for ships with LBSI main engines. In Equation 1, we subtract any CO₂ from pilot fuel, engines operating in diesel mode, and diesel auxiliary engines for LBSI ships from the CH₄-to-CO₂ ratio measured in the plume. This leaves uncombusted methane from LNG consumption in the numerator and CO₂ from combusted LNG in the denominator. This CH₄-to-CO₂ ratio is multiplied by the ratio of the molar mass of methane to carbon (16/12) and the fuel carbon content of LNG (0.75); when multiplied together, this equals 1. Equation 2 then converts the fuel methane factor to methane slip by dividing the uncombusted methane by the sum of the combusted and uncombusted LNG.

Figure 26 shows the unadjusted results compared with the results presented earlier. The unadjusted results assume that all the CO₂ measured in the plume is a consequence of burning LNG, even though some of the CO₂ is from pilot fuel, fuel oil consumption for 2-stroke engines operating in diesel mode at low loads, and diesel auxiliary engines for LBSI ships. The unadjusted results are useful for understanding the sensitivity of the results to assumptions about pilot fuel consumption and main engine operations in diesel mode. Moreover, the unadjusted results demonstrate the lowest ship-level methane slip that could be calculated if one did not adjust for fuel oil consumption. While the unadjusted results do not account for CO₂ from non-LNG sources, they do eliminate the uncertainties quantified in the previous section, except for the uncertainty of the measured ratio of CH₄-to-CO₂ in the plume.

As expected, the unadjusted values result in lower estimates of methane slip because they treat all CO₂ as originating from LNG. For H2L4 ships, the unadjusted values are substantially lower than the adjusted values because two of the three data points are

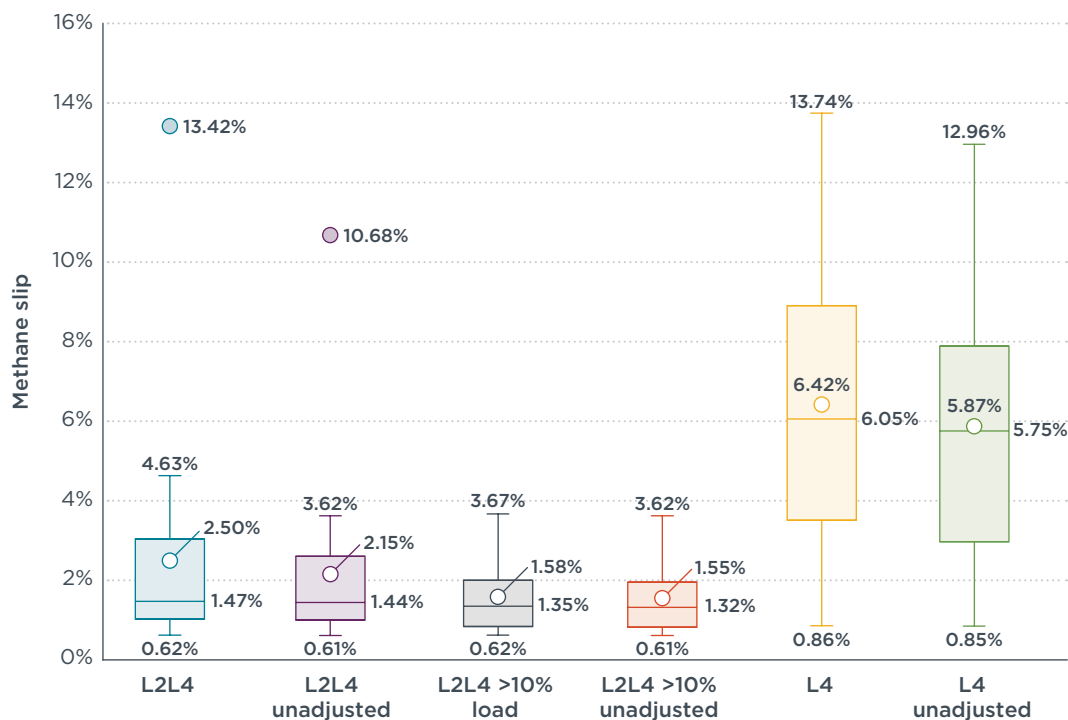
associated with low-load diesel-mode operations for the HPDF 2-stroke main engine. For L2L4, the two highest methane slip estimates are substantially lower because they are associated with low-load diesel-mode operations for the LPDF 2-stroke main engine. Note that the unadjusted data points are not always in the same rank order as the adjusted data points. For example, the second-highest adjusted methane slip estimate for L2L4 is 4.63% but is 2.24% unadjusted. The remaining adjusted and unadjusted estimates follow a similar range and distribution.



Note: H2L4 are ships with HPDF 2-stroke main engines and LPDF 4-stroke auxiliary engines; LBSI ships are those with only LBSI LNG-fueled engines; L2L4 are ships with LPDF 2-stroke main engines and LPDF 4-stroke auxiliary engines; L4 are ships are those with only LPDF 4-stroke engines.

Figure 26. Sensitivity analysis: Methane slip estimates with and without adjusting for CO₂ from fuel oil consumption from pilot fuel or for two-stroke dual-fuel engines in diesel mode.

Figure 27 shows the adjusted and unadjusted methane slip results for L2L4 and L4 ships. The maximum unadjusted methane slip for the L2L4 ship is 10.68% and the minimum is 0.61%, with a mean of 2.15% and median of 1.44%. These are lower than the adjusted values, as expected. However, the median values are similar: 1.47% for adjusted and 1.44% for unadjusted. For L2L4 ships operating >10% combined main engine load, there is less of a difference, and the maximum, minimum, mean, and median values are similar. For example, the mean is 1.58% adjusted and 1.55% unadjusted, and the median is 1.35% adjusted and 1.32% adjusted. For L4 ships, like L2L4, the unadjusted values are lower than the adjusted, as expected. The maximum unadjusted methane slip is 12.96%, compared with 13.74% adjusted, but the minimum values are the similar: 0.86% adjusted and 0.85% unadjusted. The unadjusted mean is 5.87%, while adjusted was 6.42%. The median values are 5.75% unadjusted and 6.05% adjusted.



Note: Dots show outliers; bars show minimum and maximum (excl. outliers); circle inside box is the average; horizontal line is the median; box is the interquartile range

Figure 27. Sensitivity analysis: Methane slip results for L2L4 and L4 ships with and without adjusting for CO₂ from fuel oil consumption from pilot fuel or for two-stroke dual-fuel engines operating in diesel mode.

Takeaways

An analysis of the plume campaign results yielded eight main takeaways:

1. Ships which exclusively use LPDF 4-stroke engines (L4) emitted the most methane slip.
 - a. L4 ships emitted the highest methane slip in our dataset, with a maximum of 13.74%, a mean of 6.42%, and a median of 6.05%.
 - b. For L4 ships, 77% of measurements were greater than 3.1% methane slip or 3.5% methane slip, which are the assumed default methane slip values for LPDF 4-stroke engines for the EU and the IMO, respectively.
 - c. Six of 22 measurements (27%) were associated with greater than or equal to 50% combined engine load and had a range of 3.89%–7.78% methane slip, and an average of 6.07%.
2. LPDF 4-stroke auxiliary engines increase ship-level methane slip for ships that use high or low pressure 2-stroke main engines (H2L4 and L2L4 ships).
 - a. The highest methane slip measurements for H2L4 and L2L4 ships occurred at main engine loads of <10%, when only the LPDF 4-stroke auxiliary engines were assumed to be operating on LNG.
 - b. For L2L4 ships, LPDF 4-stroke auxiliary engine LNG consumption is positively correlated with methane slip: every 10 percentage-point increase in auxiliary engine LNG consumption is expected to increase ship-level methane slip by 0.5 percentage points.
3. L2L4 ships emitted the lowest ship-level methane slip.
 - a. L2L4 ships emitted an average of 2.50% methane slip across all engine loads and 1.58% when operating above 10% main engine load. Median values were 1.47% and 1.35%, respectively.

4. H2L4 ships and LBSI ships require more data to fully understand how their ship-level methane slip compares to L2L4 and L4 ships.
5. Low-load operations can increase ship-level methane slip.
 - a. L2L4 ships had a maximum methane slip of 13.42%, a mean of 2.50%, and a median of 1.47% across 18 measurements; however, when considering only measurements with >10% combined main engine load, the maximum methane slip falls from 13.42% to 3.67%, the average decreases from 2.50% to 1.58%, and the median is reduced from 1.47% to 1.35%. This is because when operating with >10% combined main engine load, both the LPDF 2-stroke engines and the LPDF 4-stroke engines are expected to be operating in gas mode, whereas with a <10% combined main engine load, only the LPDF 4-stroke auxiliary engines are assumed to be operating on gas mode and the LPDF 2-stroke main engines would be expected to operate in diesel mode.
 - b. The highest methane slip measurements for H2L4 ships occurred at <10% main engine load, when the HPDF 2-stroke main engines were assumed to operate in diesel-mode, leaving only the LPDF 4-stroke auxiliary engines as the source of methane; however, we have only three measurements for these ships, two of which were <10% main engine load.
 - c. For L4 ships, five of the six highest methane slip estimates occurred at or below 12% combined main engine load.
 - d. The same ship with only one LPDF 4-stroke main engine had 12% methane slip at approximately 10% engine load and 7% methane slip at approximately 60% engine load.
6. Engine age (using ship build year as a proxy) is not statistically associated with methane slip for L2L4 and L4 ships.
 - a. For L2L4 ships, the confounding influence of LPDF 4-stroke auxiliary engines and only a four-year spread of ship build years may affect our ability to detect any relationship between the age of the ship and its methane emissions, if there is one.
 - b. For ships which use exclusively LPDF 4-stroke engines (L4), several engines could be operating at different engine loads and, therefore, emitting different methane slip, which could make it harder to detect any relationship between methane slip and build year. This can be the case if the influence of engine load is greater than the influence of build year on methane emissions.
7. Ships with dual-fuel engines were shown to achieve low NO_x emissions without the use of exhaust aftertreatment technology such as SCR and EGR.
 - a. 86% of measurements were below 3.4 g NO_x/kWh and 62% were below 2.0 g NO_x/kWh.
 - b. Ships with L2L4 engines showed both low NO_x and low methane slip.
8. The results are robust, despite the uncertainties.
 - a. The distribution, range, mean, and median values for our estimates of methane slip, which account for CO₂ from non-LNG sources, are similar to unadjusted methane slip estimates for L2L4 and L4 ships that do not account for CO₂ from non-LNG sources. Unadjusted estimates would be the lowest methane slip that could be calculated based on the raw data.

ONBOARD CAMPAIGN RESULTS

Drone and in-stack comparison

Table 10 shows the tests and load points that were set for the LPDF 4-stroke engine that was measured (ME4) on the Aurora Botnia roll-on/roll-off passenger ferry. Simultaneous measurements with the drone in the plume and onboard in the stack were conducted at these points while the ship was at berth. For more information on the ship and engines, refer to Table 3 and Table 4 in the methods section.

Table 10. Tests to compare the drone measurements and in-stack measurements of methane emissions from one LPDF 4-stroke main engine. The other main engines and boilers were shut down during these tests.

Date [dd.mm.yyyy]	Time engine room (CEST, UTC+2)	Engine load, based on control room screen [%]	LNG fuel consumption based on engine screen [kg/h]
31.05.2023	17:50	19	149
31.05.2023	17:59	44	313
01.06.2023	10:42	21	171
01.06.2023	11:00	45	315
01.06.2023	11:06	34	247
01.06.2023	15:06	73	490
01.06.2023	15:18	46	324
01.06.2023	19:27	62	427
01.06.2023	19:36	57	392

The results of the comparison between the in-stack measurements with FTIR and the drone sensors are depicted in Figure 28 and Figure 29, which compare the measured molar ratio of CH₄ to CO₂ and NO_x to CO₂, respectively. Both plots show a linear regression with FTIR as the explanatory variable (x-axis) and the drone as the dependent variable (y-axis). Although the results obtained with the FTIR are subject to uncertainty, we do not use a regression model with a stochastic regressor because the precision of the FTIR is considered significantly higher than the one of the drone, which also includes the influence of weather conditions. For both regressions, the calculated parameters with their 95th percentiles are given. Furthermore, the confidence and prediction intervals at the 95% level are plotted in magenta and cyan lines respectively. The determination of these intervals is based on the assumption of stochastic uncertainties which lead to deviations between the model and the measurements. The deviations are modeled as an independent and identically normally distributed random variable.

The plot in Figure 28 shows that there is a linear relationship between the drone and in-stack measurement of the molar ratio of CH₄ to CO₂, with a coefficient of 0.974 ± 0.132 , a constant of 0.000 ± 0.006 and a correlation coefficient (*r*) of 0.957. Practically, this means that there is a one-to-one relationship between the methane slip we measure in the stack with the methane slip we measure by the drone. Additionally, the standard deviation of ± 0.132 is well-aligned with the assumption of a 15% standard deviation for the CH₄-to-CO₂ ratio in Table 9.

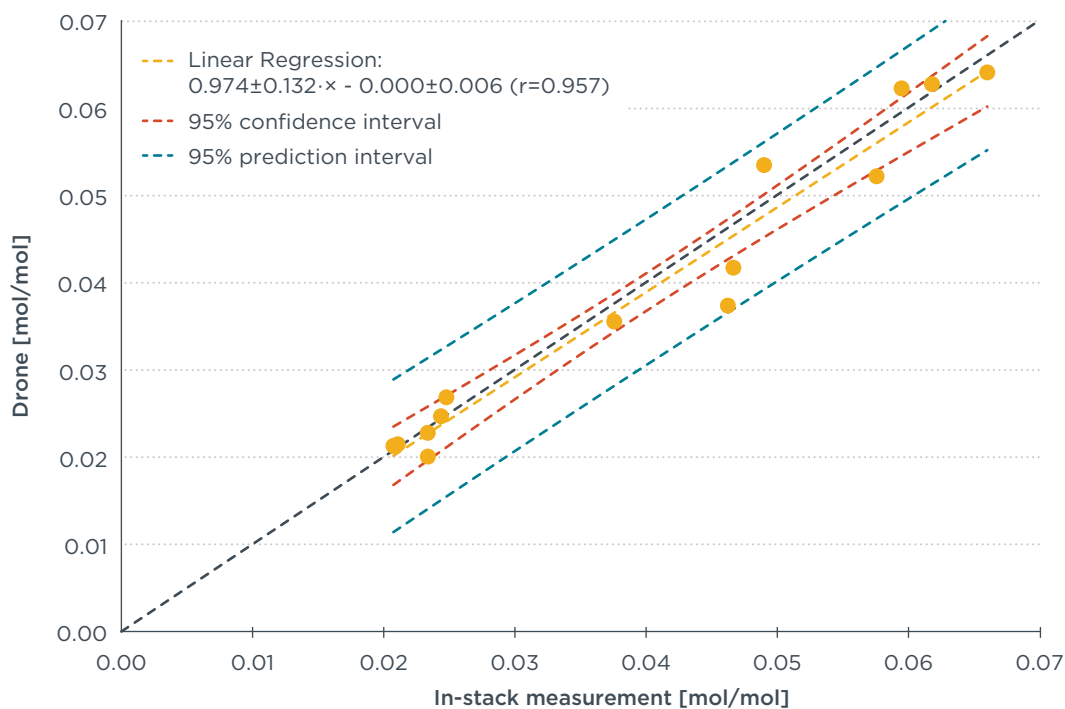


Figure 28. Plot of the linear regression of the measurement of the ratio of CH_4 to CO_2 [mol/mol] with the in-stack measurement (FTIR) as explanatory variable (x-axis) and the drone measurement in the plume as the dependent variable (y-axis).

Figure 29 shows a correlation between the drone and in-stack measurement of NO_x per CO_2 in mol/mol ($r = 0.941$) with some linearity, indicated by a coefficient of 0.631 ± 0.102 and a constant of 0.001 ± 0.001 . The drone measured less NO_x per CO_2 in the plume than the FTIR measured in the stack, especially at higher concentrations in the measurement range corresponding to low engine loads. The measurements are concentrated in the range from 0.0045–0.007 where the deviation of the drone measurements from in-stack is 0.001 mol/mol (roughly 0.5 g/kWh), with exception of one point at about 0.012 where the deviation from the in-stack instrument is the largest with 0.0035 mol/mol (roughly 2 g/kWh).

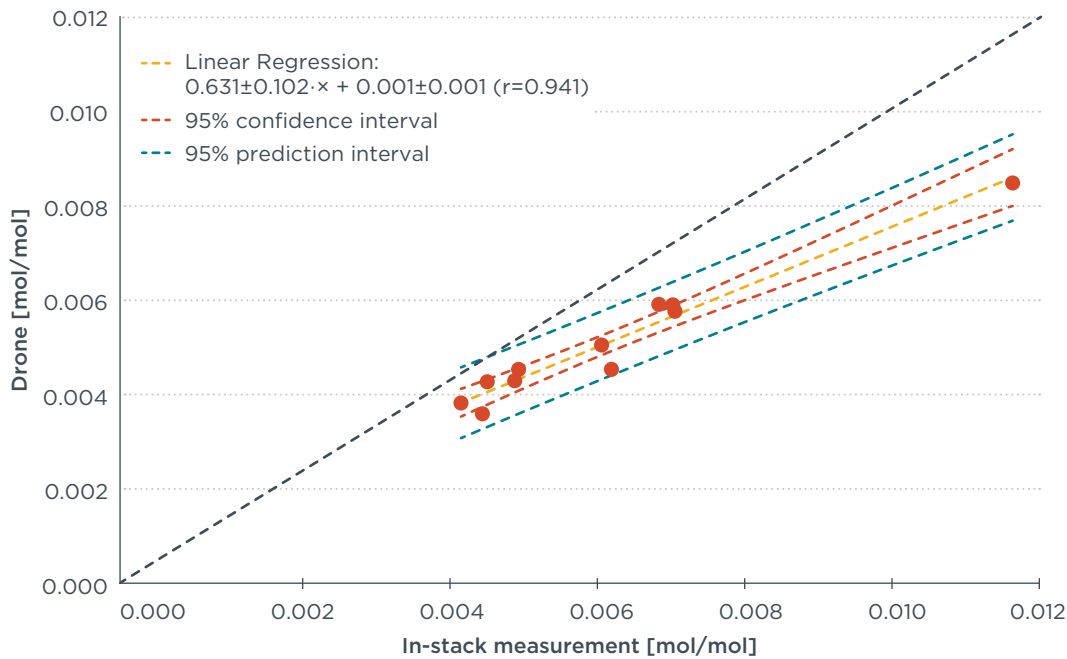


Figure 29. Plot of the linear regression of the measurement of the ratio of NO_x/CO_2 [mol/mol] with the in-stack measurement (FTIR) as explanatory variable and the drone as the dependent variable.

In-stack work specific emissions

Since the exhaust mass flow could not be measured directly during the onboard campaign, it was determined from the fuel mass flow to be able to report work-specific mass emissions of CO_2 , CH_4 , NO_x , and CO . The exhaust mass flow of CO_2 in the stack was calculated by using Equation 6:

Equation 6. Mass flow of carbon dioxide

$$\dot{m}_{\text{CO}_2} = C_{f_{\text{LNG}}} \times \dot{m}_{\text{LNG}} + C_{f_{\text{MDO}}} \times \dot{m}_{\text{MDO}}$$

Where \dot{m}_{CO_2} , \dot{m}_{LNG} , and \dot{m}_{MDO} denote the mass flows of CO_2 , LNG, and pilot fuel, respectively.

The carbon conversion factors of LNG and pilot fuel $C_{f_{\text{LNG}}} = 2.750$ and $C_{f_{\text{MDO}}} = 3.206$ were used, respectively. LNG mass flow (kg/h) and engine power were obtained from the screen in the engine control room. The pilot fuel mass flow was tabulated using Wärtsilä engine documentation for the load range 50%–100%.¹⁴ The pilot fuel mass flow (kg/h) is almost the same for each load point in this range. For lower loads the same mass flow was used. It was confirmed by Wärtsilä that the mass flow is roughly the same across the load range.

The work-specific exhaust mass flow of CH_4 , NO_x and CO is obtained from the CO_2 mass flow by multiplying with the ratio of concentrations and the ratio of molar masses according to Equation 7:

Equation 7. Work-specific exhaust mass flow

$$\dot{m}_{\text{gas}} = \dot{m}_{\text{CO}_2} \times \frac{[\text{gas}]}{[\text{CO}_2]} \times \frac{M_{\text{gas}}}{M_{\text{CO}_2}}$$

Where $[\]$ and M , Denote the volume concentration and the molar mass of an exhaust component.

¹⁴ <https://www.wartsila.com/marine/engine-configurator>

We measured this engine near the D2 test cycle load points of 10%, 25%, 50%, 75%, and 100% engine load. The D2 cycle is part of the NO_x certification procedure for engines used as constant-speed auxiliary engines contained in the IMO NO_x Technical Code 2008 (International Maritime Organization, 2008). When this engine is used as a main engine, it is certified under the E2 cycle for constant-speed main propulsion applications. The E2 cycle measures emissions at 25%, 50%, 75%, and 100% load, but not 10% load, and the weighting factors at each test mode point are different for the D2 and E2 cycles. The D2 cycle weights the emissions at each load point as follows: 0.1 at 10% load; 0.3 at 25% load; 0.3 at 50% load; and 0.25 at 75% load; and 0.05 at 100% load. The E2 cycle weights emissions at each load point as follows: 0.15 at 25% load; 0.15 at 50% load; 0.50 at 75% load; and 0.20 at 100% load. Thus, the E2 cycle weights emissions at higher engine loads more than the D2 cycle. The D2- and E2-weighted results for methane slip and NO_x are presented in Table 11.

The resulting work-specific mass emissions of CO₂ are depicted in Figure 30. The blue dots represent the average value in bins of a width of 10% engine power (e.g., 10%–20% engine load is binned to 15%; 20%–30% is binned to 25%, etc.) and the whiskers mark the range of one standard deviation. Specific mass emissions during the different load points of the D2 cycle measured during this campaign are also shown. As will be the case for the other images of the current section, the onboard results of Lehtoranta et al. (2023) have been added for reference.

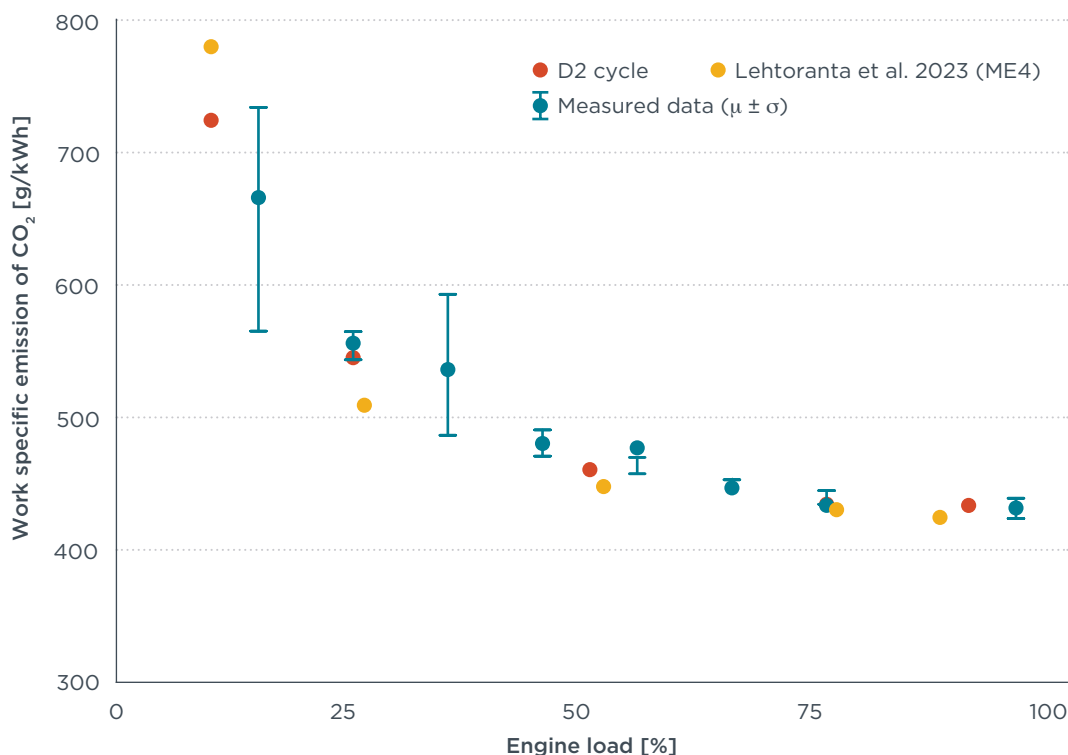


Figure 30. Work-specific CO₂ measured from the stack under constant engine loads for the D2 cycle and binned by engine load for all the measured data, which also contains data from transient operations near that load. Results are compared to a different campaign conducted on the same ship and engine (Lehtoranta et al., 2023). The result is calculated from the broadcasted fuel flow, an estimate of the pilot fuel rate, the fuels’ carbon content, and broadcasted engine power.

The trend of CO₂ mass emissions over the D2 cycle can be compared with Lehtoranta et al. (2023), who measured emissions on the same cycle on the same engine. The CO₂ trends for the D2 cycles are similar between our study and theirs but there is a clear difference at lower loads. Two possible explanations are the uncertainty regarding the amount of pilot fuel used and the fact that neither fuel flow nor engine power have been measured directly but have been read from screens in the engine room. In

the load bin between 30% and 40% engine load, only a limited amount of data were available and mainly at transient conditions. Therefore, the standard deviation is higher in this range.

The work-specific methane emissions are presented in Figure 31. The work-specific methane emissions and the methane slip are highest at low engine loads, at around 13 g/kWh (equivalent to 6.1% methane slip; see Table 11) and decrease towards high engine loads to around 3.5 g/kWh (equivalent to 2.3% methane slip). This is a common trend for LPDF 4-stroke engines. The level is comparable to the values reported in Lehtoranta et al. (2023) for the same engine, but at the lower end of those reported by others on different LPDF 4-stroke engines (e.g., Ushakov et al., 2019). For low engine loads, the results of both the D2 cycle and all measured data are somewhat higher than reported in Lehtoranta et al. (2023). The spread and deviation of all measured data is large in the low to medium load range, but this may be due to transient conditions which may cause a spread and an average increase of actual CH₄ emissions. The D2 cycle load points represent stable engine loads, like the results presented by Lehtoranta et al. (2023) and thus can be compared.

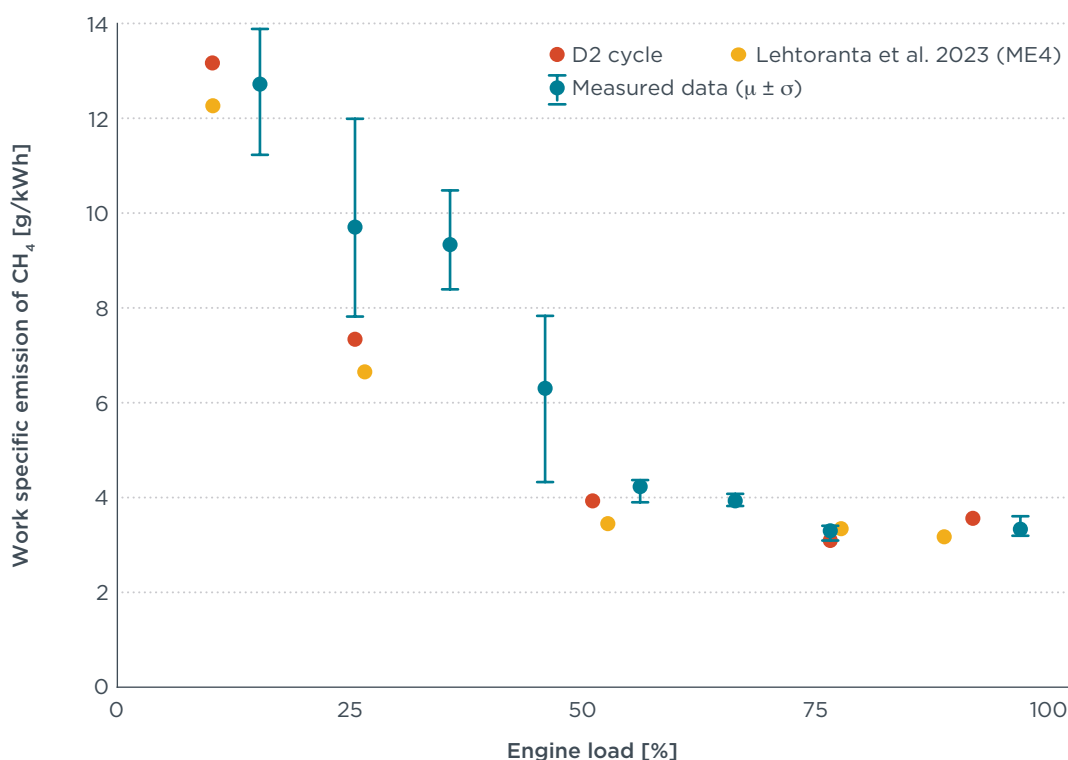


Figure 31. Work-specific CH₄ emissions measured in the stack under constant engine loads for the D2 cycle and binned by engine load for the measured data, which also contains data from transient operations near that load. Results are compared to a different campaign conducted on the same ship and engine (Lehtoranta et al., 2023).

Figure 32 depicts the work-specific mass emissions of NO_x. There is good agreement the measurements of Lehtoranta et al. (2023) across most engine loads. Only at the lowest load bin of the D2 cycle there is a significant difference. The spread of work-specific NO_x emissions is very large at 40% engine load and below. This is due to transient conditions which can cause a spread in actual emissions but also make time alignment more difficult.

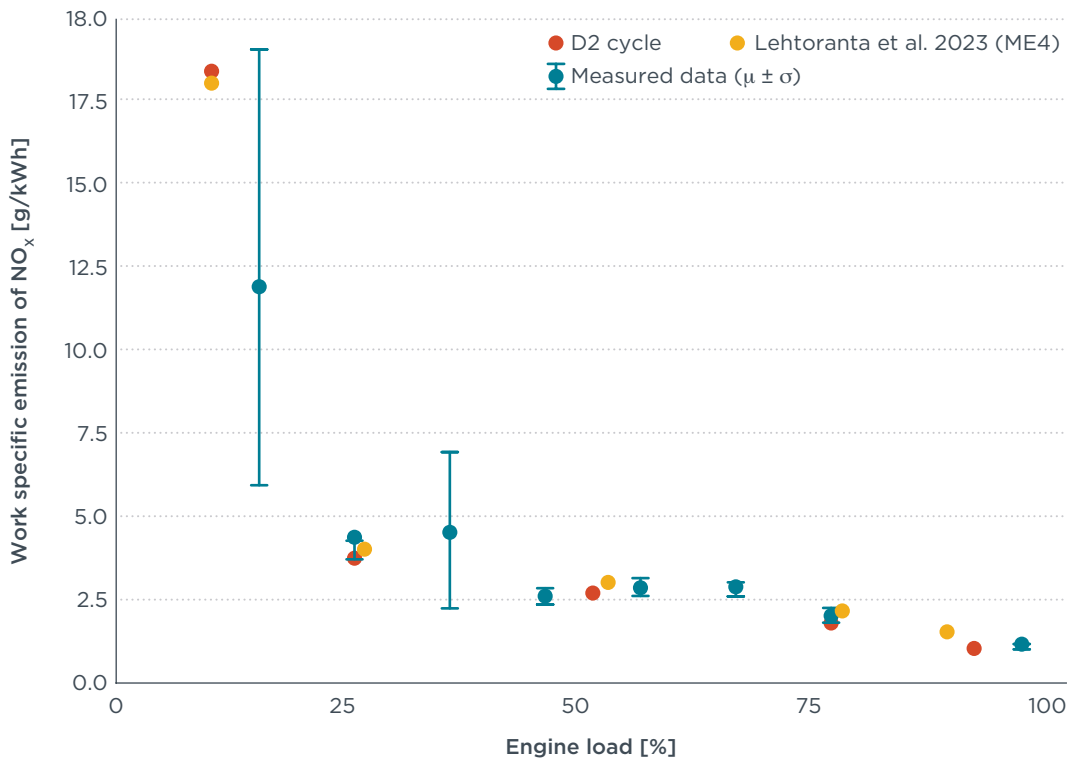


Figure 32. Work-specific NO_x emissions measured in the stack under constant engine loads for the D2 cycle and binned by engine load for the measured data, which also contains data from transient operations near that load. Results are compared to those of a different campaign conducted on the same ship and engine (Lehtoranta et al. 2023).

The work-specific mass emissions of CO are plotted in Figure 33. At high loads there is good agreement with Lehtoranta et al. (2023), but our measured values in the low and medium load range are higher.

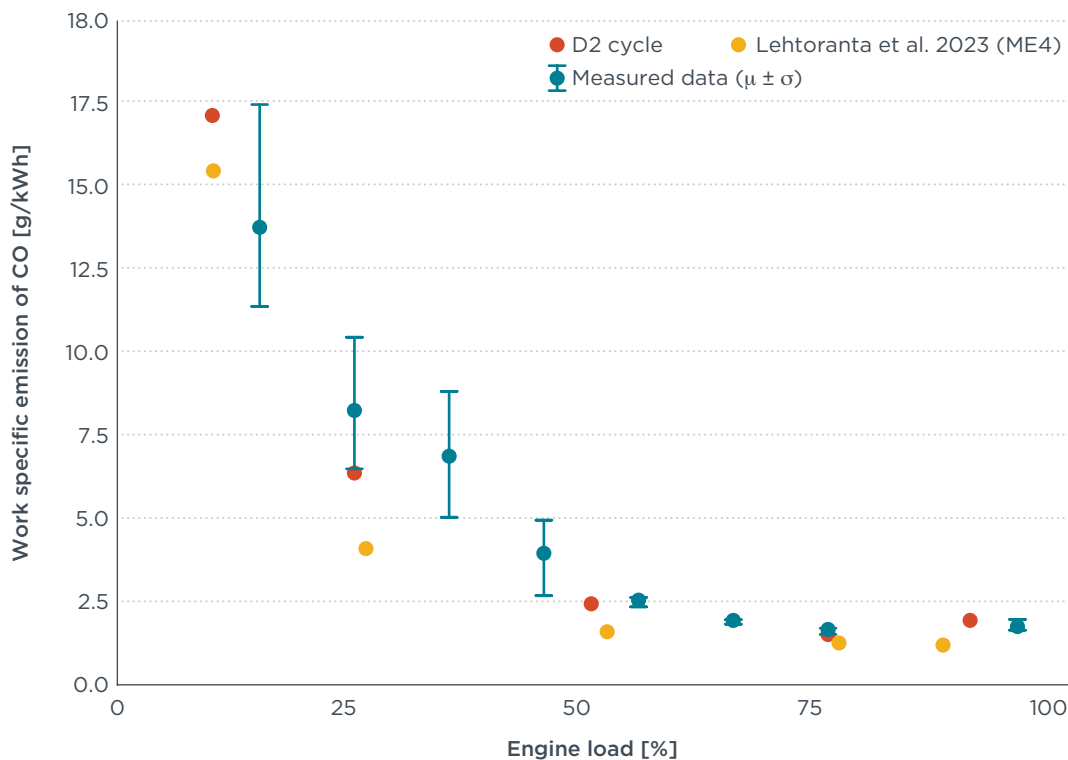


Figure 33. Work-specific CO emissions as measured from the stack over various constant engine loads and off all measured data binned, which also contains data from transients. Engine load points are shown of the D2 test cycle, as binned data from all measurement data as tested during the campaign and of a different campaign conducted on the same ship and engine (Lehtoranta et al. 2023).

In-stack methane slip

Methane slip results are depicted in Figure 34. The blue dots mark the average of the instantaneous methane slip, and the whiskers span a range of one standard deviation. The highest average methane slip of nearly 7% occurs at the lowest load bin centered on 15% engine load. The minimum methane slip values, which are just above 2%, occur at the 75% and 95% load bins. At 50% engine load on the D2 cycle and in the 55% engine load bin for all measured data, methane slip is approximately 2.5%. Like previous results, the spread is lower at high engine loads, which correlate with more stable operating conditions, and higher at lower engine loads, when there tend to be more transient operations. We observe that the methane slip measured on the D2 cycle, which were done at constant engine loads, were generally lower than the binned measurement data, which include transient engine loads. This is especially pronounced at lower engine loads. The D2 measured methane slip was slightly higher than the binned measurement data at the highest engine load points.

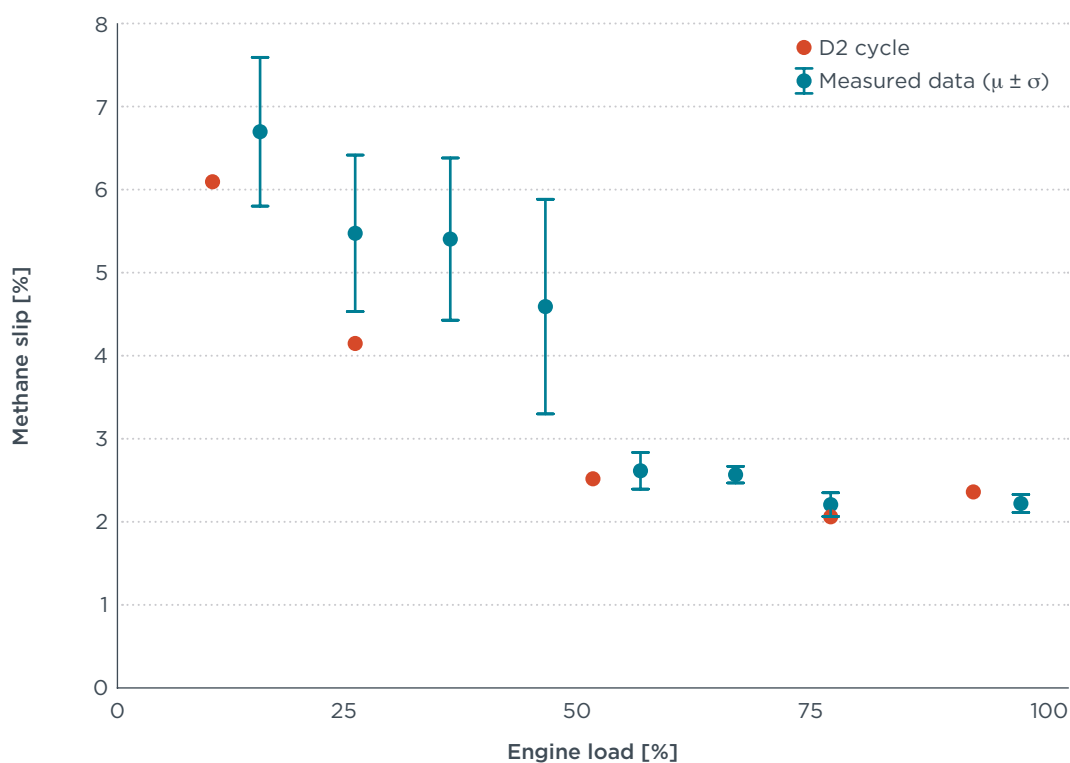


Figure 34. Methane slip measured on the D2 cycle and all measured data binned by engine load (e.g., the first bar is centered at 15% engine load, the second at 25% engine load, etc.).

D2/E2 test cycle

A test sequence based on the D2 test cycle was included in the program. The D2 cycle is meant for constant speed auxiliary engines, such as the ones used in generator sets. For constant speed propulsion engines, the E2 cycle is used. Aurora Botnia engines are certified on both the E2 and D2 test cycles.¹⁵ The D2 cycle consists of five modes to be tested, each at a different constant engine load (100%, 75%, 50%, 25%, and 10%) but at the same engine speed (rpm). The E2 cycle does not include the 10% load point and uses different weighting factors to calculate the final result. It should be noted that the test cycles provide little or no incentive for manufacturers to reduce NO_x emissions below 25% engine load. When engines are certified to Tier III requirements, which these engines are, the NO_x emissions at each individual test cycle load point cannot exceed

¹⁵ For details see ISO 8178 (ISO 8178, 2020) and NO_x technical code chapter 3.2.

the weighted average limit value by more than 50%. This requirement applies to all load test points except for the 10% load point of the D2 cycle.

At the ship, the engine could not be set to the highest load setting of 100% due to the ship control system, which is calibrated to start the next engine if more power is needed. As such, 92% was the highest attainable load, and was, therefore, used as maximum load for the D2 test cycle. The lowest attainable load setting was 11%, just above the 10% D2 test point. The constant loads were run from high to low after each load change, allowing engine temperatures to stabilize. The last 60 seconds of each mode were used to determine the average concentrations of CO₂, CO, CH₄, and NO_x. Because the conditions during the onboard measurements do not fulfil all the requirements of a valid test cycle, the calculated NO_x emissions over the D2 and E2 cycle are only indicative.

Table 11 shows the measurement results for the mode points of the D2 cycle and the weighted results for the applicable D2 and E2 cycle. The g/kWh emissions are calculated based on the CH₄ and CO₂ concentrations measured in the exhaust stack, the LNG fuel mass flow rate and engine power from the engine room data screen, and pilot fuel consumption rates from the engine manufacturer.

The absolute methane emissions increase with higher engine load, ranging from 6.6 kg/h at the lowest load to 14.3 kg/h to the highest load. NO_x emissions are highest (9.1 kg/h) at the lowest load and lowest (4.2 kg/h) at the highest load and vary between 4.3 and 6.1 kg/h at other load points. Note that NO_x emissions are presented as measured and are uncorrected for humidity and temperature. The final weighted work-specific CH₄ emissions are 4.3 g/kWh or 2.7% on the D2 cycle and 3.5 g/kWh or 2.0% on the E2 cycle. NO_x emissions are 2.7 g/kWh (D2) and 1.8 g/kWh (E2). Because this ship has a keel-laid date in 2020, it only needs to achieve Tier II NO_x compliance with a limit of 9.6 g/kWh. Since the formal procedure for onboard NO_x verification was not applied, the result for D2 and E2 cycle weighted NO_x needs to be regarded as indicative; however, we can conclude that the engine is likely complying with its required Tier II NO_x limits because the weighted D2 and E2 values are well-below the weighted Tier II limit. It is also likely that the engine would comply with Tier III under the E2 cycle.

The NO_x g/kWh at 11% engine load is an order of magnitude higher than what we measured at 77% load. This is consistent with literature showing that NO_x emissions from marine engines operating on all fuels, not just LNG, are highest below 25% engine load (Comer et al., 2023). NO_x values below 25% engine load are usually not used for certifying engines, except for when an engine is used as a constant-speed auxiliary engine and therefore certified under the D2 cycle. When a low load test point (10% engine load) is used for NO_x certification, as in the D2 cycle, it is only weighted 0.1, meaning emissions at this test point represent a relatively small component of the overall weighted emission factor.

Table 11. Results over the D2 cycle modes and the weighted result of NO_x and CH₄ emissions and methane slip for the D2 and E2 cycle.

Load ^a [%]	D2 weighting factors	E2 weighting factors	Generator Power ^a [kW]	Engine Power ^b [kW]	Fuel (LNG) ^a [kg/h]	Fuel (pilot) ^c [kg/h]	CH ₄ rate [kg/h]	CH ₄ [g/kWh]	CH ₄ slip	NO _x ^e [kg/h]	NO _x ^e [g/kWh]
92	0.05	0.2	3938	4031	608	19.8	14.26	3.54	2.3%	4.15	1.03
77	0.25	0.5	3332	3410	512	19.5	10.49	3.08	2.0%	6.10	1.79
50	0.3	0.15	2179	2239	350	19.6	8.75	3.91	2.5%	6.00	2.68
26	0.3	0.15	1094	1152	204	19.6 ^d	8.41	7.30	4.1%	4.29	3.73
11	0.1		455	500	108	19.6 ^d	6.55	13.10	6.1%	9.12	18.24
D2 weighted result								4.3	2.7% ^f		2.7
E2 weighted result								3.5	2.0% ^f		1.8

^a From engine data screen.

^b Engine output power is calculated from the specified generator efficiency at given loads.

^c From <https://www.wartsila.com/marine/engine-configurator> (8V31DF).

^d Pilot fuel consumption for these engine load setting are assumed to be the same as for the higher loads ones provided in^c. Pilot fuel consumption is said to be approximately constant across the engine load range, according to Wärtsilä personnel.

^e NO_x emissions are presented as measured without corrections. Formally, according to the IMO NO_x verification procedure, measured NO_x needs to be corrected for ambient temperature and humidity and the air charge is to be referenced to 25^oC sea water temperature. We prefer to present actual NO_x emissions as measured.

^f Weighted based on fuel consumption instead of engine work.

Carbon dioxide equivalent emissions

Methane is a stronger GHG than carbon dioxide; the global warming potential (GWP) of methane over 20 years (GWP20) is 82.5 and its 100-year GWP (GWP100) is 29.8 (Intergovernmental Panel on Climate Change, 2021). The work-specific carbon dioxide equivalent emissions of CO₂ and CH₄ emitted by the engine using all measurement data are presented in Figure 35. The left stacked bar in each load bin represents the CO₂ equivalent emissions of CO₂ and CH₄ using GWP20, whereas the right bar shows the same using GWP100. While the work specific emission of CO₂ stays the same (GWP always equals 1.0, no matter the timeframe), the contribution of CH₄ is higher, especially when considering methane's 20-year GWP.

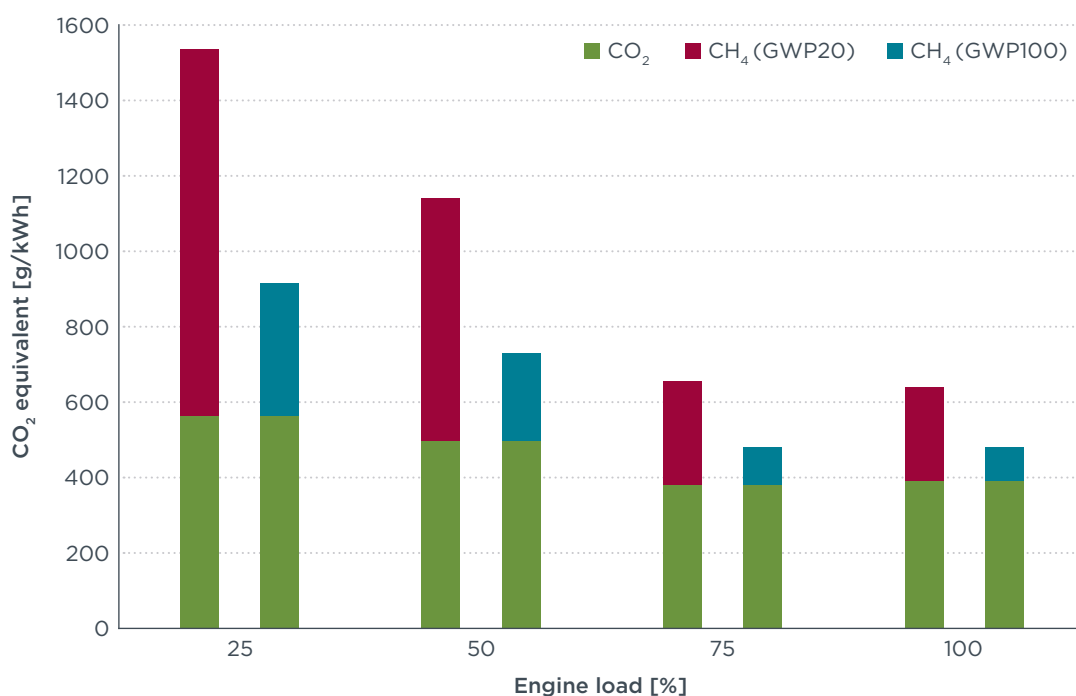


Figure 35. CO₂-equivalent emissions based on the GWP of CO₂ and CH₄ emissions per engine load bin using all measured emissions data.

The CO₂ equivalent emissions rate in kg/h shows the inverse behavior compared to the work-specific emissions (g/kWh), as shown in Figure 36. The emissions rate increases with engine load. This is due to increased hourly fuel consumption as engine load increases, which increases CO₂ emissions.

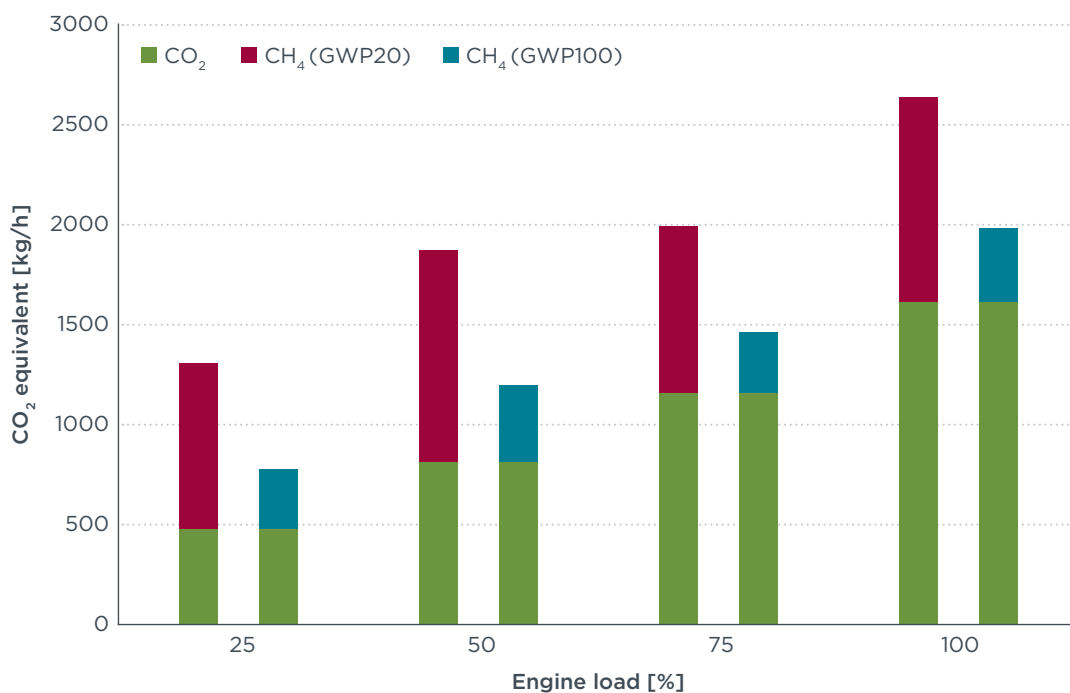


Figure 36. CO₂-equivalent emissions in kg/h based on the GWP of CO₂ and CH₄ per load bin using all measured emissions data.

Whole trip emission trends

The exhaust gas concentrations of various gases measured over the trip are shown in Figure 37. Concentration peaks can be observed for CH₄ and NO_x after engine start and when the engine operation is transient or changing load.

After the main engine is started, the ship can sail at a fixed engine load almost immediately while exiting the port. During the trip, engine loads are mostly stable but can change depending on requested power for maintaining the cruising speed and charging the onboard batteries. At the end of the trip, the engine runs in a more transient manner as the ship maneuvers into the quay. Figure 38 shows that, with exception of the final maneuvering, the engine load of ME4 is mostly stable and starts at about 90%. Figure 39 shows that the other engine (ME2) is switched on, causing the load of both engines drop to around 70%. Later in the trip, ME2 is switched off and ME4 load increases to about 90%. Toward the end of the trip, ME2 is switched on again, causing both engine loads to fall. When the ship is maneuvering, the load of both engines drop to 15%-25%. Note that the proportion of time spent at different load points varies from the weighting factors applied to both the D2 and E2 test cycles, with a greater proportion of time spent at higher engine loads than implied by the weighting factors. The engine measured (ME4) was operated at around 90% load for about half of the time (46%) and around 70% load for about one-third of the time (32%), compared to D2 weighting factors of 0.05 at 100% load and 0.25 at 75% load, and E2 weighting factors of 0.2 at 100% load and 0.5 at 75% load. Conversely, Comer et al. (2023) found that ships tend to operate at lower engine load ranges than implied by the E2 test cycle. This suggests that the weighting factors that are used to estimate emissions from marine engines may need to be individualized depending on how the engine is intended to be used.

Less methane is emitted when one engine is running at high load compared to two engines each at lower loads. The same is true for fuel consumption. The hybrid powertrain of the ship enables flexible use of the main engines by switching on auxiliary engines depending on the power need, while keeping engines at high load to optimize fuel consumption and to reduce methane slip.

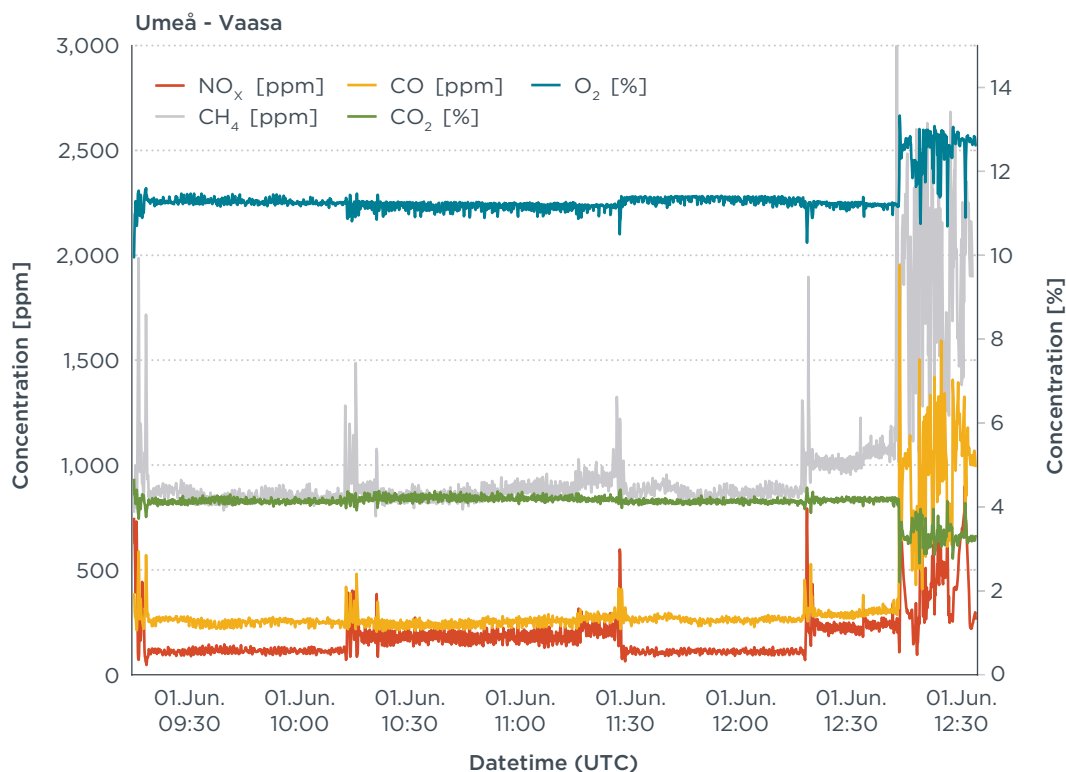


Figure 37. Concentration of exhaust components during a trip from Umeå to Vaasa.

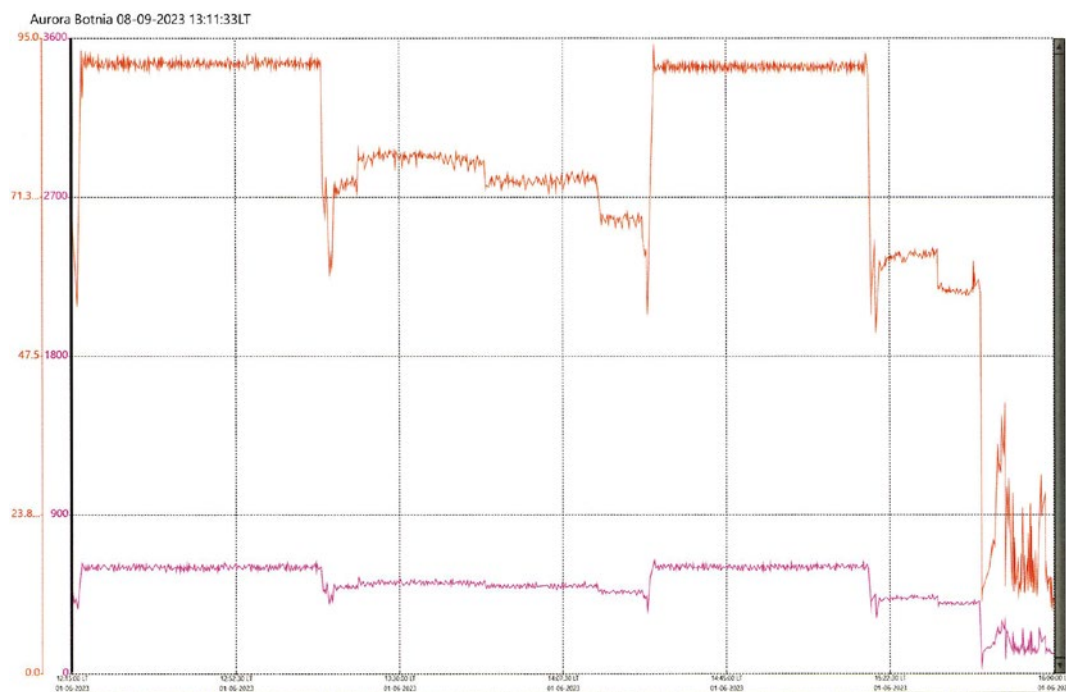


Figure 38. Screen of the engine load and fuel consumption of Main Engine 4 during a trip from Umeå to Vaasa. Orange line represents engine load in % of ME4. The pink line represents the fuel consumption of ME4 in kg/h.

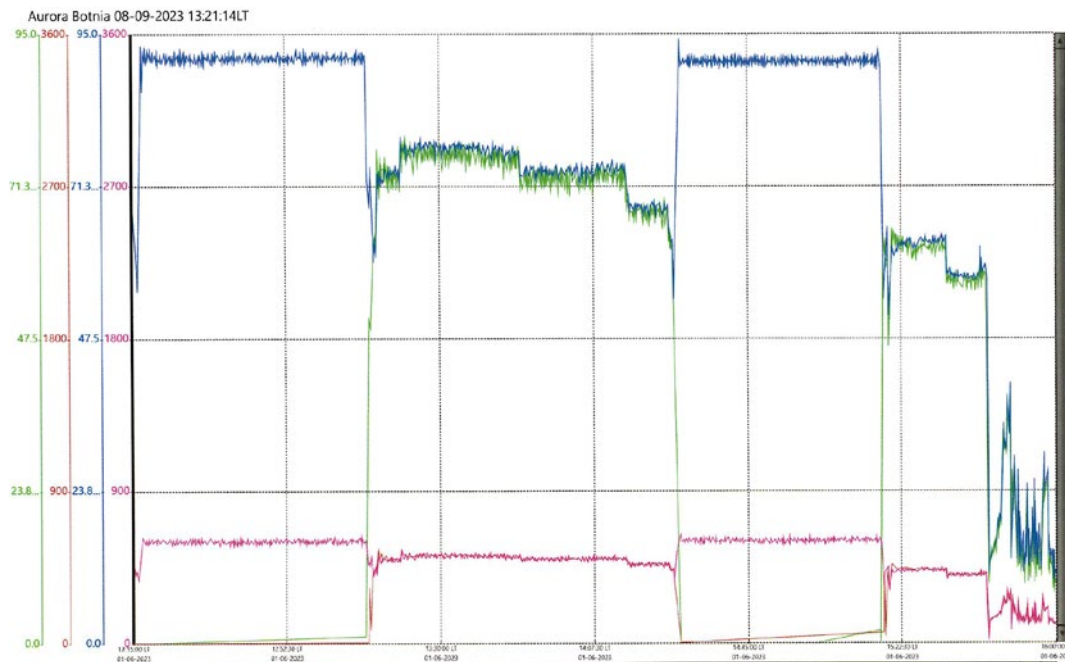


Figure 39. Screen of the engine load and fuel consumption of ME2 and 4 during a trip from Umeå to Vaasa. Blue line (ME4) and green line (ME2) represent load in %. Pink (ME4) and red (ME2) represent gas consumption in kg/h.

Takeaways

Onboard key takeaways:

1. A modern LPDF 4-stroke engine can emit lower methane slip than the default EU and IMO values.
 - a. When measured on the D2 test cycle under constant engine loads, methane slip ranged from a minimum of approximately 2% at 77% load and 2.3% at 92% load, to about 4% at 26% load and 6% at 11% load. Methane slip was 2.5% at approximately 50% engine load, which is lower than the EU assumption of 3.1%.
2. Real sailing emissions can be higher than those measured using an onboard test-cycle.
 - a. When measuring real sailing emissions, methane emissions at lower loads tended to be higher than emissions measured at similar load points on the test cycle. While the minimum methane slip under real sailing conditions was similar at and above 50% engine load, it was higher at and below approximately 25% load compared to the test cycle. Real-sailing methane slip near 25% load was approximately 5.5%, on average, compared to 4% on the D2 cycle. Real sailing emissions measured near 15% load were approximately 6.7%, compared to 6.1% near 10% load on the D2 cycle.
3. Methane slip decreases as engine load increases.
 - a. Methane slip varies with engine load; the highest methane slip was measured at low engine load and decreased towards the highest load. This means that the lower the load is, the higher the fraction of the fuel that leaves the stack unburned. For work specific methane emissions, the trend is the same.
 - b. Due to the increase of fuel consumption with engine load, the absolute methane emissions measured from the stack are the lowest at constant low loads and increase towards high constant loads. Methane slip was much more variable below 50% engine load than above 50% engine load; this seems to be caused by the transient operation of the engine in this load range.

- c. The hybrid diesel-electric propulsion system with four main engines used on the Aurora Botnia enabled optimized engine loads for higher fuel efficiency and lower methane slip by avoiding low load operations for most of the trip. Wasaline applies this strategy on their daily trips.
4. Real engine load distributions did not match test cycle weighting factors.
 - a. We observed that the engine mainly operated at high loads, spending about 46% of the time at about 90% load and 32% of the time at around 70% load, compared to D2 weighting factors of 0.05 at 100% load and 0.25 at 75% load, and E2 weighting factors of 0.2 at 100% load and 0.5 at 75% load.
5. NO_x emissions are highest at low engine loads.
 - a. Work-specific NO_x emissions were 18.2 g/kWh at 11% engine load compared to just 1.0 g/kWh at 92% load and 1.8 g/kWh at 77% engine load, meaning that NO_x emissions were ten-times higher at 11% engine load compared with those at and above 77% engine load. There is little or no incentive to reduce NO_x emissions below 25% load because the E2 cycle does not contain a test point below 25% load and the D2 cycle weights the emissions at 10% load by a factor of only 0.1.
 - b. Absolute NO_x emissions were 9.12 kg/h at 11% engine load compared with 4.15 kg/h at 92% engine load, despite fuel consumption being six-times greater at 92% load compared with 11% load.
6. Transient operations temporarily increase both methane and NO_x emissions.
 - a. We observed peaks of CH₄ and NO_x concentrations when the engines switched from one operating mode to another (e.g., ~70% load to ~90% load) and during maneuvering.
7. Other engine technologies and emissions sources should be measured.
 - a. Additional measurements of CH₄ from sea-going ships with other representative main engine types, such as the LPDF 2-stroke and HPDF 2-stroke, plus their LPDF 4-stroke auxiliary engines would provide a more complete representation of emissions. Other methane sources onboard of ships, such as the crankcase ventilation, should also be measured.

Drone validation key takeaways:

8. Drone-mounted sensors can effectively measure methane slip.
 - a. Although drone measurements are considered less accurate than in-stack measurements, they showed good correlation ($r = 0.957$) and linearity (linear regression coefficient = 0.974) with the in-stack measurements for the observed CH₄-to-CO₂ ratios in the range measured onboard.
9. Drone-mounted sensors may underestimate NO_x emissions.
 - a. The correlation to the in-stack measurement was good ($r=0.941$), but the linearity was poor (linear regression coefficient = 0.631), suggesting that drone measurement underestimates NO_x emissions in the range measured in this study.

CROSS-INSTRUMENT COMPARISON (ON-LAND) RESULTS

Before investigating the correlation between the remote plume measurement by the drone and in-stack measurement onboard, a cross-instrument comparison was first conducted in a land-based experimental set-up to study the correlation and reliability of the remote measurements in comparison to measurements in the exhaust stack. More details on the experimental set up can be found in the methods section and in a separate report (Paschinger et al., 2023). The CH₄ to CO₂ concentration ratios as measured by the drone in an exhaust gas plume was compared to a reference measurement of the concentrations in the tailpipe and known quantities of methane

injected in the exhaust gas. As a basis for comparison of in-stack and remote measurement data, the emissions of CH₄ and NO_x have been determined as their respective ratios to the concentration of CO₂ in the exhaust. The results are depicted in Figure 40. The averages of the PEMS data during the time slots when the drone was moved through the exhaust plume have been calculated and are depicted as violet bars. The calculated average ratios as determined by the drone are depicted as blue bars with the duration of the respective flight.

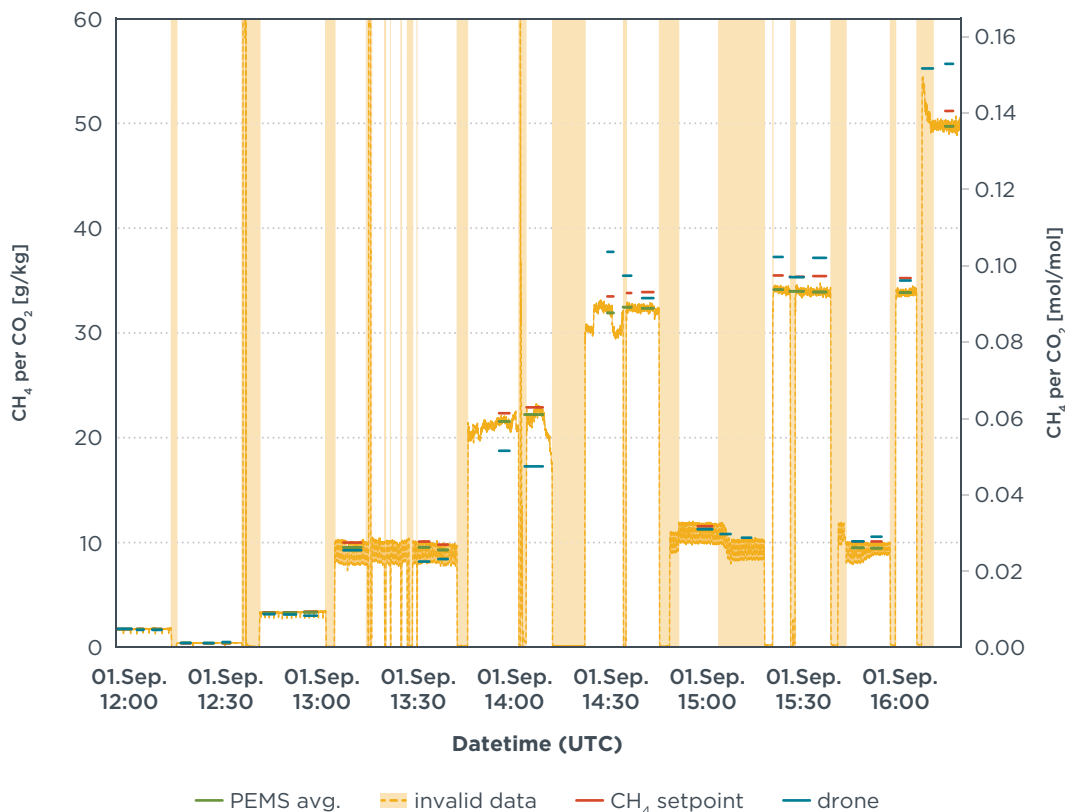


Figure 40. Methane emissions expressed per unit of CO₂ in g/kg and mol/mol as adjusted and measured by the mass flow controllers (CH₄ setpoint), as measured by PEMS and as measured by the drone for the various methane slip levels selected in the program.

A comparison of the in-stack PEMS and drone measurements to the setpoints is shown for methane in Figure 41. A comparison of the in-stack measurements by PEMS and the remote results obtained by the drone is depicted for methane in the scatter plot in Figure 42. A linear regression suggests that the remote measurements yield somewhat higher values of CH₄ per CO₂ compared to in-stack measurements, although the actual drone measurements are sometimes lower or higher compared to in-stack. The readings of the in-stack measurement differ by less than 0.004 mol CH₄ per mol CO₂ from the values calculated based on the methane mass flow controller setting and the measured exhaust mass flow. The relative deviations are generally within ±5%, but there are a few outliers of up to +9%. The correlation coefficient (*r*) of the PEMS to the setpoints is 0.99993. The readings of the drone measurement differ by less than 0.015 mol CH₄ per mol CO₂. The relative deviations are generally within ±15%, with outliers up to 30%. A possible explanation for the variability with the drone measurements is the relatively small plume of the genset, which was affected by wind gusts during the tests. Nevertheless, the drone measurement for the on-land test had a correlation coefficient (*r*) of 0.9934 for the correlation with the setpoints of the mass flow controllers (Figure 41) and 0.9933 with the PEMS (Figure 42). It is expected that the larger plumes of seagoing vessels provide much more stable conditions and are therefore better suited for the remote measurements. Indeed, in the onboard campaign, we found even better linearity (linear regression coefficient = 0.974 ± 0.132) and good correlation (*r* = 0.957)

between the drone and in-stack measurements (using FTIR instead of PEMS) during onboard tests, as shown in Figure 28.

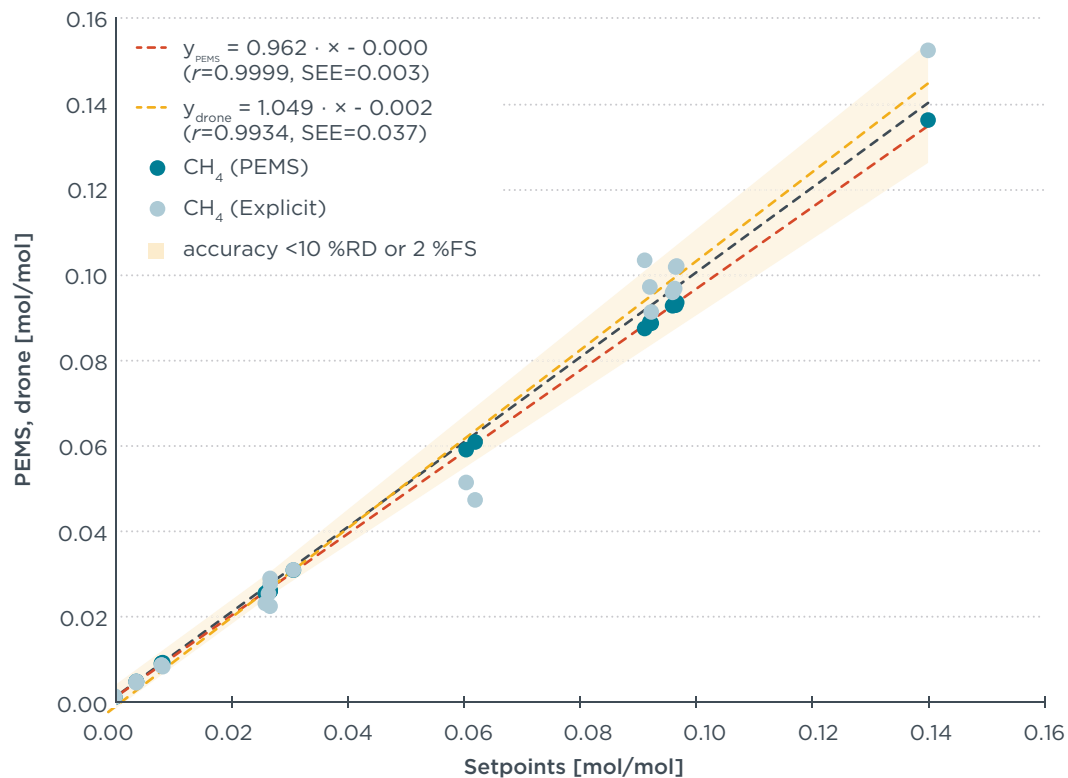


Figure 41. Methane emissions expressed per unit of CO₂ in mol/mol as adjusted and measured by the mass flow controllers (CH₄ setpoint), compared to PEMS and drone (Explicit) measurements during the on-land cross-instrument comparison.

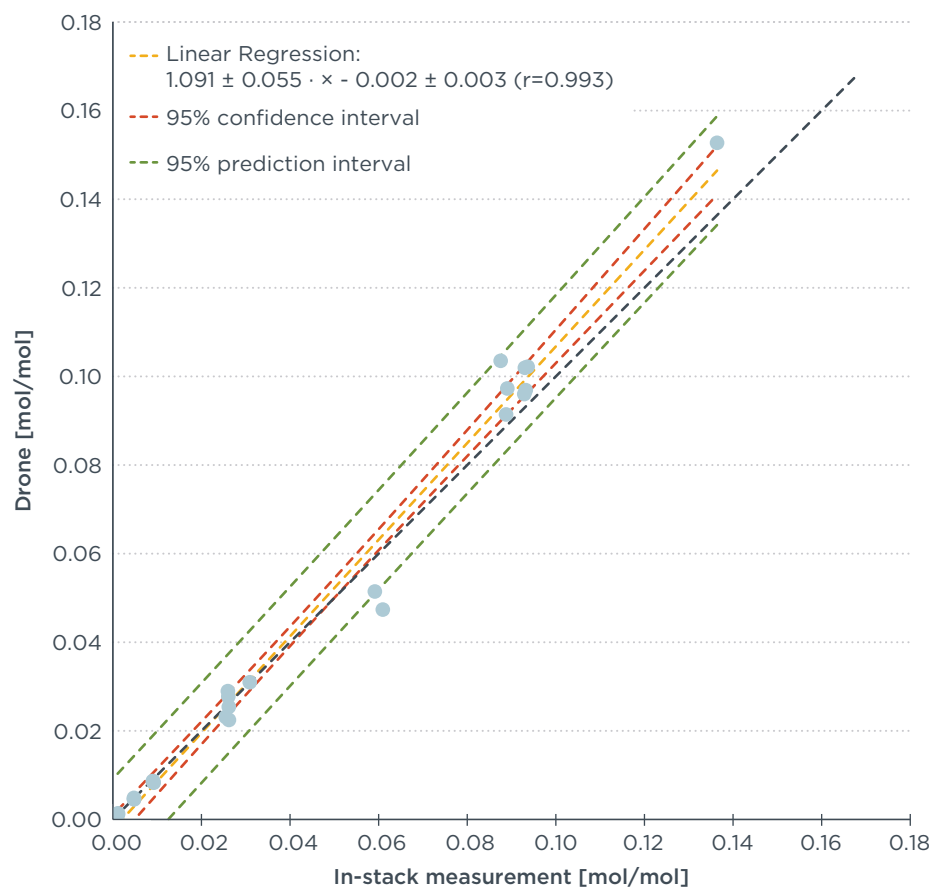


Figure 42. Comparison of methane-to-CO₂ concentrations (mol/mol) measured in-stack by the PEMS and in the plume by the drone (Explicit) for the various methane slip levels selected in the on-land cross-instrument comparison.

A comparison of the in-stack measurements by PEMS and the remote results obtained by the drone is depicted for NO_x in the scatter plot in Figure 43. The plot shows that the NO_x per CO₂ concentration ratio of the genset varied little for the individual measurements due to a stable engine load. The scatter is caused by the small variation of NO_x per CO₂ concentrations at the fixed engine load points that were used for the measurements. Almost all individual NO_x per CO₂ results of the drone are higher than the results of PEMS, on average about 18% and within -0.0001 to 0.0007 mol/mol and -1% to 24%.

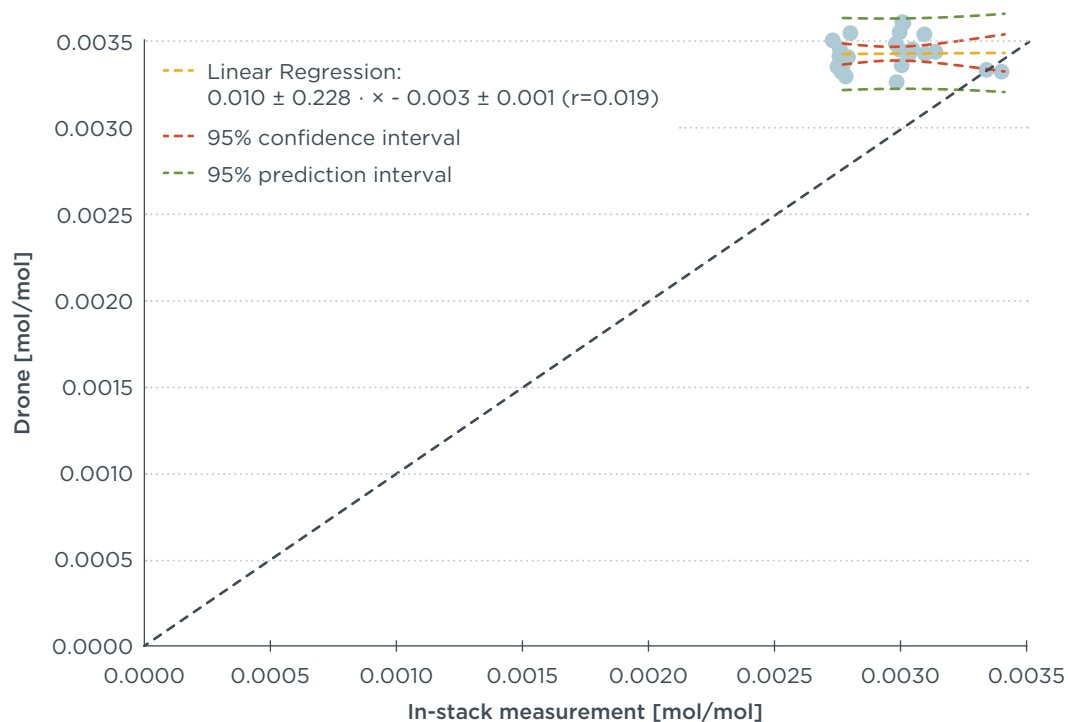


Figure 43. NO_x emissions expressed per unit of CO₂ in mol/mol measured by the drone during the on-land cross-instrument comparison, compared to NO_x emissions measured by PEMS in the stack.

Takeaways

An analysis of the cross-instrument comparison results yielded three takeaways:

1. In-stack measurements are more accurate than plume measurements, but for the CH₄-to-CO₂ ratio the plume measurement nevertheless showed a linear relationship with a correlation coefficient of 0.993 and a regression coefficient of 1.09 ± 0.055 relative to the PEMS.
2. For NO_x, the results of the drone deviated on average about 18%, between about -1%–24% from reference measurements done with PEMS.
3. The small unstable plume of the land-based set-up proved to be a challenging condition for the drone to measure emissions ratios. Much larger plumes of sea-going ships likely yield more stable results. Hence, the results provided the confidence to take the next step to compare the drone with in-stack measurements aboard a sea-going ship.

FUGITIVE CAMPAIGN RESULTS

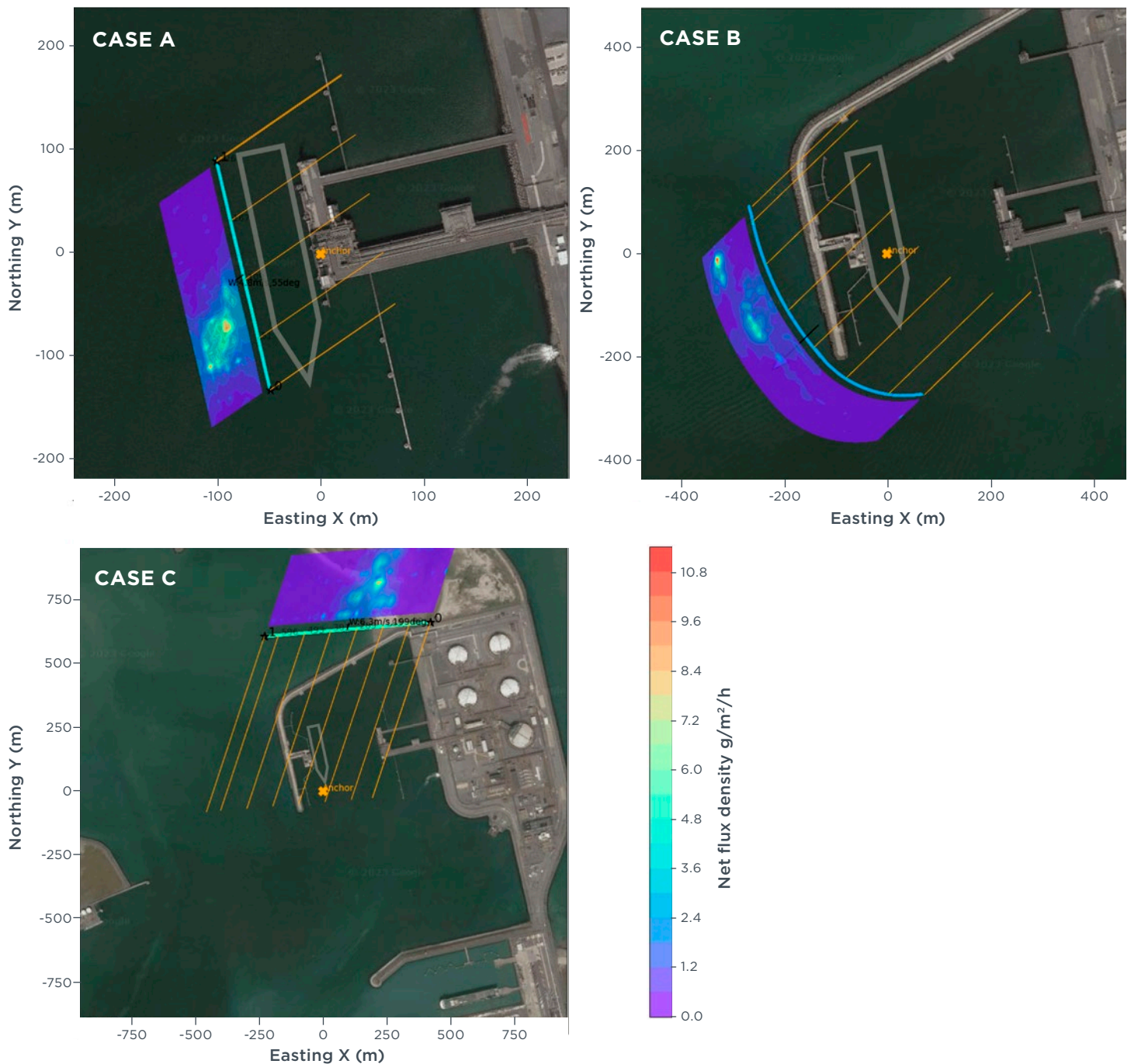
Measurements to evaluate the overall fugitive emissions of vessels unloading LNG as cargo were conducted in September 2022. In total, three different vessels (cases A, B, and C) were measured using the DFM method while they were connected for LNG cargo unloading operations at either of the two jetties of the terminal. Although confidentiality agreements prevent us from identifying individual vessels, general information about the ships can be reported. For case A, the ship is a gas tanker built in 2010, with a cargo capacity of 10,000 cubic meters (m³). The case A ship uses 4-stroke diesel engines, i.e., it does not run on LNG. For case B, the ship is an LNG carrier with LPDF 4-stroke engines (L4) built in 2021, with a cargo capacity of 174,000 m³. For case C, the ship is an LNG carrier built in 2009 with LPDF 4-stroke engines (L4) and a cargo capacity of 162,400 m³.

The LNG terminal is equipped with two jetties (see Figure 44). The storage and production units of the terminal are located on the land-side to the east of both jetties. Both jetties are equipped with a set of loading arms to load or unload LNG to or from moored vessels. Case A was measured at Jetty 1 and cases B and C were measured at Jetty 2.



Figure 44. Map of the LNG Terminal with the marked locations of Jetty 1 where Case A was measured and Jetty 2 where Cases B and C were measured (Maps data: Google, ©2022, 2023 CNES / Airbus, Maxar Technologies).

During the measurements of cases A and B the predominant wind was from northeast at around 4 and 3 meters per second (m/s), respectively, and hence from the directions of other facilities at the LNG terminal. In case C, the wind came from the south at around 6 m/s, which is from the inner areas of harbor and inland direction. Despite the possible influence of other terminal facilities or other potential sources in the background, the distinct patterns of the measured flux distributions in visualizations of individual measurement walls, as shown in Figure 45, can clearly be related by location and elevation to sources that were either on or near the moored vessels. Possible emissions from other sources farther away are more dispersed, and they were accounted for as part of the background, which was subtracted for the calculation of the net emissions from the vessel-related sources of methane.



Notes: The results are mapped on satellite images (Maps data: Google, ©2022, 2023 CNES / Airbus, Maxar Technologies). The anchor points indicate the location of the vessels along the respective jetties. At the time of the measurements, these were the only ships moored at either of the two jetties. All ships were moored with their respective bows heading southwards. Vessel sizes indicated by the ship outlines on the map are approximations.

Figure 45. Visualization of measured fugitive methane emissions while three different vessels were present for bunkering operations at two jetties of the LNG terminal. The visualized emission rates are combined emissions from the measurement scene.

The overall emission rates of methane that can be related to the individual vessels or the loading/unloading facilities near the respective vessel at the time of the measurements were between 10.9–40.5 kg/h. The results for the individual cases are listed in Table 12. (See Figure 45 for spatially resolved visualizations of the measured emission rates of the respective cases.) Average methane emissions for cases B and C were similar, at 30.6 and 32.4 kg/h, respectively, whereas methane emissions for case A were approximately half as much, at 15.1 kg/h.

Table 12. Summary of the measured emission rates from bunkering operations.

Case ID	number of repetitions	overall period of observation [h:mm]	lowest emission rate [kg/h]	highest emission rate [kg/h]	average emission rate [kg/h]	Uncertainty [kg/h]
Case A	5	3:50	10.94	20.78	15.09	2.29
Case B	2	0:41	28.96	32.22	30.59	7.35
Case C	6	2:56	23.68	40.45	32.44	12.05

The main sources of methane appear to be near to the locations of the connections between the vessels and the jetties where LNG was being unloaded, as well as the engine exhaust stacks for case B and case C, which involve ships with LPDF 4-stroke engines. The measurement walls could be erected aside of the vessels in cases A and B, so that the visualization allowed for a more distinct source discrimination. In both cases, a hotspot was found near the location of the bunkering connections between the vessels and the jetties. In case A, where the vessel was moored to jetty 1, the major emissions are dispersed between a 12 and 36 m elevation with a peak around 20 m above ground level of the jetty, meaning that the source of emissions is likely to be in this range.

In case B, a second emission hotspot appears to be from the exhaust stack of the vessel based on the location of the stack and elevation around 50 m with respect to the ground level. Again, a hotspot can be seen downwind of the location of the connection facilities at an elevation of around 40 m.

Case C is an example of when the wind is opposite the heading of the vessel. In this case, the determination of locations of sources is more difficult, as the emissions are measured behind the short stern side. However, the measurements show a hotspot around 40 to 60 m elevation above the jetty ground level. This would match with the findings in case B, and the upper hotspot indicates a likely contribution of methane from the ship's engine exhaust stacks.

Importantly, for case A where the ship does not run on LNG, we do not observe an exhaust hotspot, offering some additional evidence that the emissions for cases B and C include methane slip from the engines. Case A had the lowest methane emissions rate, which could be at least partly because of a lack of methane emissions from the exhaust stack. The ship in case A also had a much smaller LNG cargo capacity than in cases B and C, but the difference in LNG cargo capacity may be less important with regards to the fugitive emissions rate than the rate at which the LNG cargo is delivered from the ship to the bunkering connections and deserves further investigation. Cases B and C had similar ship types, LNG cargo capacities, and engine equipment, and they had similar methane emissions rates.

Engine methane slip may be on the order of 8 kg/h based on quantifying the rates associated with the hotspots that match the height of the stack for case B. We expect ships of this size to draw approximately 2.5 MW of power while they are at berth (Appendix A). During the onboard campaign for the FUMES project, when the Aurora Botnia's LPDF 4-stroke engine was operating at 2.15 MW, we estimated that it emitted approximately 8.75 kg/h of methane. Therefore, an estimate of 8 kg/h of methane emissions from an LPDF 4-stroke marine engine may be reasonable.

Assuming 8 kg/h of methane emissions from the LPDF 4-stroke engines, the remaining fugitive methane emissions rate is 23 and 24 kg/h for cases B and C, respectively. This means that during LNG unloading, fugitive methane emissions can be up to several times higher than the onboard engines. The results of this study show that fugitive emissions during LNG cargo unloading operations can be large compared to those that were emitted through the stack. However, over the entire voyage, engine emissions will still dominate.

The total loss of the transported LNG can be estimated, assuming that the measured average emission rates for the three cases are representative throughout the duration of the unloading operation. For the calculation, the respective average emission rates are assumed. For cases B and C, an engine methane slip of 8 kg/h was assumed and subtracted from the total average emission rate before further calculation. Then, the total mass of the emitted fugitive emissions from the cargo during this operation is put in relation to the total volume of the unloaded LNG. For the conversion of the LNG cargo volume to its weight, the density was assumed to be 456 kg/m³, based on data from the U.S. Department of Energy (2004). The calculation leads to an estimated fraction of the LNG that is lost through fugitive emissions ranging from 0.0004% to 0.0036% for the measured cases, as shown in Table 13.

Table 13. Estimated fraction of the LNG cargo lost as fugitive methane emissions during unloading operations.

Case ID	Duration of unloading operation [hh:mm]	Volume of unloaded LNG [m ³]	Mass of unloaded LNG [kg]	Measured emission rate appointed to fugitive emissions from LNG cargo* [kg/h]	Total mass of emitted fugitive methane emission from LNG cargo [kg]	Fraction of fugitive methane to total amount of unloaded cargo
Case A	10:30	9,540	4,350,240	15.1	158	0.0036%
Case B	14:22	164,349	74,943,144	22.6	325	0.0004%
Case C	06:18	30,019	13,688,664	24.4	154	0.0011%

* Average total emission rates for cases B and C were reduced by 8 kg/h appointed to engine emissions. Case A was not affected by engine emissions.

Takeaways

An analysis of the fugitive campaign results yielded four main takeaways:

1. Drone measurements can be used to quantify and visualize fugitive methane emissions from LNG cargo unloading operations.
 - a. We presented a novel and unique approach to quantify and visualize fugitive emissions during unloading operations of LNG cargo vessels. This is the first time a top-down approach using a drone was conducted to quantify such emissions.
 - b. The measurements did not interfere with the operation of the ships or the port.
2. There are measurable fugitive releases of CH₄ during LNG cargo bunkering operations.
 - a. Unloading operations can release 11–21 kilograms of methane per hour (kg/h) for a small, 10,000 cubic meter (m³) capacity LNG tanker that uses conventional diesel engines (i.e., does not use LNG as a fuel).
 - b. Unloading operations of large 162,000–174,000 m³ capacity LNG tankers that use LPDF 4-stroke engines can cause emissions between 24 and 40 kg/h of methane, including approximately 8 kg/h in the form of methane slip from the engines.
3. Fugitive methane emissions sources can be identified.
 - a. Depending on wind conditions and measurement geometry, the data results can be used to pinpoint to the sources of the emissions.
 - b. Emissions related to the bunkering operations can be separated from other sources, including engine stack emissions, and quantified.
4. Additional measurements of fugitive emissions from bunkering operations are warranted.
 - a. Only three cases were examined. Further measurements covering more cases would give a more complete picture of emissions.

LIMITATIONS AND FUTURE WORK

For the plume campaign, in addition to the uncertainty in the sensor itself, assumptions about individual main engine load and the resultant pilot fuel consumption limit our ability to precisely estimate methane slip based on the methane-to-CO₂ ratio measured in the plume. Individual engine loads and pilot fuel consumption could be obtained if ship operators would share this information with researchers at the time the ship exhaust is sampled. However, as shown in the sensitivity analysis, even if one used a drone or helicopter to measure the CH₄-to-CO₂ ratio and did not adjust for the influence of pilot fuel consumption or when 2-stroke engines were operating in diesel mode, the results would still be useful to understand the magnitude of methane emissions from ships.

An additional limitation for the plume campaign was limiting measurements to near-shore areas where ships would tend to, but not always, sail at slower speeds and lower combined engine loads than their typical operations. However, as we have noted, combined engine load is not the same as individual engine loads, especially for L4 ships. For L2L4 and H2L4 ships, when operating below 10% combined engine load, we assume that all methane is from LPDF 4-stroke engines. It is difficult to precisely estimate combined engine load, and even more challenging to estimate individual engine load, when there is more than one main engine. It is possible that LPDF 2-stroke and HPDF 2-stroke engines are making some contribution to methane emissions below 10% combined engine load. However, it may also be the case that the main engines switch to diesel mode at engine loads higher than 10% in some cases. If so, all the methane would be from LPDF 4-stroke engines at higher combined main engine loads that we have estimated here. Efforts could be made to use helicopters to intercept plumes of ships farther offshore; for now, drones will be limited to near-shore operations unless they are deployed from offshore ships or platforms.

We were only able to measure three H2L4 ships and two LBSI ships. This is perhaps unsurprising, given that L4 and L2L4 ships are more common. While LBSI ships have consistently represented a relatively insignificant share of installations and LNG consumption, the use of H2L4 ships has been growing. It would be useful to obtain additional ship-level measurements for H2L4 ships, and individual engine measurements for HPDF 2-stroke engines, given that the only data available (that we are aware of) on methane slip from these engines is provided by engine manufacturers. With additional measurements, researchers could independently verify engine manufacturer claims of low methane slip emissions from these engines. Our own efforts to get onboard a ship with an HPDF 2-stroke main engine were unsuccessful, due to a limited number of willing shipowners, paired with inconvenient departure locations and long, transoceanic voyages that would have required spending many weeks onboard. Lastly, we were unable to isolate methane slip from HPDF or LPDF 2-stroke engines without interference from LPDF 4-stroke auxiliary engines. Obtaining isolated measurements of these engines could be accomplished in future research campaigns.

For the onboard campaign, measurements in the stack have the advantage that they can be done with high accuracy. However, a formal test method is yet to be established to measure methane emissions from marine engines in both the testbed and onboard. Several measurement techniques are available to measure methane (and other components) which all have advantages and disadvantages. The onboard reproducibility is lower than a testbed and affected by conditions such as sea state and weather. Measurement results often rely on the use of engine parameters to be retrieved from onboard devices, which are hard to verify. For instance, the engine power, which is needed to calculate the engine work, is calculated by the engine computer, but there are no formal requirements set to check the accuracy of these data. The results of onboard measurements represent real sailing emissions; however,

to be able to determine emissions over a trip including all engine operating conditions would require longer term testing. It is difficult to find shipowners willing to participate in testing programs and much effort is needed to make all the arrangements to get aboard for a test program. It is hard to fit a test program within the operations of a ship, as ships may be at sea for days or weeks. Future work could focus on measuring methane emissions across additional engine load points and for longer periods of time. This could include the use of continuous monitoring equipment to measure methane emissions across a wide range of engine loads, sea states, weather conditions, and operating parameters.

For the fugitive campaign, measurements using the DFM method need to be conducted when the vessels are not moving, i.e., when they are anchored or at berth. Also, erecting each measurement wall with the DFM method takes up to 25 minutes. Preferably each measurement should then be repeated three times. This usually requires collaboration with the site owners which might restrict the opportunities for such measurements. However, this study shows the capability of the DFM method to measure fugitive emissions even for objects that are otherwise hard to assess. Future work could complement the findings of this study with further measurements of fugitive methane emissions from ships either at loading/unloading or bunkering operations, or individually when anchoring.

POLICY RECOMMENDATIONS

Regulators have a responsibility to ensure that climate policies accurately account for all methane emissions from ships to determine shipping's contribution to global warming. Two EU policies will soon regulate methane emissions in the sector: the FuelEU Maritime regulation and the EU Emissions Trading System (ETS). The FuelEU maritime regulation, which enters into force in 2025, gradually reduces the allowable well-to-wake GHG intensity of the fuels (or energy) used by ships on voyages to, from, or between EU ports. The EU ETS requires emitters to purchase market-traded allowances based on their direct GHG emissions. The ETS has been extended to the shipping sector in 2024, initially covering only CO₂ emissions, and will cover methane beginning in 2026. Later, the IMO will incorporate methane slip into its policies by applying its LCA guidelines.

EU and IMO policymakers should consider increasing the default methane slip value for LPDF 4-stroke engines from 3.1% (EU) or 3.5% (IMO) to at least 6%. Across all combined engine loads, methane slip from 22 measurements of 18 unique ships using exclusively LPDF 4-stroke engines (L4 ships) averaged 6.42% with a median of 6.05%. For six measurements at or above 50% combined engine load, the average was 6.07% and the median was 6.59%. Methane slip was greater than 3.1% in 77% of the measurements, and these measurements were also greater than 3.5%. Based on the results, the default LPDF 4-stroke methane slip value could be increased from 3.1% to at least 6% in FuelEU and EU ETS. IMO delegations, including EU Member States, could propose the default methane slip emission factor for LPDF 4-stroke engines in the IMO LCA Guidelines be increased from 3.5% to at least 6%. For the EU, this change could be made during the FuelEU Maritime review, which will be completed by the end of 2027, or sooner through an “implementing act” of the European Commission. For the IMO, this change could be implemented as part of its ongoing development of its LCA Guidelines. We cannot say whether the methane slip default values for HPDF 2-stroke or LPDF 2-stroke engines are reasonable because we were not able to isolate methane slip emissions from these engines without interference from LPDF 4-stroke auxiliary engines. More real-world data should be obtained on methane slip from 2-stroke, dual fuel engines.

Shipowners may certify that the engines they use emit less than the default values. Shipowners that do not wish to take the default values may certify that the engines used on their ships emit less than the default methane slip values. This would incentivize shipowners to reduce methane emissions from their ships. Engine manufacturers would also have an incentive to reduce methane slip from their engines to meet shipowner demand. The FuelEU Maritime regulation and the EU ETS allow for the possibility of certifying that the engines used on the ship emit less than the default EU values. The IMO also has a provision to allow for replacing the default values with certified replacement values. If certified, ships with lower-emission engines would be able to use LNG as a compliant fuel for longer under the FuelEU Maritime regulation. Under the EU ETS, they would pay a smaller GHG fee because their total GHG emissions would be lower. Additionally, these ships would face an easier compliance pathway for global IMO regulations that incorporate methane.

Procedures to certify engines to lower than the default methane slip values should be carefully designed to ensure they reflect real-world operations. We found in the onboard campaign that using a modern LPDF 4-stroke engine can result in lower-than-default emission values. However, any certification procedure should accurately reflect how the engine is operated in the real world because methane slip varies by engine load. Certification options could include a test-cycle, continuous emissions monitoring, or reporting engine load distribution and calculating annual emissions based on measured methane slip for that engine across loads. We caution that test-

cycle approaches require careful consideration of the number and value of load test points, as well as the weighting factors applied to those test points due to evidence that the test cycle used to certify compliance with NO_x regulations has resulted in newer Tier II engines emitting higher rates of NO_x than older Tier I engines (Comer et al., 2023). Additionally, a lack of a test point below 25% engine load for most engines has resulted in higher NO_x emissions near shore;¹⁶ we found NO_x emissions (g/kWh) were an order of magnitude higher near 10% engine load compared to those near 75% engine load. Continuous monitoring could provide a more complete emissions profile for the engine, but it would likely be more expensive compared to estimating it on a test cycle. Calculating the methane slip based on the reported engine load distribution has the advantage of using real-world operations data while only needing to measure emissions from the engine once in the lab and at regular intervals onboard but emissions over a broad engine load range would need to be established for the engine.

EU policymakers should consider requiring LNG-fueled ships to plug into shore power or otherwise eliminate their at-berth emissions. Requiring LNG-fueled ships to plug into shore power or otherwise eliminate their at-berth emissions would eliminate the use of LPDF 4-stroke auxiliary engines, the engine technology we found to have the highest methane slip. Until then, if LPDF 4-stroke auxiliary engines must be used, ship operators should operate them at higher engine loads; for example, use one auxiliary engine at 50% load rather than two engines at 25% load. Shipowners can also invest in batteries or fuel cells to provide auxiliary power.

EU policymakers should consider requiring monitoring, reporting, and verification of methane emissions at LNG storage and refueling points. We found that fugitive methane emission rates during LNG cargo unloading operations can be greater than the rate of methane slip from LPDF 4-stroke engines. If data collected from a monitoring program or additional research campaigns confirms that there can be substantial methane emissions from LNG storage and refueling infrastructure, policymakers should consider regulating them. In the EU, these fugitive emissions could be incorporated into the FuelEU well-to-tank equation by amending the values for the “emissions from transport and distribution” (e_{td}) variable to account for these emissions. For the IMO, these fugitive emissions could also be incorporated into the equation used to calculate well-to-tank emissions in the LCA Guidelines.

IMO policymakers should consider adding a low-load test point to all engine emission certification test cycles. In the onboard measurements, we found that methane slip and work-specific NO_x emissions were highest at the lowest engine loads. To address this, IMO policymakers should consider adding a 10% engine load test point to all engine certification test cycles. They should also consider adjusting how emissions at each engine load test point are weighted to more accurately reflect real-world operations.

¹⁶ See the results of the SCIPPER project, reported here: https://www.scipper-project.eu/wp-content/uploads/2023/02/scipper-d5.5_s.pdf

CONCLUSIONS

Before the FUMES project, it was understood that LNG-fueled ships emit unburned methane, but real-world measurements of methane slip were scarce and the magnitude of ship-level methane emissions were largely unknown. The FUMES project resulted in the most comprehensive dataset of real-world methane emissions from LNG-fueled ships to date. We were able to obtain 45 measurements from 34 unique ships using a combination of drones and helicopters. We measured onboard one LNG-fueled ferry using in-stack sensors complemented by drone-mounted sensors in the plume. We also estimated methane emissions rates associated with LNG cargo unloading operations for three LNG carriers using a drone and a novel flux wall approach.

Overall, we conclude that the use of LNG-fueled ships results in releases of methane to the atmosphere in the form of methane slip from their engines, as well as fugitive methane emissions from LNG cargo unloading operations.

From the plume campaign, we conclude that LPDF 4-stroke engines, on average, emit 6.4% methane slip, which is more than twice as much methane slip as assumed by the EU (3.1%) and over 80% more than assumed by the IMO (3.5%). We cannot say whether the default methane slip values for HPDF 2-stroke or LPDF 2-stroke engines used by the EU or IMO are reasonable because we were not able to isolate methane slip emissions from these engines without interference from LPDF 4-stroke auxiliary engines. While the focus of our study was primarily on methane emissions, we found that most of the ships we measured in the plume campaign could achieve NO_x emissions below weighted Tier III limits without the use of exhaust aftertreatment technologies.

From the onboard campaign, we conclude that modern LPDF 4-stroke engines can emit lower methane slip than assumptions from EU regulations and the IMO, but methane slip can still be substantial, especially at low loads. Average real-sailing methane slip emissions ranged from a minimum of approximately 2% for measurements near 75% load and above 6.7% for measurements near 15% load. Methane slip was about 2.5% at approximately 50% engine load. This is lower than the EU assumption of 3.1% at 50% load and at the lower end of what is reported in literature. The E2 test cycle measurements yielded a weighted methane slip of 2.0%, lower than IMO's assumption of 3.5% methane slip for this engine technology. We found that the engine can achieve weighted NO_x emissions that could comply with Tier III standards under the E2 test cycle, even though the engine is only required to be certified to Tier II standards. However, we found that NO_x emissions (g/kWh) at around 10% engine load, which is not used in the E2 cycle, were 10-times higher than NO_x emissions at near 75% engine load.

From the fugitive campaign, we conclude that LNG cargo unloading operations can release 11–21 kg/h of methane for a small, 10,000 m³ capacity LNG tanker that uses conventional diesel engines. The unloading operations of large 162,000–174,000 m³ capacity LNG tankers that use LPDF 4-stroke engines can cause emissions of 24–40 kg/h of methane, including approximately 8 kg/h in the form of methane slip from the engines. While the amount of methane released as a percentage of cargo unloaded is small, the methane emissions rates from unloading operations were estimated to be greater than the emissions rates from LPDF 4-stroke engines, the engine technology we found emits the most methane.

Regarding measurement approaches, we found that mounting sensors to drones and helicopters is useful for estimating ship-level methane slip from LNG-fueled ships and for estimating fugitive methane emissions from LNG cargo unloading operations. While measuring in the plume introduces more uncertainty compared with in-stack sensors, we nevertheless found good agreement in measured methane concentrations between the two approaches. Using drones and helicopters allows for sampling more

ships at a lower cost than in-stack measurements. Moreover, the barriers to making the measurement are lower. In-stack measurements are useful for accurately measuring methane emissions from individual engines onboard the ship, which is not possible when measuring in the plume, unless only one engine is operating at a time. When measuring onboard, the emissions from the stack can be determined over the range of real sailing engine loads and other methane sources can also be monitored.

In light of our findings, EU and IMO policymakers should consider increasing the default methane slip value for LPDF 4-stroke engines to at least 6%. Shipowners that do not wish to take the default values can certify that the engines used on their ships emit less than the default methane slip values. EU policymakers should consider requiring LNG-fueled ships to plug into shore power or otherwise eliminate their at-berth emissions to avoid using LPDF 4-stroke auxiliary engines. Additionally, because we found that LNG cargo unloading operations can emit higher rates of methane emissions than LPDF 4-stroke engines, EU policymakers should consider requiring monitoring, reporting, and verification of methane emissions at LNG storage and refueling points. Lastly, because we found that methane slip and work-specific NO_x emissions were highest at the lowest engine loads, IMO policymakers should consider adding a 10% engine load test point to all engine certification test cycles. They should also consider adjusting how emissions at each engine load test point are weighted to more accurately reflect real-world operations.

REFERENCES

- Anderson, M., Salo, K., & Fridell, E. (2015). Particle- and gaseous emissions from a LNG powered ship. *Environmental Science*, 49(20), 12568–12575. <https://doi.org/10.1021/acs.est.5b02678>
- Balcombe, P., Heggo, D. A., & Harrison, M. (2022). Total methane and CO₂ emissions from liquefied natural gas carrier ships: The first primary measurements. *Environmental Science & Technology*, 56(13), 9632–9640. <https://doi.org/10.1021/acs.est.2c01383>
- Beecken, J., Irijala, M., Weigelt, A., Conde, V., Mellqvist, J., Proud, R., ... Duyzer, J. (2019). *Review of available remote systems for ship emission measurements* (No. D2.1). The SCIPPER Project (European Commission - Horizon 2020 No. 814893). https://www.scipper-project.eu/wp-content/uploads/2020/01/scipper_d2_1_20191220.pdf
- Bernard, M. R. (2023). *European Union Alternative Fuel Infrastructure Regulation (AFIR)*. International Council on Clean Transportation. <https://theicct.org/publication/afir-eu-april2023/>
- Carr, E. W., McCabe, S., Elling, M., & Winebrake, J. J. (2023). *Options for Reducing Methane Emissions from New and Existing LNG-fueled Ships*. International Council on Clean Transportation. <https://theicct.org/publication/options-for-reducing-methane-emissions-from-new-and-existing-lng-fueled-ships-oct23/>
- Comer, B., McCabe, S., Carr, E. W., Elling, M., Sturup, E., Knudsen, B., ... Winebrake, James. J. (2023). *Real-world NOx emissions from ships and implications for future regulations*. International Council on Clean Transportation. <https://theicct.org/publication/real-world-nox-ships-oct23/>
- Comer, B., O'Malley, J., Osipova, L., & Pavlenko, N. (2022). *Comparing the future demand for, supply of, and life-cycle emissions from bio, synthetic, and fossil LNG marine fuels in the European Union*. International Council on Clean Transportation. <https://theicct.org/publication/lng-marine-fuel-sep22/>
- Corbin, J. C., Peng, W., Yang, J., Sommer, D. E., Trivanovic, U., Kirchen, P., Gagné, S. (2020). Characterization of particulate matter emitted by a marine engine operated with liquefied natural gas and diesel fuels. *Atmospheric Environment*, 220, 117030. <https://doi.org/10.1016/j.atmosenv.2019.117030>
- De Rossi, L. (2021). *Quantification of Methane Emissions from a Biogas Plant using a Drone-Based Method* (Master's thesis). Polytechnic University of Milan. <https://www.politesi.polimi.it/handle/10589/181747>
- De Rossi, L., & Knudsen, J. (2022). *DFM Method: Controlled Release Campaign at TADI, 21-23 June 2022*. Explicit.
- DNV. (2023). EU ETS: Preliminary agreement to include shipping in the EU's Emission Trading System from 2024. <https://www.dnv.com/news/eu-ets-preliminary-agreement-to-include-shipping-in-the-eu-s-emission-trading-system-from-2024-238068>
- European Parliament (2023). *Reducing methane emissions in the energy sector*. <https://www.europarl.europa.eu/legislative-train/package-fit-for-55/file-reducing-methane-emissions-in-the-energy-sector>
- European Parliament and the Council of the European Union. (2023). *Regulation (EU) 2023/957 of the European Parliament and of the Council of 10 May 2023 amending Regulation (EU) 2015/757 in order to provide for the inclusion of maritime transport activities in the EU Emissions Trading System and for the monitoring, reporting and verification of emissions of additional greenhouse gases and emissions from additional ship types*. <https://eur-lex.europa.eu/eli/reg/2023/957/oj>
- European Parliament and the Council of the European Union. (2023). *Regulation (EU) 2023/1805 of the European Parliament and of the Council of 13 September 2023 on the use of renewable and low-carbon fuels in maritime transport, and amending Directive 2009/16/EC*. <https://eur-lex.europa.eu/legal-content/EN/TXT/?uri=CELEX%3A32023R1805>
- Explicit. (2016). *Patent No. EP3100022, US10416672, CN106170685*.
- Explicit ApS. (2018). *Airborne Monitoring of Sulphur Emissions from Ships in Danish Waters: 2017 Campaign Results*. Danish Environmental Protection Agency. <https://www2.mst.dk/Udgiv/publications/2018/04/978-87-93710-00-9.pdf>
- Faber, J., Hanayama, S., Zhang, S., Pereda, P., Comer, B., Hauerhof, E., ... Xing, H. (2020). *Fourth IMO GHG Study 2020*. <https://www.imo.org/en/ourwork/Environment/Pages/Fourth-IMO-Greenhouse-Gas-Study-2020.aspx>
- Gozillon, D. (2022). *FuelEU Maritime: T&E analysis and recommendations*. Transport & Environment. <https://www.transportenvironment.org/wp-content/uploads/2022/02/TE-Report-FuelEU-Maritime-1.pdf>
- Grönholm, T., Mäkelä, T., Hatakka, J., Jalkanen, J.-P., Kuula, J., Laurila, T., Kukkonen, J. (2021). Evaluation of methane emissions originating from LNG ships based on the measurements at a remote marine station. *Environmental Science & Technology*, 55(20), 13677–13686. <https://doi.org/10.1021/acs.est.1c03293>

- International Maritime Organization. (2008). *Resolution MEPC.177(58) Amendments to the Technical Code on Control of Emission of Nitrogen Oxides from Marine Diesel Engines (NOx Technical Code 2008)*. [https://wwwcdn.imo.org/localresources/en/KnowledgeCentre/IndexofIMOResolutions/MEPCDocuments/MEPC.177\(58\).pdf](https://wwwcdn.imo.org/localresources/en/KnowledgeCentre/IndexofIMOResolutions/MEPCDocuments/MEPC.177(58).pdf)
- International Maritime Organization. (2023). *Resolution MEPC.376(80) Guidelines on Life Cycle GHG Intensity of Marine Fuels (LCA Guidelines)*. [https://wwwcdn.imo.org/localresources/en/KnowledgeCentre/IndexofIMOResolutions/MEPCDocuments/MEPC.376\(80\).pdf](https://wwwcdn.imo.org/localresources/en/KnowledgeCentre/IndexofIMOResolutions/MEPCDocuments/MEPC.376(80).pdf)
- Intergovernmental Panel on Climate Change. (2021). *Climate Change 2021: The Physical Science Basis. Contribution of Working Group I to the Sixth Assessment Report of the Intergovernmental Panel on Climate Change* [Masson-Delmotte, V., P. Zhai, A. Pirani, S.L. Connors, C. Péan, S. Berger, N. Caud, Y. Chen, L. Goldfarb, M.I. Gomis, M. Huang, K. Leitzell, E. Lonnoy, J.B.R. Matthews, T.K. Maycock, T. Waterfield, O. Yelekçi, R. Yu, and B. Zhou (eds.)]. <https://doi.org/10.1017/9781009157896>
- ISO 8178, *Reciprocating internal combustion engines—Exhaust emission measurement*. (2020).
- Knudsen, B., Lallana, A. L., & Ledermann, L. (2022). *NOx Emissions from Ships in Danish Waters: Assessment of Current Emission Levels and Potential Enforcement Models*. Danish Environmental Protection Agency. <https://www2.mst.dk/Udgiv/publications/2022/01/978-87-7038-384-4.pdf>
- Knudsen, J., & De Rossi, L. (2022). *The Plane Project: Mapping and quantification of GHGs from diffuse emission sources using drone technology and vertical measuring walls*. Danish Environmental Protection Agency. <https://www2.mst.dk/Udgiv/publications/2022/04/978-87-7038-413-1.pdf>
- Korakianitis, T., Namasivayam, A. M., & Crookes, R. J. (2011). Natural-gas fueled spark-ignition (SI) and compression-ignition (CI) engine performance and emissions. *Progress in Energy and Combustion Science*, 37(1), 89–112. <https://doi.org/10.1016/j.peccs.2010.04.002>
- Kuittinen, N., Heikkilä, M., Jalkanen, J.-P., Aakko-Saksa, P., & Lehtoranta, K. (2023, June). *Methane slip emissions from LNG vessels—Review*. Presented at the CIMAC congress. https://cris.vtt.fi/ws/portalfiles/portal/85067970/CIMAC_paper_629.pdf
- Kuittinen, N., Heikkilä, M., & Lehtoranta, K. (2023). *Review of Methane Slip from LNG Engines*. https://greenray-project.eu/wp-content/uploads/2023/04/D1.1_Review_of_methane_slip_from_LNG_engines.pdf
- Laskar, I. I., & Giang, A. (2023). Policy approaches to mitigate in-use methane emissions from natural gas use as a marine fuel. *Environmental Research: Infrastructure and Sustainability*, 3(2), 025005. <https://doi.org/10.1088/2634-4505/acff33>
- Lehtoranta, K., Aakko-Saksa, P., Murtonen, T., Vesala, H., Ntziachristos, L., Rönkkö, T., Timonen, H. (2019). Particulate mass and nonvolatile particle number emissions from marine engines using low-sulfur fuels, natural gas, or scrubbers. *Environmental Science & Technology*, 53(6), 3315–3322. <https://doi.org/10.1021/acs.est.8b05555>
- Lehtoranta, K., Koponen, P., Vesala, H., Kallinen, K., & Maunula, T. (2021). Performance and regeneration of methane oxidation catalyst for LNG ships. *Journal of Marine Science and Engineering*, 9(2). <https://doi.org/10.3390/jmse9020111>
- Lehtoranta, K., Kuittinen, N., Vesala, H., & Koponen, P. (2023). Methane emissions from a state-of-the-art LNG-powered vessel. *Atmosphere*, 14(5). <https://doi.org/10.3390/atmos14050825>
- Maersk Mc-Kinney Møller Center for Zero Carbon Shipping. (2022). *Reducing methane emissions onboard vessels*. <https://cms.zerocarbonsshipping.com/media/uploads/publications/Reducing-methane-emissions-onboard-vessels.pdf>
- Nielsen, J. B., & Stenersen, D. (2010). *Emission Factors for CH₄, NO_x, particulates and black carbon for domestic shipping in Norway, revision 1*. MARINTEK. <https://kudos.dfo.no/dokument/9321/emission-factors-for-ch4-nox-particulates-and-black-carbon-for-domestic-shipping-in-norway-revision-1>
- Olczak, M., Piebalgs, A., & Balcombe, P. (2022). Methane regulation in the EU: Stakeholder perspectives on MRV and emissions reductions. *Environmental Science & Policy*, 137, 314–322. <https://doi.org/10.1016/j.envsci.2022.09.002>
- Olmer, N., Comer, B., Roy, B., Mao, X., & Rutherford, D. (2017). *Greenhouse gas emissions from global shipping, 2013–2015*. International Council on Clean Transportation. <https://theicct.org/publication/greenhouse-gas-emissions-from-global-shipping-2013-2015/>
- Paschinger, P., Kranendonk, M. R., Spijker, S., Verhagen, V. E., & Vermeulen, R. J. (2023). *TNO 2023 R11001 FUMES: land-based comparison of remote and in-stack measuring equipment* (No. 2023 R11001).
- Pavlenko, N., Comer, B., Zhou, Y., Clark, N., & Rutherford, D. (2020). *The climate implications of using LNG as a marine fuel*. International Council on Clean Transportation. <https://theicct.org/publication/the-climate-implications-of-using-lng-as-a-marine-fuel/>
- Peng, W., Yang, J., Corbin, J., Trivanovic, U., Lobo, P., Kirchen, P., ... Cocker, D. (2020). Comprehensive analysis of the air quality impacts of switching a marine vessel from diesel fuel to natural gas. *Environmental Pollution*, 266, 115404. <https://doi.org/10.1016/j.envpol.2020.115404>

- Republic of Korea. (2022). *REDUCTION OF GHG EMISSION FROM SHIPS Measurement of actual methane slip in terms of Tank-to-Wake emission factors by using the relevant procedures in the NOx Technical Code 2008* (No. MEPC 78/7/13).
- Rochussen, J., Jaeger, N. S. B., Penner, H., Khan, A., & Kirchen, P. (2023). Development and demonstration of strategies for GHG and methane slip reduction from dual-fuel natural gas coastal vessels. *Fuel*, 349, 128433. <https://doi.org/10.1016/j.fuel.2023.128433>
- Schuller, O., Kupferschmied, S., Hengstler, J., & Whitehouse, S. (2021). *2nd Life Cycle GHG Emission Study on the Use of LNG as Marine Fuel*. sphera. <https://sphera.com/research/2nd-life-cycle-ghg-emission-study-on-the-use-of-lng-as-marine-fuel/>
- Sommer, D. E., Yereimi, M., Son, J., Corbin, J. C., Gagné, S., Lobo, P., Kirchen, P. (2019). Characterization and reduction of in-use CH4 emissions from a dual fuel marine engine using wavelength modulation spectroscopy. *Environmental Science & Technology*, 53(5), 2892-2899. <https://doi.org/10.1021/acs.est.8b04244>
- Stamatis, F. (2021). *LNG as marine fuel and methane slip*. Safety4Sea. <https://safety4sea.com/cm-lng-as-marine-fuel-and-methane-slip/>
- Stenersen, D., & Thonstad, O. (2017). *GHG and NOx emissions from gas fuelled engines* (No. OC2017 F-108). SINTEF. <https://www.nho.no/siteassets/nox-fondet/rapporter/2018/methane-slip-from-gas-engines-mainreport-1492296.pdf>
- Thinkstep. (2019). *Life cycle GHG emission study on the use of LNG as marine fuel*. sphera. <https://sphera.com/research/life-cycle-ghg-emission-study-on-the-use-of-lng-as-marine-fuel/>
- Trivanovic, U., Corbin, J. C., Baldelli, A., Peng, W., Yang, J., Kirchen, P., ... Rogak, S. N. (2019). Size and morphology of soot produced by a dual-fuel marine engine. *Journal of Aerosol Science*, 138, 105448. <https://doi.org/10.1016/j.jaerosci.2019.105448>
- Uncertainty of measurement—Part 3: Guide to the expression of uncertainty in measurement (GUM:1995)*. (2008). International Organization for Standardization. <https://www.iso.org/standard/50461.html>
- U.S. Department of Energy. (2004). *Liquefied natural gas: Understanding the basic facts*. <https://www.energy.gov/fe/downloads/liquefied-natural-gas-understanding-basic-facts>
- Ushakov, S., Stenersen, D., & Einang, P. M. (2019). Methane slip from gas fuelled ships: A comprehensive summary based on measurement data. *Journal of Marine Science and Technology*, 24(4), 1308-1325. <https://doi.org/10.1007/s00773-018-00622-z>
- Zhao, Y., Fan, Y., Fagerholt, K., & Zhou, J. (2021). Reducing sulfur and nitrogen emissions in shipping economically. *Transportation Research Part D: Transport and Environment*, 90, 102641. <https://doi.org/10.1016/j.trd.2020.102641>

APPENDIXES

APPENDIX A: AUXILIARY ENGINE DEMAND ASSUMPTIONS

Table A1. Energy demand assumptions for auxiliary engines.

Ship type	Size	Units	Berth (kW)	Anchor (kW)	Maneuvering (kW)	Cruising (kW)
Chemical tanker	0-4999	dwt	110	170	190	200
Chemical tanker	5000-9999	dwt	330	490	560	580
Chemical tanker	10000-19999	dwt	330	490	560	580
Chemical tanker	20000-39999	dwt	790	550	900	660
Chemical tanker	40000-+	dwt	790	550	900	660
Container	0-999	TEU	370	450	790	410
Container	1000-1999	TEU	820	910	1750	900
Container	2000-2999	TEU	610	910	1900	920
Container	3000-4999	TEU	1100	1350	2500	1400
Container	5000-7999	TEU	1100	1400	2800	1450
Container	8000-11999	TEU	1150	1600	2900	1800
Container	12000-14499	TEU	1300	1800	3250	2050
Container	14500-19999	TEU	1400	1950	3600	2300
Container	20000-+	TEU	1400	1950	3600	2300
Liquefied gas tanker	0-49999	m ³	240	240	360	240
Liquefied gas tanker	50000-99999	m ³	1700	1700	2600	1700
Liquefied gas tanker	100000-199999	m ³	2500	2000	2300	2650
Liquefied gas tanker	200000-+	m ³	6750	7200	7200	6750
Cruise	0-1999	gt	450	450	580	450
Cruise	2000-9999	gt	450	450	580	450
Cruise	10000-59999	gt	3500	3500	5500	3500
Cruise	60000-99999	gt	11500	11500	14900	11500
Cruise	100000-149999	gt	11500	11500	14900	11500
Cruise	150000-+	gt	11500	11500	14900	11500
Roll-on/roll-off ferry	0-4999	dwt	750	430	1300	430
Roll-on/roll-off ferry	5000-9999	dwt	1100	680	2100	680
Roll-on/roll-off ferry	10000-14999	dwt	1200	950	2700	950
Roll-on/roll-off ferry	15000-+	dwt	1200	950	2700	950
Offshore	0-+	gt	320	320	320	320
Service-other	0-+	gt	220	220	220	220

APPENDIX B: PLUME RESULTS FIGURES IN GRAMS OF METHANE PER KILOWATT HOUR (g CH₄/kWh)

This appendix reproduces relevant figures from the plume campaign results in units of g CH₄/kWh.

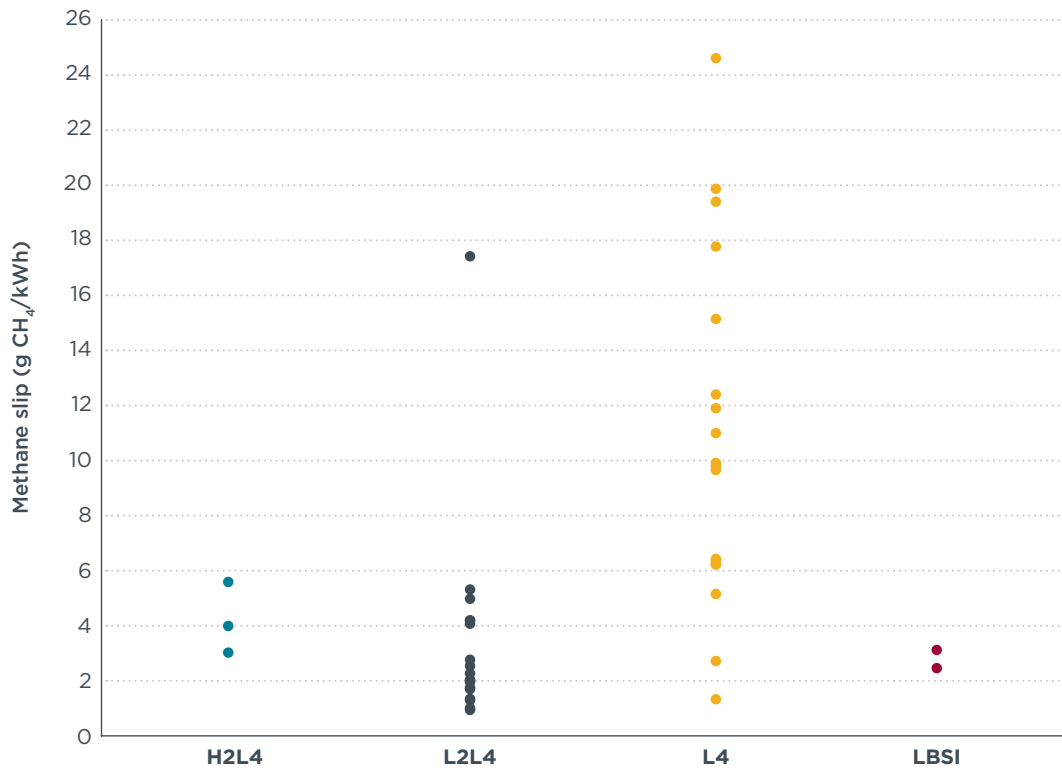


Figure B1. Ship-level methane slip from all engine sources (g/kWh).

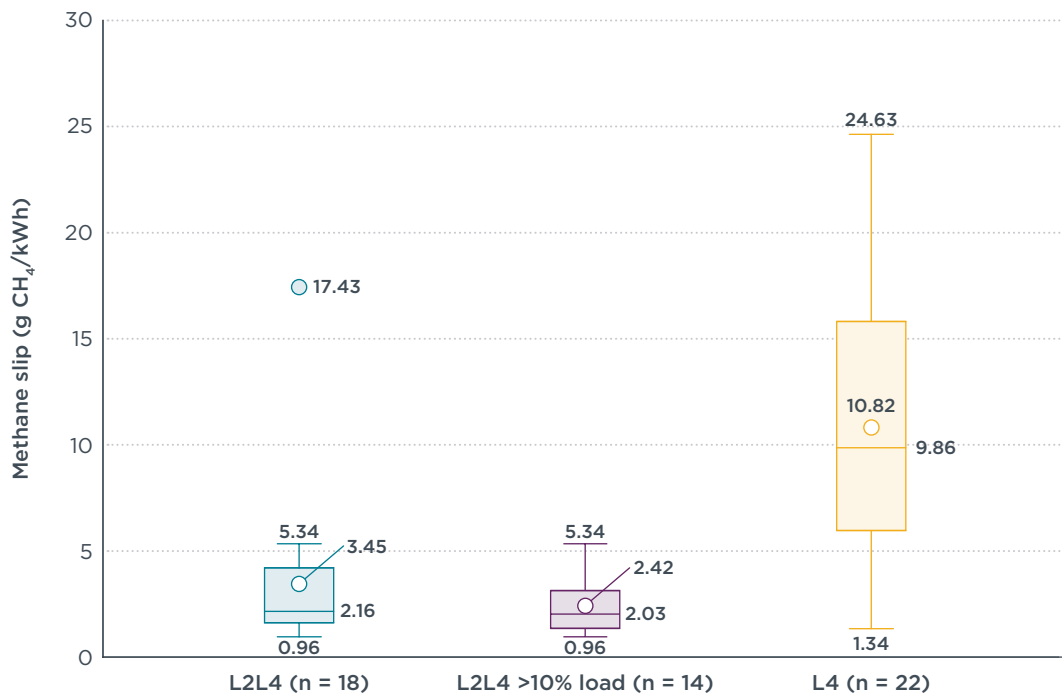


Figure B2. Boxplot of ship-level methane slip for ships with LPDF 2-stroke main engines and LPDF 4-stroke auxiliary engines (L2L4) and ships with only LPDF 4-stroke engines (L4) in g/kWh.

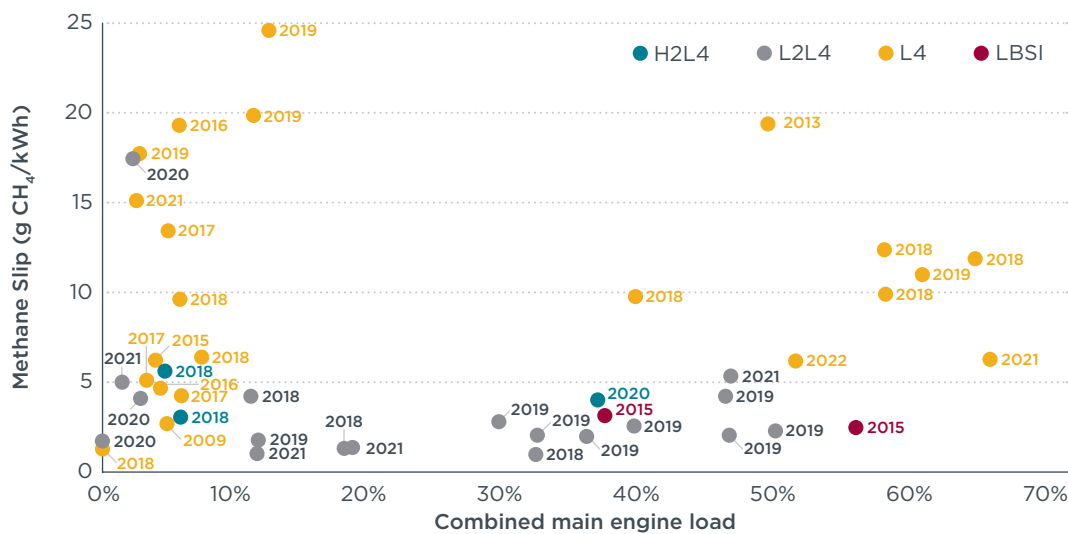


Figure B3. Methane slip (g/kWh) versus combine main engine load.

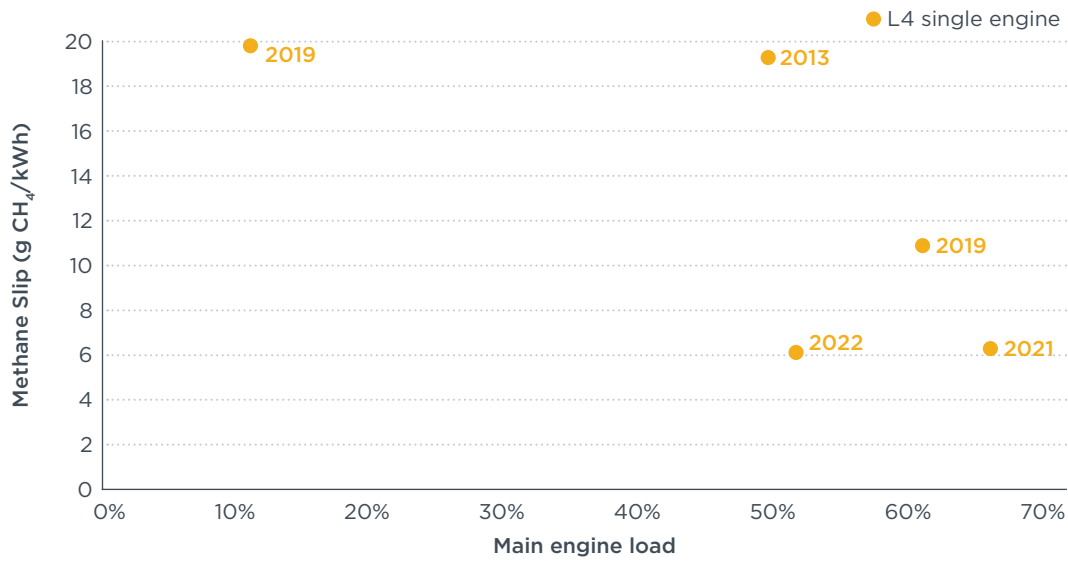


Figure B4. Methane slip (g/kWh) by engine load for ships that have only one LPDF 4-stroke main engine, with build year of the ship indicated.

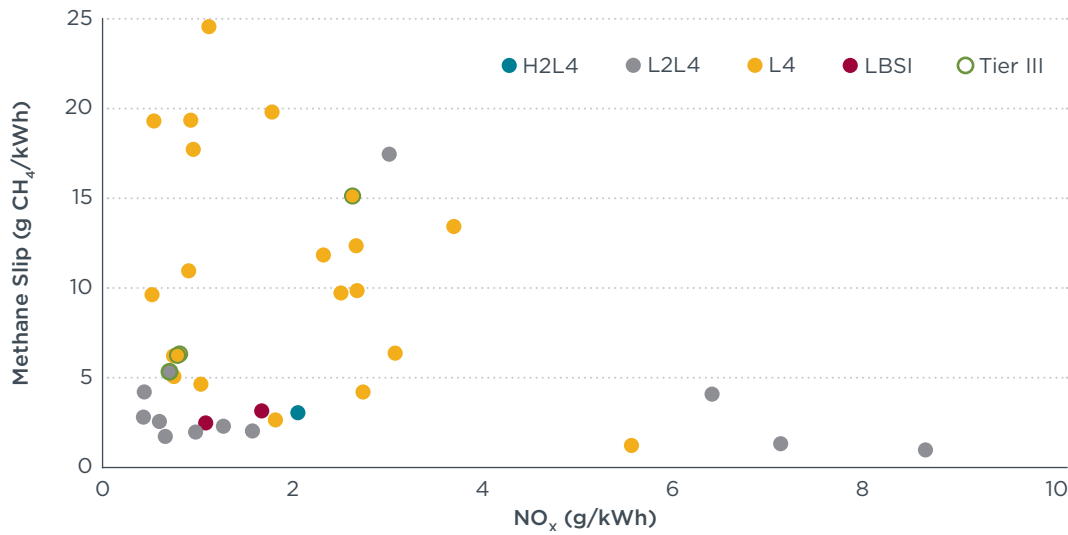


Figure B5. Methane slip (g/kWh) versus NO_x.

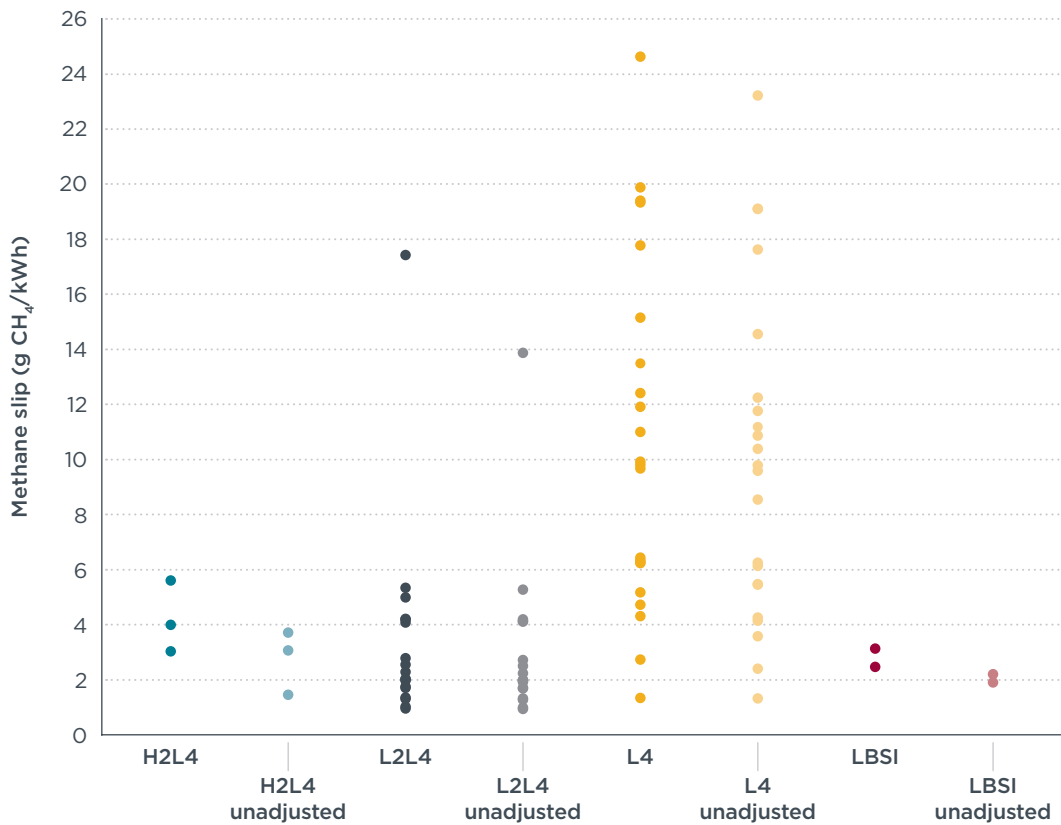


Figure B6. Sensitivity analysis: Methane slip estimates (g/kWh) with and without adjusting for CO₂ from fuel oil consumption from pilot fuel or for two-stroke dual-fuel engines in diesel mode.

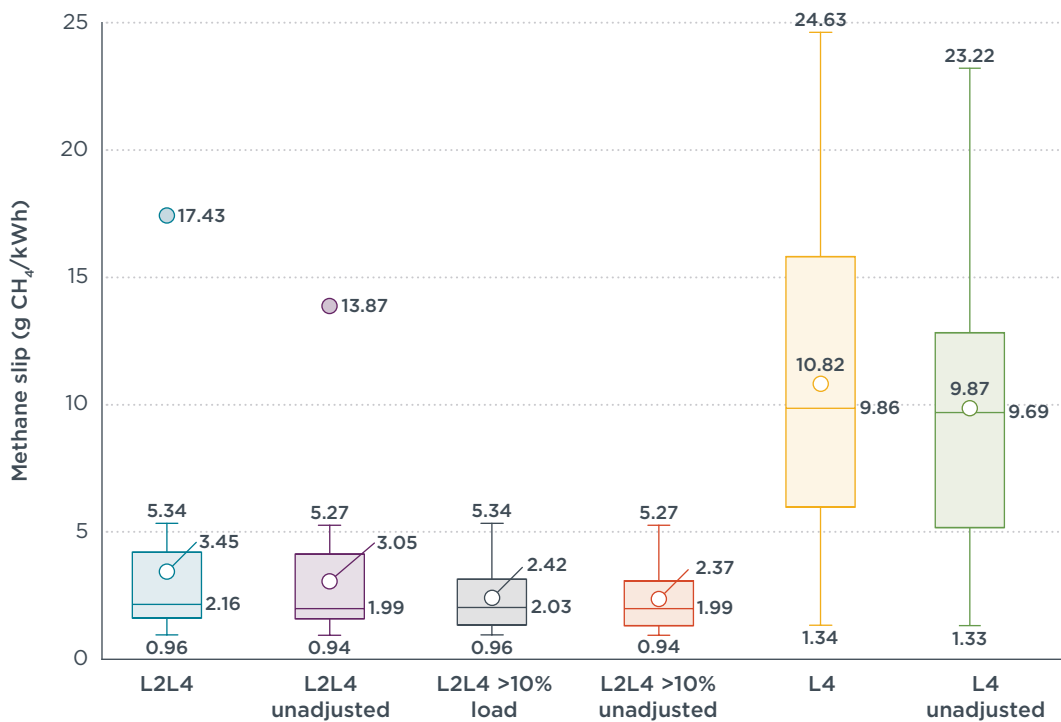


Figure B7. Sensitivity analysis: Methane slip results (g/kWh) for L2L4 and L4 ships with and without adjusting for CO₂ from fuel oil consumption from pilot fuel or for two-stroke dual-fuel engines operating in diesel mode.

APPENDIX C: ANNUAL COMBINED MAIN ENGINE LOAD DISTRIBUTIONS FOR SHIPS MEASURED IN THE PLUME CAMPAIGN

The supplemental material file labeled “FUMES_measurements_by_load.xlsx” has been published alongside this report at www.theicct.org/publication/fumes-characterizing-methane-emissions-from-lng-fueled-ships-using-drones-helicopters-and-on-board-measurements-jan24/. It reports the annual combined main engine load distribution for each ship that was measured in the plume campaign. For each ship, we report which combined engine load bin the measurements were associated with. This shows whether the ship was measured when it was operating at an engine load that is typical for that ship over the course of the year, or whether it was atypical.

We also devised a way to quantify the results. There are 11 engine load bins for each ship. For each ship, if we measured in the most-common engine load bin, we recorded a 1. If we measured in the least-common bin, we recorded an 11. If a ship was measured more than once, we used the lowest value to calculate the fleet-level average—e.g., if we measured in bin 2 and bin 8, we use bin 2.

Across the fleet of ships, measurements were taken in bins 1 through 11, with an average of bin 5.8, a median of bin 6.5, and a mode of bin 8. This suggests that our measurements tended to occur away from typical engine loads for most ships—usually lower. However, as we explain in the report, the combined engine load is not representative of individual engine loads, especially for L4 ships.

APPENDIX D: SUPPLEMENTAL MATERIAL FOR PLUME AND FUGITIVE MEASUREMENTS

The supplemental material file “FUMES_plume_measurements_vf.xlsx” contains the necessary information to reproduce our plume measurement results. The supplemental material file labeled “Fugitive_reports.zip” contains additional information on the data collected and analyzed in the fugitive campaign. Both files can be found at www.theicct.org/publication/fumes-characterizing-methane-emissions-from-lng-fueled-ships-using-drones-helicopters-and-on-board-measurements-jan24/.

